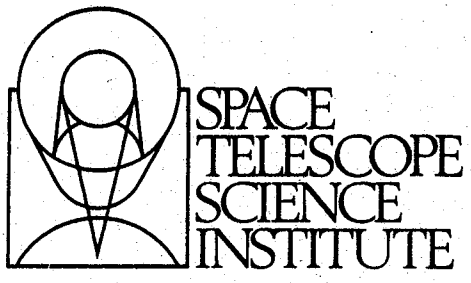

Hubble Space Telescope

Wide Field and Planetary Camera Instrument Handbook

Version 2.1

May 1990

Revision History

Version 1.0	October 1985; edited by Richard Griffiths
Version 2.0	May 1989; edited by Richard Griffiths
Version 2.1	May 1990; edited by Richard Griffiths

The Space Telescope Science Institute is operated by the Association of Universities for Research in Astronomy, Inc., for the National Aeronautics and Space Administration.

SCREEN IMAGE USER=*EBB SESSION=T20BRO8 4/15/92-10:14:46-AM

DISPLAY 92N17484/2

92N17484*# ISSUE 8 PAGE 1386 CATEGORY 89 RPT#: NASA-CR-189753 NAS 1.26:189753 CNT#: NAS5-26555 90/05/00 85 PAGES UNCLASSIFIED DOCUMENT

Revised

UTTL: Hubble Space Telescope: Wide field and planetary camera instrument handbook. Version 2.1

AUTH: A/GRIFFITHS, RICHARD PAT: A/ed.

CORP: Space Telescope Science Inst., Baltimore, MD.

SAP: Avail: NTIS HC/MF A05

CIO: UNITED STATES

MAJS: /*CAMERAS/*HANDBOOKS/*HUBBLE SPACE TELESCOPE/*SPECTROPHOTOMETERS/*WIDE ANGLE LENSES

MINS: / CALIBRATING/ CONSTRUCTION/ PIXELS/ POLARIMETRY

ABA: Author

ABS: An overview is presented of the development and construction of the Wide Field and Planetary Camera (WF/PC). The WF/PC is a duel two dimensional spectrophotometer with rudimentary polarimetric and transmission grating capabilities. The instrument operates from 1150 to 11000 A with a resolution of 0.1 arcsec per pixel or 0.043 arcsec per pixel. Data products and standard calibration methods are briefly summarized.

ENTER:

CONTENTS

1.0 INTRODUCTION 1
2.0 INSTRUMENT OVERVIEW 2
2.1 Brief Description of Science Objectives 2
2.2 Overall Instrument Description 2
3.0 INSTRUMENT DESCRIPTION 8
3.1 WF/PC Configurations, Fields of View and Resolution 8
3.2 Optical Filters and Spectral Elements 8
3.3 Neutral Density or 'Baum' Spot 13
3.4 Shutter 13
3.5 CCD Orientation and Read-out 47
4.0 INSTRUMENT PERFORMANCE 52
4.1 Quantum Efficiency 52
4.2 Quantum Efficiency Stability 58
4.3 Linearity 59
4.4 CCD Read-out Noise, Full Well and 'Gain' 60
4.5 Point-spread Function 60
4.6 Cosmic Ray Background 60
4.7 Instrument Anomalies 63
5.0 ESTIMATION OF EXPOSURE TIME AND SIGNAL-TO-NOISE RATIO 67
5.1 Point Sources 67
5.2 Extended Sources 77
6.0 CALIBRATION AND DATA REDUCTION 80
6.1 Calibration Frames 80
6.2 Data Reduction and Data Products 81

1.0 INTRODUCTION

The development and construction of the Wide Field and Planetary Camera (WF/PC) was led by Prof. J. A. Westphal, Principal Investigator, of the California Institute of Technology. The Investigation Definition Team (IDT) also included J. E. Gunn (deputy P. I.), W. A. Baum, A. D. Code, D. G. Currie, G. E. Danielson, T. F. Kelsall, J. A. Kristian, C. R. Lynds, P. K. Seidelmann, and B. A. Smith. The instrument was built at the Jet Propulsion Laboratory, Caltech.

The material contained in this *Handbook* was largely provided by the WF/PC IDT members or by the engineering team at JPL.

WF/PC is a dual two-dimensional spectrophotometer with rudimentary polarimetric and transmission-grating capabilities. The instrument operates from 1150Å to 11,000Å with a resolution of 0.1 arcsec per pixel (wide field camera, f/12.9) or 0.043 arcsec per pixel (planetary camera, f/30).

A brief description of the instrument is contained in section 2, with a more detailed description of relevant components and parameters in section 3. The details necessary to formulate an observing proposal are described in section 5, using the information supplied in Sections 3 and 4.

Data products and standard calibration methods are briefly summarized in section 6.

The information contained in this document summarizes the performance of the WF/PC as known in March 1990.

2.0 INSTRUMENT OVERVIEW

2.1 BRIEF DESCRIPTION OF SCIENCE OBJECTIVES

The scientific objectives of the wide field and planetary camera are to provide photometrically and geometrically accurate, multiband images of astronomical objects over a relatively wide field-of-view (FOV), with high angular resolution across a broad range of wavelengths.

2.2 OVERALL INSTRUMENT DESCRIPTION

The wide-field and planetary camera, illustrated in Figure 2.2.1, occupies the single radial bay allocated to a scientific instrument. Its field of view is centered on the optical axis of the telescope and it therefore receives the highest quality images. The WF/PC operates in two basic configurations. The wide-field camera at f/12.9 provides a field-of-view of 2.57 $\times$ 2.57 arc min with each 15 μm detector pixel subtending 0.10 arc sec on the sky. In the planetary camera at f/30, the field-of-view is 66 $\times$ 66 arc sec, and a pixel subtends 0.043 arc sec. In wide-field use the camera undersamples the point-spread function of the optical telescope assembly (OTA) by a factor of 2 in the visible to provide an adequate field-of-view for studying galaxies, clusters of galaxies, etc. The planetary camera has a resolution in the visible nearly at the OTA limit, a field-of-view that is more than adequate to provide full-disk images of the planets, and a focal ratio which permits the short exposure times required for some observations. It should be emphasized that the planetary camera has numerous extra-solar applications, including studies of galactic and extra-galactic objects in which high angular resolution and excellent red-light sensitivities are needed. The WF/PC can be used as the prime instrument, as a target acquisition 'finder,' and also for parallel observations.

Figure 2.2.2 shows the optical arrangement (not to scale) of the WF/PC in one of its two configurations. The central portion of the OTA f/24 beam is intercepted by the pick-off mirror that is attached to the WF/PC and is diverted through an entry port into the instrument. For contamination control, the entry port is sealed with an afocal MgF_2 window. The beam then passes through an opened shutter and is reduced in spectral content by a filter or is dispersed by an objective grating or is analyzed for linear polarization by a polarizing filter. A total of 48 such elements are contained in a filter wheel assembly. The beam then falls on a shallow-angle, four-faceted pyramid located at the OTA focus, each face of the pyramid being a concave spherical surface. The pyramid divides the OTA image of the sky into four parts: after leaving the pyramid, each quarter of the full field-of-view is relayed by an optical flat to a Ritchey-Chrétien repeater that forms a second field image on a charge-coupled device (CCD) of 800 $\times$ 800 pixels. Each detector is housed in a cell that is sealed by a MgF_2 window. This window is figured to serve as a field flattener. At the edge of the field-of-view (i.e., in the worst case) the computed modulation transfer function (MTF) of this optical system for the wide-field mode, combined with that of a diffraction-limited OTA at visible wavelengths, is 44% in the radial direction and 32% in the tangential direction at the 33 cycles mm^{-1} sampling frequency of the CCD detector.

After a selected integration time ($\geq$ 0.11 sec), the camera shutter is closed, and the full 1600 $\times$ 1600-pixel field-format may be recovered by reading out, assembling, and analyzing the electrical outputs from the four CCDs fed by the pyramid. Alternatively, any combination

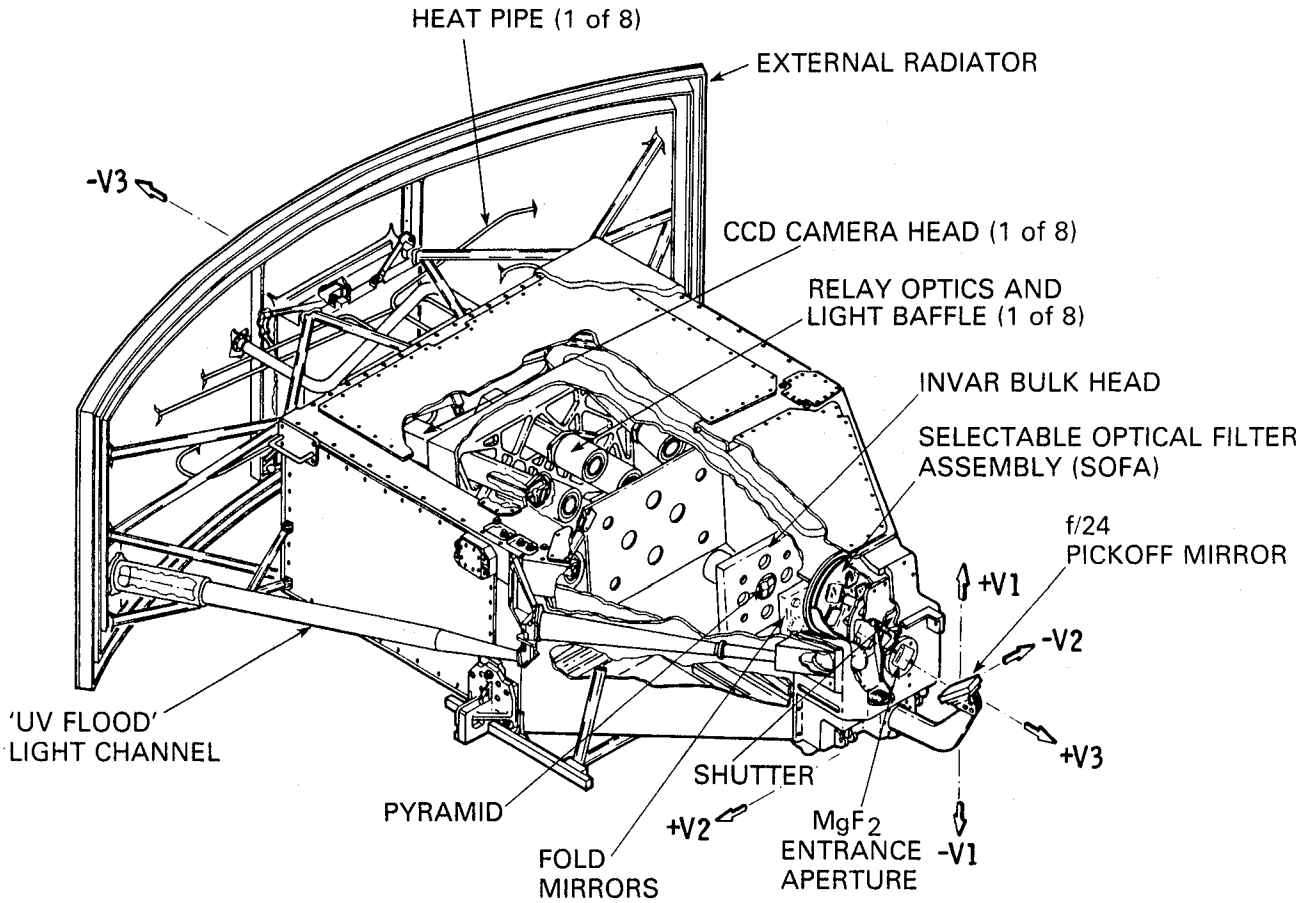

Figure 2.2.1 Wide Field/Planetary Camera Concept Illustration

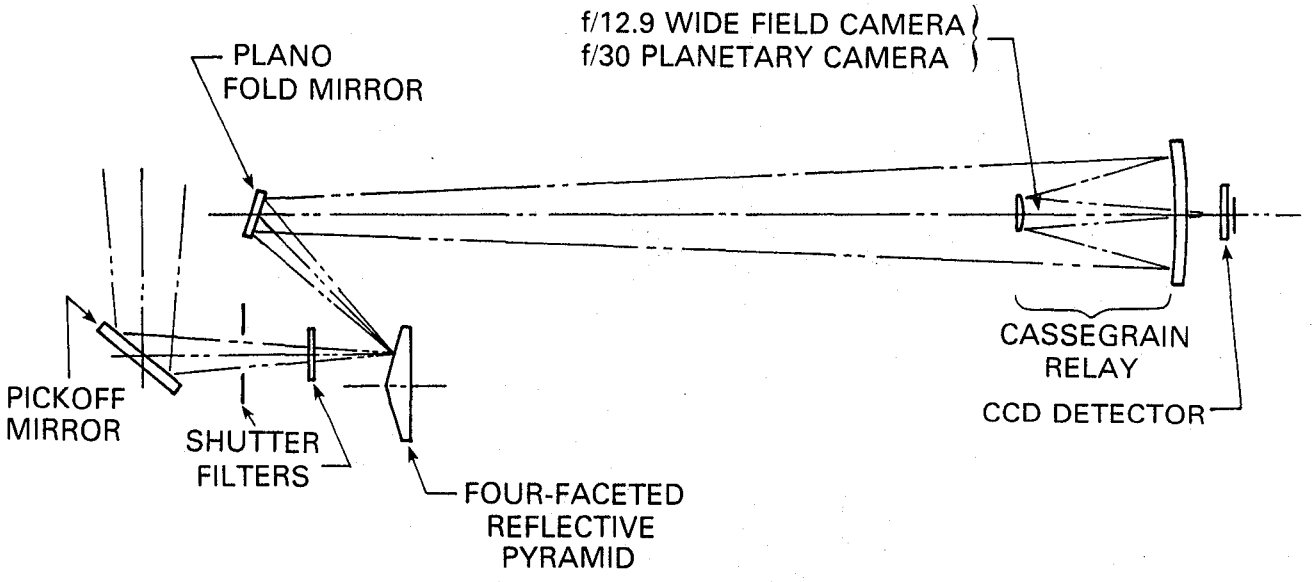

Figure 2.2.2 WF/PC Optical Configuration

of 1, 2 or 3 CCDs may be read out in numerical order. In each configuration (WF or PC) the CCDs are physically oriented and clocked such that the pixel readout direction is rotated approximately 90° in succession (see figure 3.5.1). The (1,1) pixel of each CCD array is thereby located near the apex of the pyramid. As a registration aid in assembling the four frames into a single picture, a light can be turned on at the pyramid to form a series of eleven fixed artificial "stars" (known as Kelsall spots or 'K'-spots) along the boundaries of each of the mosaic quadrants. This calibration is done in a separate exposure, because light also shines through the neutral-density or 'Baum' spot, causing blooming and residual image.

In total, the WF/PC contains eight relay mirror-repeater-CCD trains, four for the wide-field camera and four for the planetary camera. To place the desired camera into operation, the pyramid is commanded to rotate into one of two fixed orientations, separated by 45°. The pyramid can also be moved along the WF/PC optical axis to provide an optimum focus, e.g., to compensate for OTA shrinkage due to outgassing.

Each CCD is a thinned, backside-illuminated, silicon sensor, fabricated by Texas Instruments and clocked with 3 phases. A CCD, mounted on its header, is hermetically packaged in a ceramic-tube body that is filled with 0.1 atmosphere absolute of argon and sealed with a MgF_2 field flattener. This complete cell is connected with compliant silver straps to the cold junction of a thermoelectric cooler (TEC). The hot junction of the TEC is connected to the radial bay external radiator by an ammonia heat pipe. This sensor-head assembly is shown in Figure 2.2.3. During operation, each TEC cools its sensor package to a selected temperature of -92, -97, -102, -107, -111, or -115. Thereby suppressing dark current in the CCD to a level ($\leq$0.003 electrons pixel^{-1} sec^{-1}) that does not inhibit long integration times. A readout noise of $\sim$ 13 rms electrons pixel^{-1} is characteristic of these CCDs with their associated signal chains.

The WF/PC provides a useful sensitivity from 115 nm to 1100 nm in the same detector. Specifically, the full throughput detective quantum efficiency of the instrument (exclusive of filters) is shown in figure 4.1. The visible and red sensitivity of the WF/PC is a property of the thickness of the silicon from which the CCDs are fabricated ($\sim 8\mu$m). To achieve good ultraviolet response each CCD is coated with a thin ($\simeq$160 nm) film of coronene, an organic phosphor. Coronene converts photons with wavelengths $\lesssim$ 380 nm into visible photons with wavelengths peaked near 520 nm. The CCD detects these visible photons with good sensitivity. Longward of 380 nm, the coronene becomes transparent and acts to some degree as an antireflection coating. Thus, the full wavelength response is determined by the MgF_2 cutoff on the short-wavelength end, and the silicon band-gap in the infra-red at 1.1 eV (= 1.1 μm).

With such CCD sensors, images may be obtained in any spectral subregion defined by the chosen filter with high photometric quality, wide dynamic range, and excellent spatial resolution. The bright end of the dynamic range is limited by the 0.11 sec. minimum exposure time, and by the saturation level of the analog to digital converter, which has been set electronically to about 30,000 electrons per pixel. The bright end of the dynamic range can be extended by using the neutral density or "Baum" spot— see section 3.3. The faint end is limited by photon noise, instrument noise, and, for the wide-band visible and infra-red filters, the sky background. The minimum signal-to-noise ratio corresponding to a full exposed pixel will be about 200. Table 2.2.1 gives characteristic values of the expected

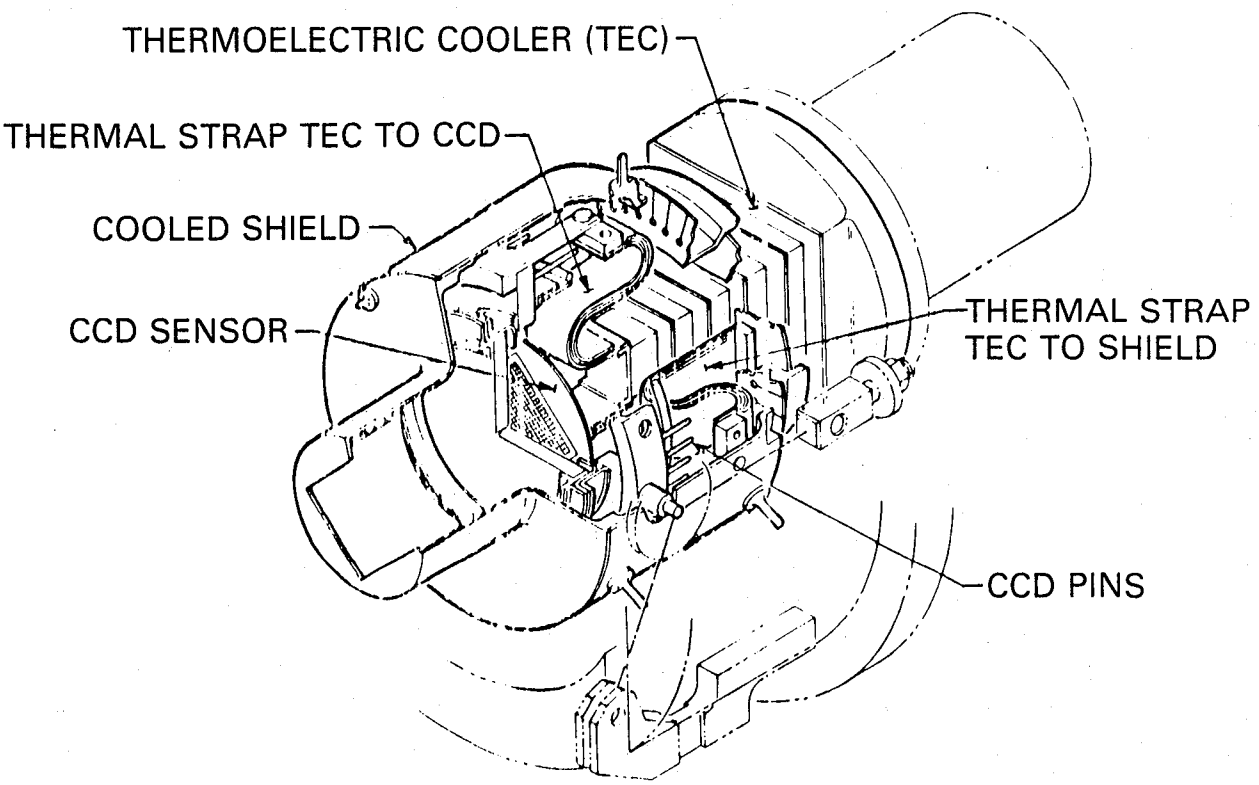

Figure 2.2.3 Cooled Sensor Assembly

dynamic range in visual magnitudes for point sources. The minimum brightness is given for a S/N ratio of 3, and the maximum corresponds to full well. The quoted values assume an effective bandwidth of 90 nm centered on 550 nm.

Note that, because the planets are not point sources they will be observable with short exposure times even though their integrated brightnesses may greatly exceed the 8.4 magnitude limit. The faint observational limit at S/N $\geq$10 in a 3000 sec exposure will be about V = 26. The ultimate limit of marginal detectability is probably V$\simeq$28 (S/N$\geq$1 in 3000 sec) for the bandwidth assumed above.

Finally, a low-reflectance spot has been placed on one of the four pyramid faces, approximately 1.23 arc secs in diameter. This neutral density or 'Baum' spot will attenuate the light from a bright source by a factor of $\sim$1000 permitting sufficiently long exposure times to bring out the fainter background object near a bright source. As an example, precise astrometric measurements of a bright object's position, relative to the background field could then be made. If repeated periodically over a sufficiently long time, such measurements may reveal the "wobbling" of the bright star's position induced by "dark" companions.

Table 2.2.1 WF/PC Dynamic Range within Single Exposure

Configuration	Exposure (sec)	Min. V Magnitude	Max. V Magnitude
Wide Field	0.11	9.3	16.6
Wide Field	3000.	20.4	27.5
Planetary	0.11	8.4	16.0
Planetary	3000.	19.5	27.0

3.0 INSTRUMENT DESCRIPTION

Figure 2.2.1 is a pictorial view of the WF/PC which has been cut away to show the various major elements of this system.

3.1 WF/PC CONFIGURATIONS, FIELDS OF VIEW AND RESOLUTION

The fields of view and angular resolutions of the wide field and planetary cameras are approximately as follows:

	Pixel and CCD Format	F.O.V.	Pixel Resolution milli arc sec (mas)	f/ratio
Wide Field Camera	800x800 x 4CCDs	$(2.6 \text{ arc min})^2$ mosaic	$(100 \text{ mas})^2$	13
Planetary Camera	800x800 x 4CCDs	$(66 \text{ arc sec})^2$ mosaic	$(43 \text{ mas})^2$	30

3.2 OPTICAL FILTERS AND SPECTRAL ELEMENTS

The optical filters define the spectral bandpass of light which is allowed to reach the CCDs. The filters are located within the Selectable Optical Filter Assembly (SOFA) placed between the shutter and the reflecting pyramid. The SOFA contains 12 filter wheels, each of which has 4 filters and a clear 'home' position. A listing of all optical elements in the SOFA mechanism and the location of each element (by wheel number 1–12, and position A to D) is shown in Table 3.2.1.

Each of the filters is equivalent to 5mm of quartz in terms of optical path length, with compensation for wavelength such that focus is maintained on the CCDs.

The three basic categories of spectral elements are as follows:

(i) Filters (F), which may be long-pass (LP), wide (W), medium (M) or narrow (N) or Neutral density (ND). Most of these filters are either flat single substrates or sandwiches (type A in Table 3.2.1, designed to be used alone in the optical path). The Neutral Density filter (F8ND) provides 7.5 mag of attenuation, i.e. a factor of 1000, and is designed for use in combination with a filter of type A.

(ii) Polarizers (POL), with relative polarization angles of 0°, 60° and 120° (Table 3.2.1). The polarizers are constructed with curved substrates, and are to be used with any one of the filters of Type A, over the wavelength range 2800Å to 8000Å.

(iii) Gratings (G), transmission gratings mated to wedged substrates or prisms. Such combinations are often called 'grisms'. The blue and red gratings have prismatic substrates wedged in one dimension only, and therefore produce linear spectra. The UV grating is wedged along two orthogonal axes and thus produces cross-dispersed spectra.

Table 3.2.1 Filters Listed by Wavelength

NAME	TYPE	WHEEL /HOLE	MEAN WAVELENGTH, Å		EFFECTIVE WIDTH, Å	PEAK FILTER TRANS. %	WAVELENGTH AT PEAK, Å
F122M	B	2-A	2329	RED LEAK!	2824	15.5	1200
F128LP	A	11-A	1275	Ca F_2 LP		92.5	
F157W	B	4-A	1682		1019	16.3	1455
F194W	B	4-B	1961		436	17.5	1870
F230W	A	4-C	2313		366	21.5	2220
F284W	A	4-D	2814		524	23.7	2820
F336W	A	2-B	3360		411	51.7	3346
F368M	A	8-A	3687		230	37.2	3577
F375N	A	7-A	3755	3727 RS	82	37.1	3734
F413M	A	8-B	4125		248	56.3	4090
F437N	A	7-C	4366	[OIII]	22	46.3	4366
F439W	A	2-C	4352		465	60.3	4094
F469N	A	11-B	4687	HeII	27	56.8	4688
F487N	A	11-C	4869	H β	31	55.7	4867
F492M	A	8-D	4906		364	60.9	4712
F502N	A	7-B	5018	OIII	29	60.3	5016
F517N	A	11-D	5170	C_2, MgII	87	62.1	5155
F547M	A	9-A	5454		438	64.8	5418
F555W	A	9-B	5416		1205	91.5	5150
F569W	A	5-A	5598		967	90.1	5320
F588N	A	7-D	5880	HeI, NaD	43	54.6	5877
F606W	A	12-B	5844	Wide V	1553	95.4	6444
F622W	A	8-C	6140		964	96.5	6030
F631N	A	6-A	6306	[OI]	29	43.5	6310
F648M	A	9-C	6469		371	53.1	6467
F656N	A	6-B	6559	Hα	19	40.9	6559
F658N	A	5-D	6576	[NII]	20	41.2	6577
F664N	A	6-C	6637	Hα RS	131	53.9	6634
F673N	A	1-B	6723	SII	50	83	6731
F675W	A	5-B	6684		910	94.9	6753
F702W	A	6-D	6898		1493	97.1	6920
F718M	A	9-D	7160		595	55.5	7120
F725LP	A	12-C	8496	(7320) LP	1987	90.0	
F785LP	A	10-C	8922	(7850) LP	1571	95.6	
F791W	A	5-C	7906		1322	86.4	7556
F814W	A	10-A	8137		1768	93.9	8580
F850LP	A	12-A	9298	(8600) LP	1153	93.0	
F875M	A	10-B	8762		556	88.5	8747
F889N	A	12-D	8888	CH_4	51	83.5	8884
F1042M	A	10-D	10167		481	91.4	10828
F1083N	A	3-D	10831	HeI	80	59.2	10847
F8ND	B	1-A	7.5 mag Neutral Density			00.1	
POL0	B	3-A	POLARIZER 0 DEGREES				
POL60	B	3-B	POLARIZER 60 DEGREES				
POL120	B	3-C	POLARIZER 120 DEGREES				

Table 3.2.1 Filters Listed by Wavelength (Cont'd.)

NAME	TYPE	WHEEL /HOLE	MEAN WAVELENGTH, Å	EFFECTIVE WIDTH, Å	PEAK FILTER TRANS. %	WAVELENGTH AT PEAK, Å
G200		2-D	UV GRATING	1st ORDER 1600–4000Å, 2nd ORDER 1300–2000Å		
G450		1-C	BLUE GRATING	3000–6000Å		
G800		1-D	RED GRATING	6000–10000Å		

F = filter, POL = polarizer (must be used with a filter for focus), G = grating, LP = longwavelength pass, RS = red shifted N means < 3%, M = 3%–15%, W > 15% (FWHM/Effective Wavelength).

The number given in parenthesis for LP is the 50% cut-on point. The mean wavelength is similar to that defined in Schneider, Gunn and Hoessel (Ap. J. **264**, 337) – see Section 5.1. It includes the CCD QE and the transmission of OTA, WF/PC and filters. The width is the FWHM of a Gaussian filter with the same second moment and is reasonably close to the FWHM.

The 'wide open' position, i.e., no filter, results in out-of-focus imaging and will not generally be used. With the exception of the Polarizers and the Neutral Density filter, all filters are designed to be used alone - combinations will result in out-of-focus images, which will not be calibrated.

Figure 3.2.1 Shows spectral response curves, obtained by combining the spectral quantum efficiency with the passbands of various WF/PC color filters. Their peaks are normalized here to unity.

(A) Narrowband filters for isolating individual spectral lines or bands. An H-alpha filter (for z $\sim$ 0) at 656 nm and an N II filter at 658 nm have been omitted from the plot to avoid graphical crowding.

(B) Mediumband filters with FWHM $\sim$ 10% of the central wavelength. Note that F368M and F413M cover the region of falling coronene response and increasing silicon response. Their usefulness, therefore, depends on the success of UV flood and the absence of hysteresis.

(C) A photometric set including approximations to UBVRI passbands and extending that series in the ultraviolet down to Lyman-alpha. Note, however, that the WF/PC UBVRI series is not the Johnson photometric series. In particular, the CCD response in the U and B bands is a strong function of wavelength, so that differences from Johnson U and B may be large. F439W spans the region of CCD response in the critical region where silicon absorption length is changing rapidly with wavelength; its response is, therefore, improved by UV flood, and is subject to any remaining hysteresis.

(D) Wideband filters with FWHM $\sim$ 25% of the central wavelength.

(E) "Wide-V" and "Wide-I." Not shown is the pure CaF_2 filter whose response function resembles Figure 4.1.1 except for cutting off Lyman-α at the extreme left end. (Also not shown are three afocal Polaroids and three grisms.)

The wide field camera CCDs view essentially the full dimensions of any given filter. The planetary camera CCDs, however, see only the central portion of any filter. This is a consequence of that camera's narrowed field of view. This narrower field is skewed 45° with respect to the wide field when the pyramid is rotated to switch the incoming image to the planetary camera (see Figure 3.5.1).

The WF/PC is designed to permit coverage of a wide spectral range. Figure 3.2.1 summarizes the normalized transmission curves for narrow, medium and wide-band spectral filters.

Filter transmission curves are shown in Figures 3.2.3 (filters alone) and 3.2.4, folded with system reponse. A few of the curves required extrapolation to zero in the wings and removal of extraneous non-real wing spikes. Note that some (UV) filters have 'red leaks,' which are quantified in figure 4.7.3.1 for F122M, F157W, F194W, F230W and F284W. The transmission of the three polarizers (nos. POL0, POL60, and POL120) is shown in Figure 3.2.4. The polarizers are afocal and must therefore *always* be used in combination with another filter which largely defines the shape of the passband. Removal of all filters from the beam results in an out-of-focus image.

Throughput curves for the gratings (figure 3.2.5) include the blaze envelope as well as OTA, WF/PC optics and CCD response. The grating dispersions, which are optimized for the WFC, are listed in Table 3.2.2. The zero order image can be used as a wavelength fiducial with any of the gratings.

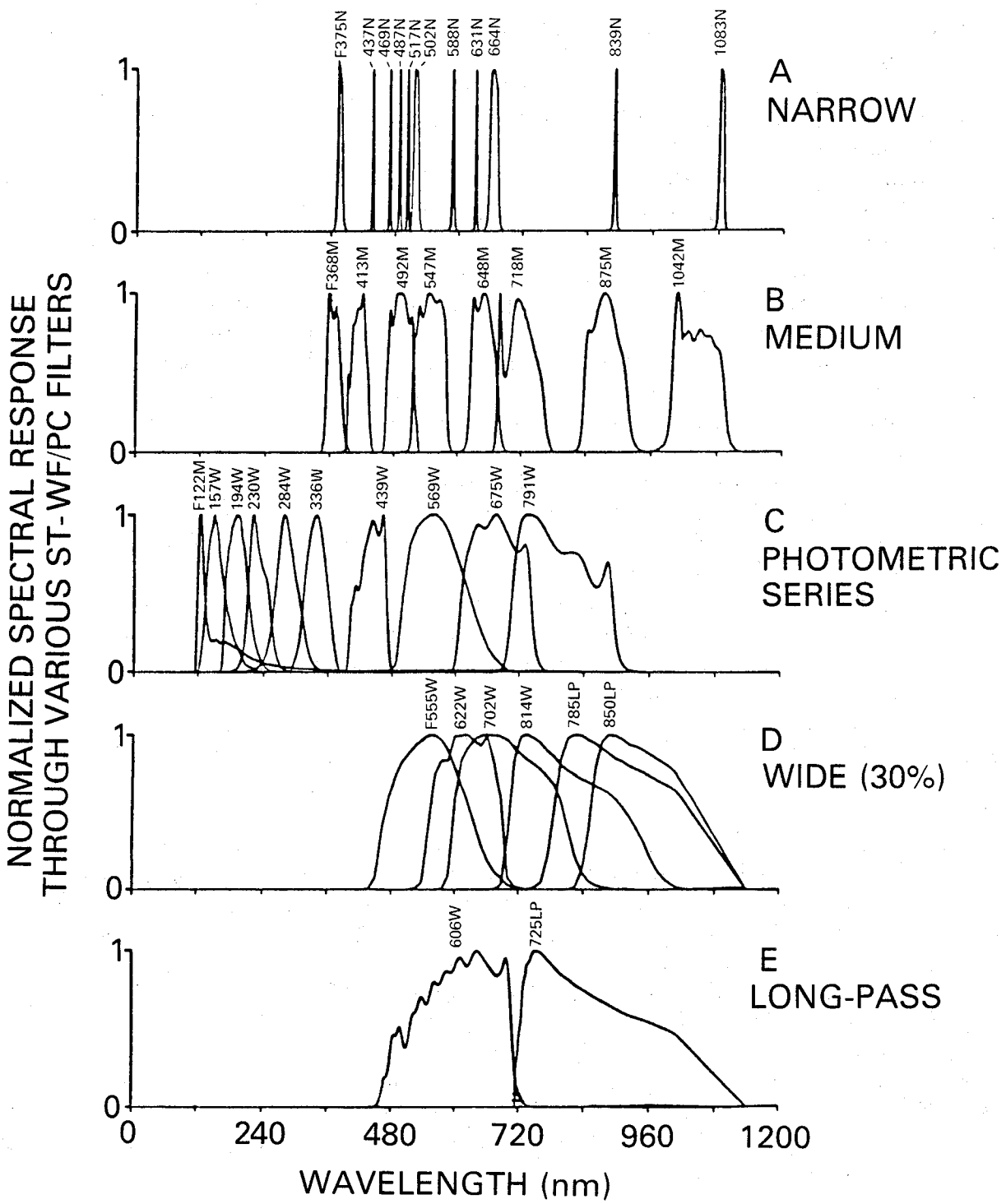

Figure 3.2.1 Normalized Spectral Response Through Various ST-WF/PC Filters

Table 3.2.2

Grating Dispersion Constants

Substrate		UV (G200) Ca F_2	Blue (G450) BG–38	Red (G800) OG–570
Blaze angle (rads)		0.01269	0.0152	0.0137
Lines mm^{-1}		25	16.2	8.22
Focal Distance mm		277	287	287
Central	1st order	2400	5000	8850
Wavelength	2nd order	1500		
Wavelength	1st order	1600–4000	3000–6000	6000–10000
range				
	2nd order	1300–2000		
Dispersion	1st order	15.0	55.5	110.8
Å/pixel (WFC)	2nd order	12.1		
Peak Efficiency	1st order	25%	65%	65%
	2nd order	15%		

Notes on second order UV grating

If d is the groove spacing, N the order, and n the index of refraction of the CaF_2 substrate, the equation for the position of the image at λ for an axial star, measured along the direction of dispersion and at right angles to the dispersion, respectively, is given by

$$x_{11} = D\theta_{11} = D\Big(\frac{N\lambda}{d} - (n-1)\gamma\Big)$$
$$x_{\perp} = D\theta_{\perp} = D(n-1)\zeta$$

where D is the distance between the grating and the focal plane = 277 mm
γ is the wedge angle in the dispersion direction = $0^o.727$
$\zeta = 0^o.47$ is the wedge angle across the dispersion
d = 0.04 mm.
and n is the refractive index

The spectra will look like this:

$$P_{11} = \frac{D\theta_{11}}{P} = .025\lambda N - 125(n-1)$$

$$P_{\perp} = \frac{D\theta_{\perp}}{P} = 80(n-1)$$

where p_{11} and $p_{\perp}$ are the displacements *in pixels*, and P is the WFC pixel size projected back to the OTA focus on the WF/PC pyramid (28μm). The template for the spectra is illustrated in the following figure 3.2.2.

Figure 3.2.2
Template for dispersed spectra using the UV grating with the WFC

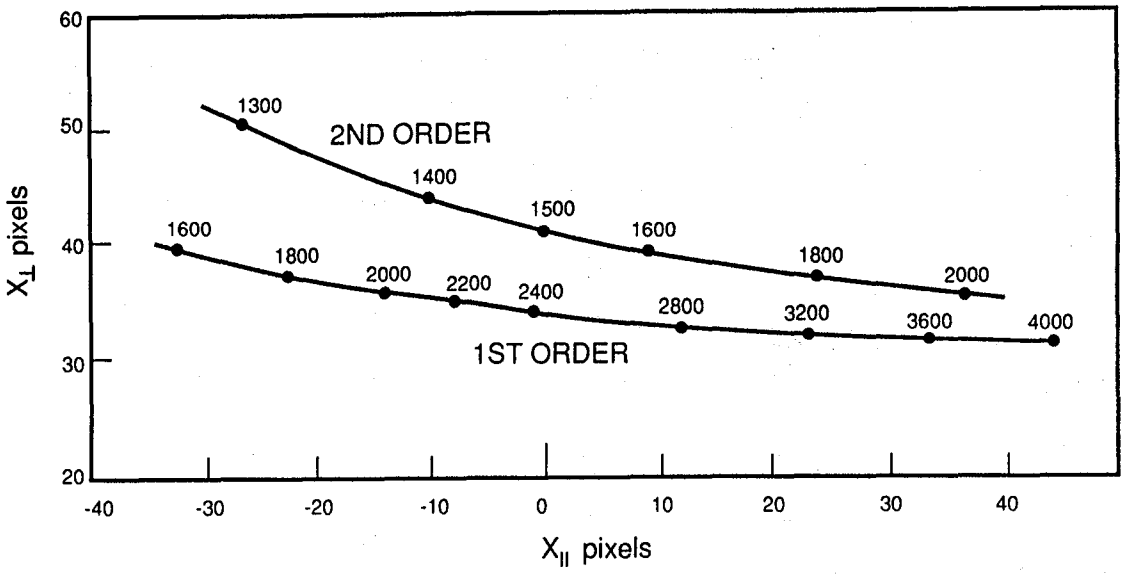

3.3 NEUTRAL DENSITY OR 'BAUM' SPOT

One facet of the pyramid has a low-reflectance spot approximately 1.23 arc sec in diameter with a reflectance approximately 0.1 percent of the other portions of the optical surface over the wavelength range 5000 to 7000Å. This low reflectance spot allows for the observation of a faint image in the presence of a bright point source, and extends the useful dynamic range of one CCD in each of the wide field and planetary cameras. It appears near the center (x=416, y=417) of PC CCD 8 and at x=195, y=197 in WF CCD 4. The measured reflectance vs. wavelength is shown in Fig. 3.3.1.

3.4 SHUTTER

The shutter is a two-blade mechanism used to control the duration of the exposure. A listing of the possible exposure times is contained in Table 3.4.1.

For the shortest times, it is necessary to determine the actual exposure time by measuring the time of flight of the shutter blades. The necessary information is contained in the WF/PC engineering data stream: encoder disks, attached to the shutter blade arms, are timed by means of a photo-transistor. The accuracy of shutter timing is $\pm$ 5 msec. (average minus minimum or maximum).

For short-exposure observations, it is not generally possible to repeat exposures on timescales less than 3 minutes (see section 4.7.4).

Figure 3.2.3
The next 10 pages show transmission curves for the WF/PC filters

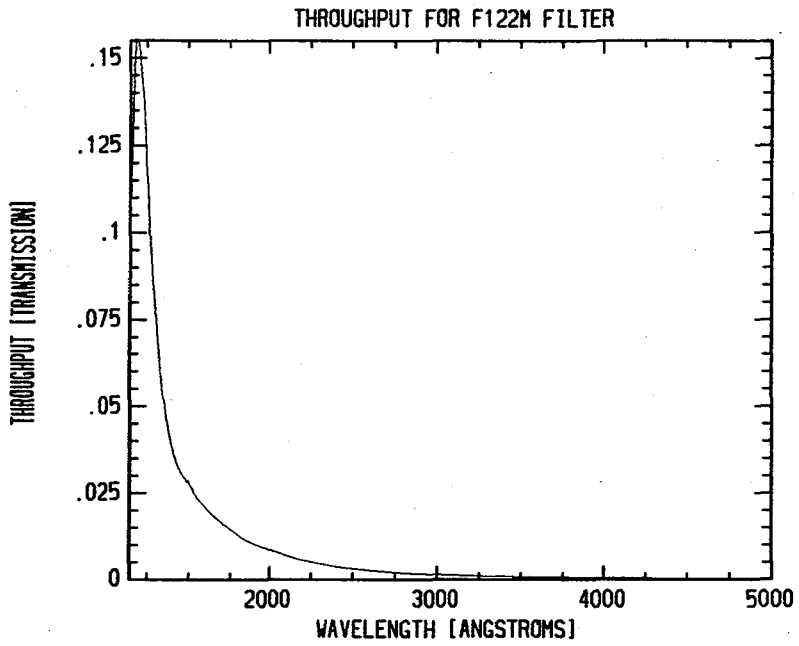
THROUGHPUT FOR F122M FILTER
THROUGHPUT [TRANSMISSION]
.15
.125
.1
.075
.05
.025
0
2000
3000
4000
5000
WAVELENGTH [ANGSTROMS]

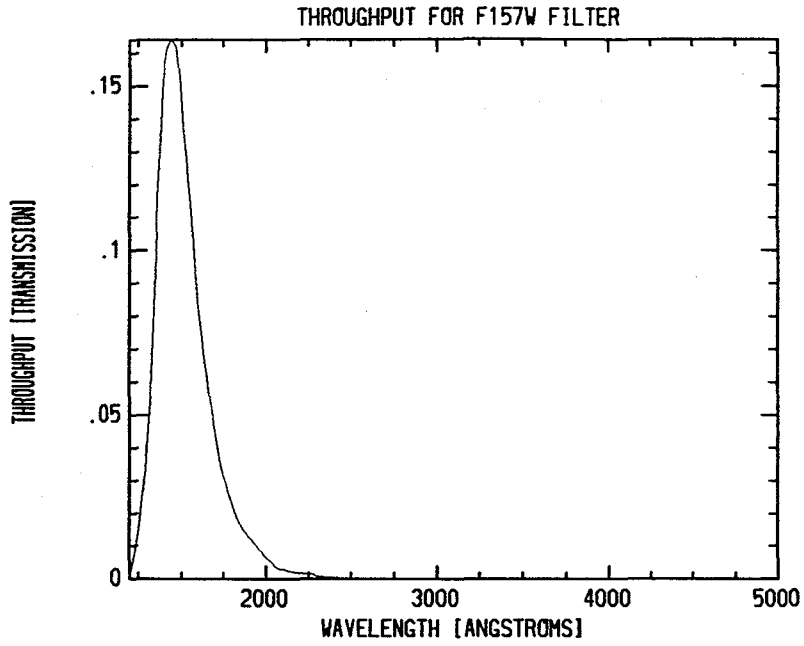
THROUGHPUT FOR F157W FILTER
THROUGHPUT [TRANSMISSION]
.15
.1
.05
0
2000
3000
4000
5000
WAVELENGTH [ANGSTROMS]

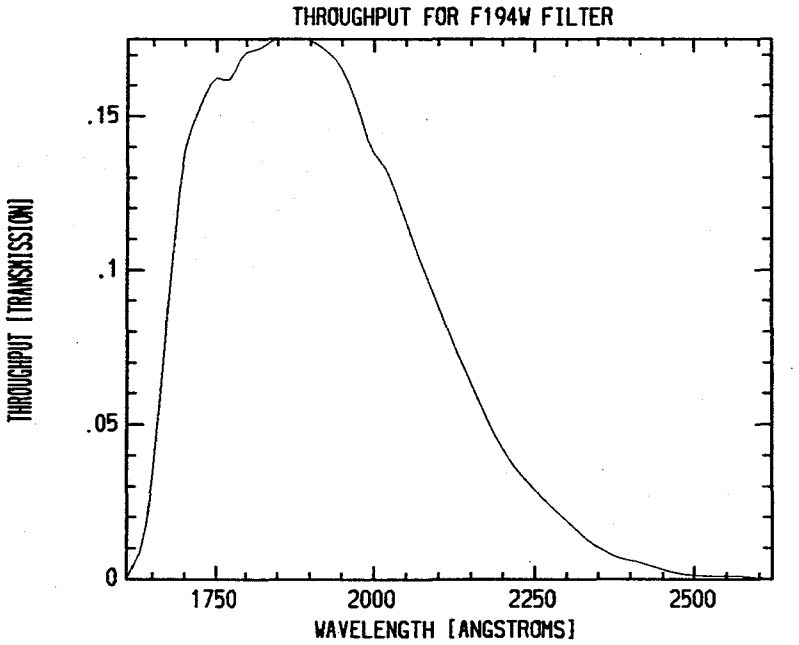
THROUGHPUT FOR F194W FILTER
THROUGHPUT [TRANSMISSION]
.15
.1
.05
0
1750
2000
2250
2500
WAVELENGTH [ANGSTROMS]

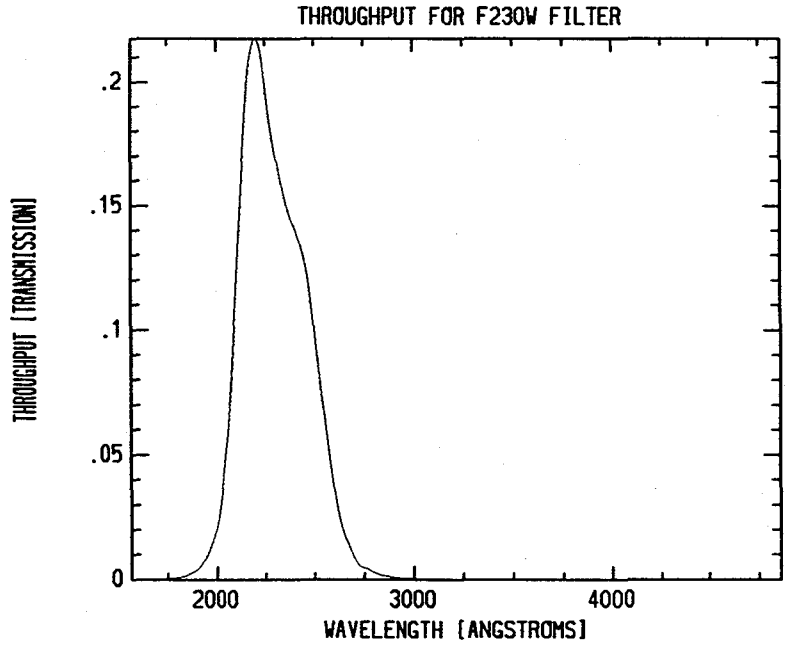
THROUGHPUT FOR F230W FILTER
THROUGHPUT [TRANSMISSION]
.2
.15
.1
.05
0
2000
3000
4000
WAVELENGTH [ANGSTROMS]

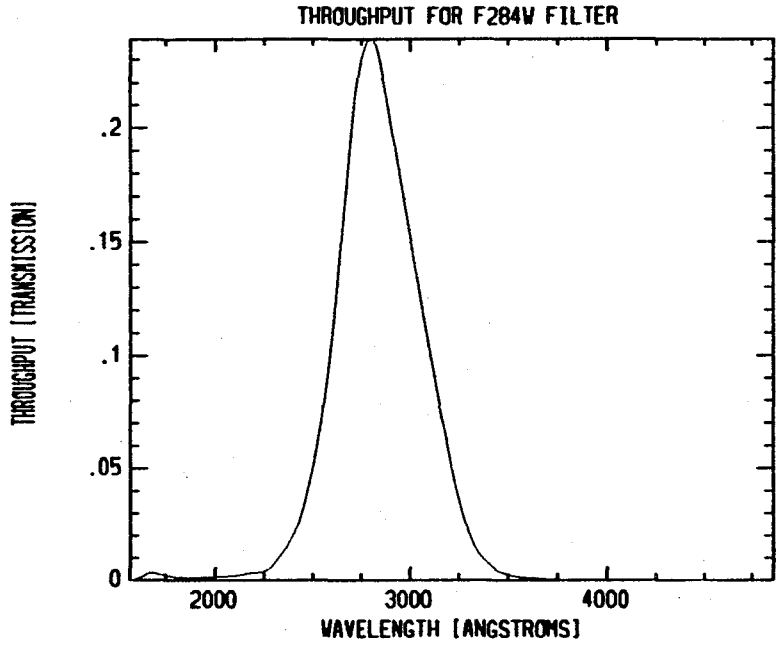
THROUGHPUT FOR F284W FILTER
THROUGHPUT [TRANSMISSION]
.2
.15
.1
.05
0
2000
3000
4000
WAVELENGTH [ANGSTROMS]

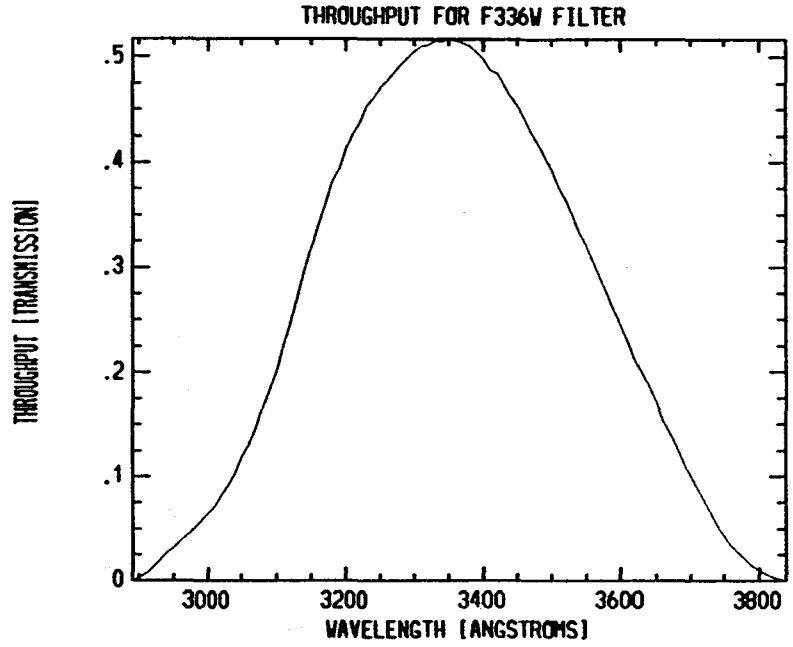
THROUGHPUT FOR F336W FILTER
THROUGHPUT [TRANSMISSION]
.5
.4
.3
.2
.1
0
3000
3200
3400
3600
3800
WAVELENGTH [ANGSTROMS]

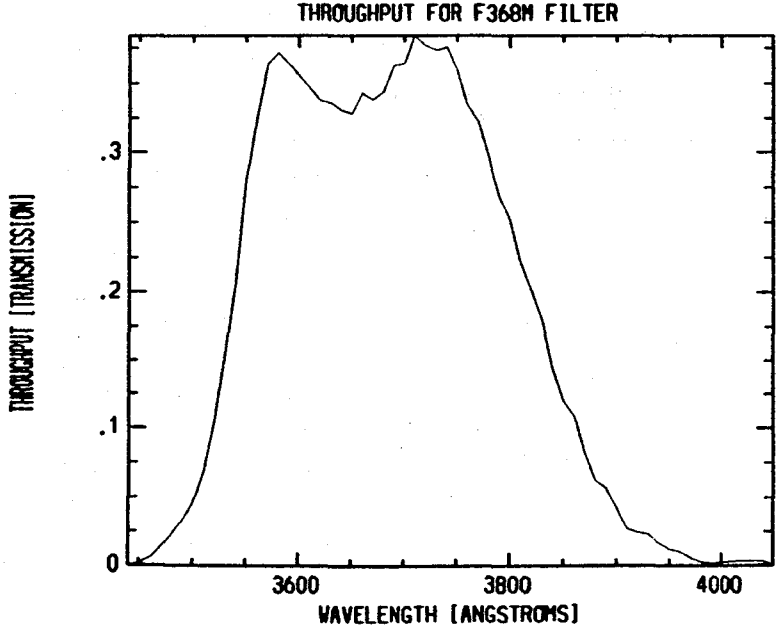
THROUGHPUT FOR F368M FILTER
THROUGHPUT [TRANSMISSION]
.3
.2
.1
0
3600
3800
4000
WAVELENGTH [ANGSTROMS]

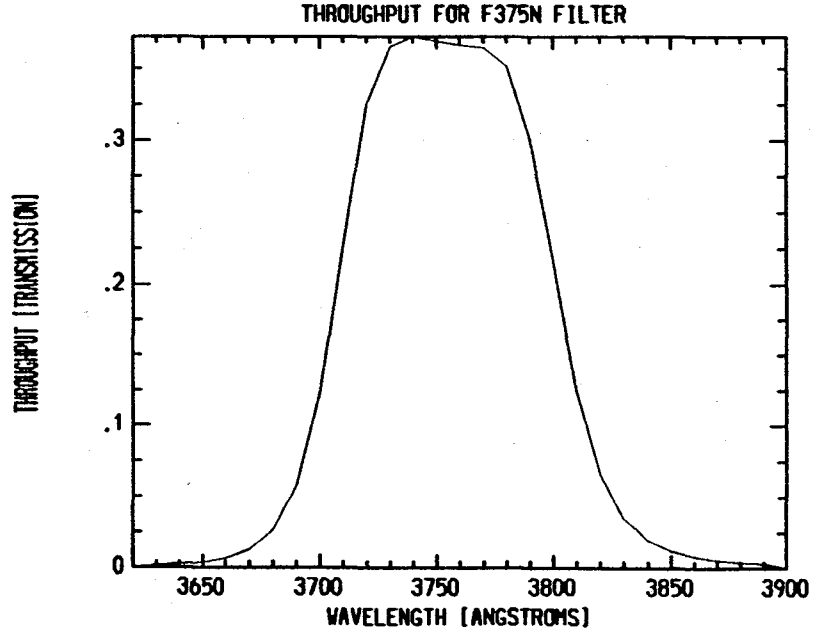
THROUGHPUT FOR F375N FILTER
THROUGHPUT [TRANSMISSION]
.3
.2
.1
0
3650
3700
3750
3800
3850
3900
WAVELENGTH [ANGSTROMS]

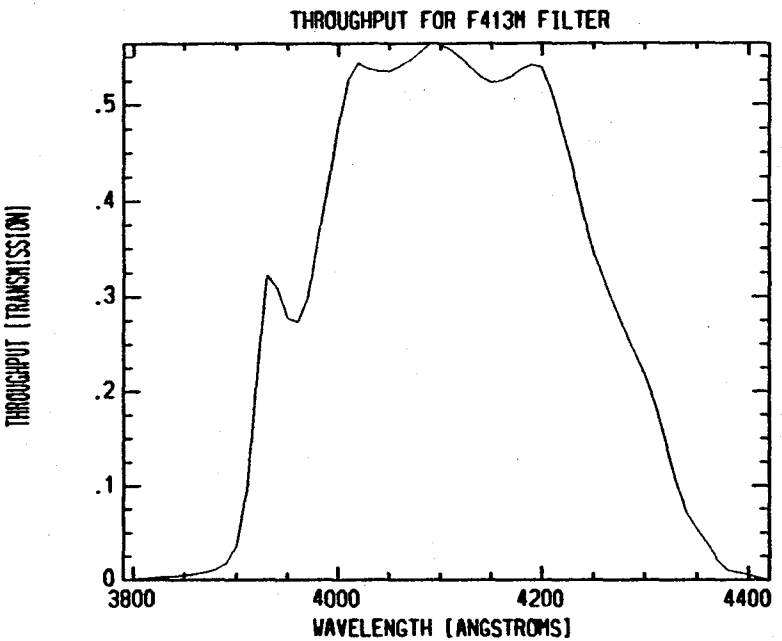
THROUGHPUT FOR F413M FILTER
THROUGHPUT [TRANSMISSION]
0
.1
.2
.3
.4
.5
3800
4000
4200
4400
WAVELENGTH [ANGSTROMS]

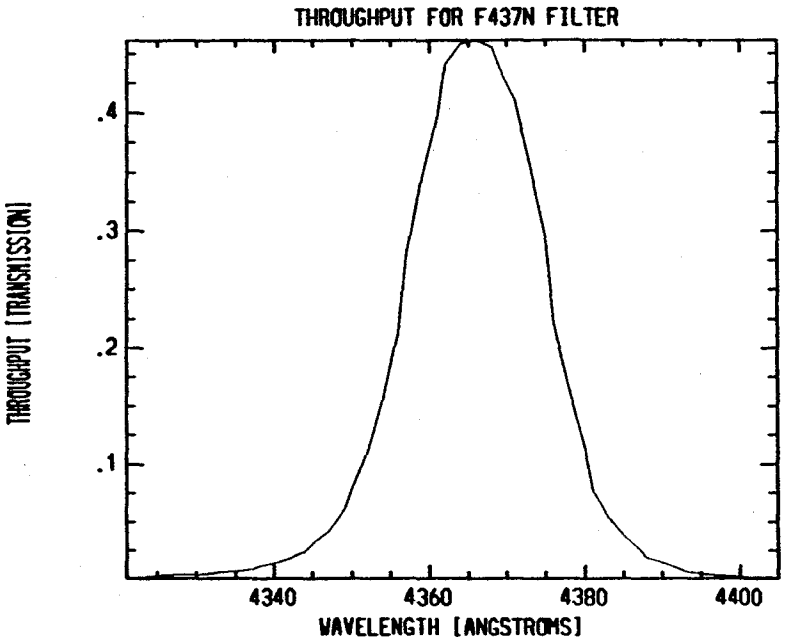
THROUGHPUT FOR F437N FILTER
THROUGHPUT [TRANSMISSION]
.1
.2
.3
.4
4340
4360
4380
4400
WAVELENGTH [ANGSTROMS]

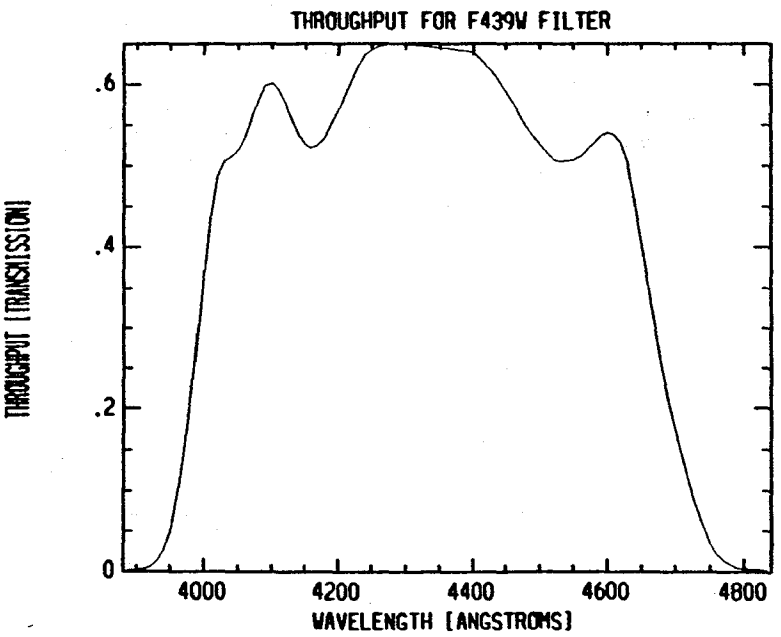
THROUGHPUT FOR F439W FILTER
THROUGHPUT [TRANSMISSION]
0
.2
.4
.6
4000
4200
4400
4600
4800
WAVELENGTH [ANGSTROMS]

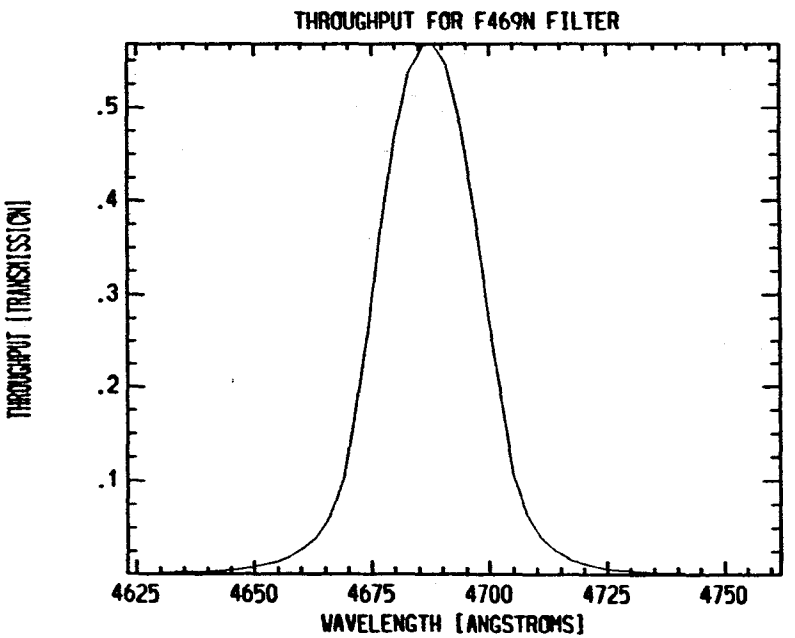
THROUGHPUT FOR F469N FILTER
THROUGHPUT [TRANSMISSION]
.1
.2
.3
.4
.5
4625
4650
4675
4700
4725
4750
WAVELENGTH [ANGSTROMS]

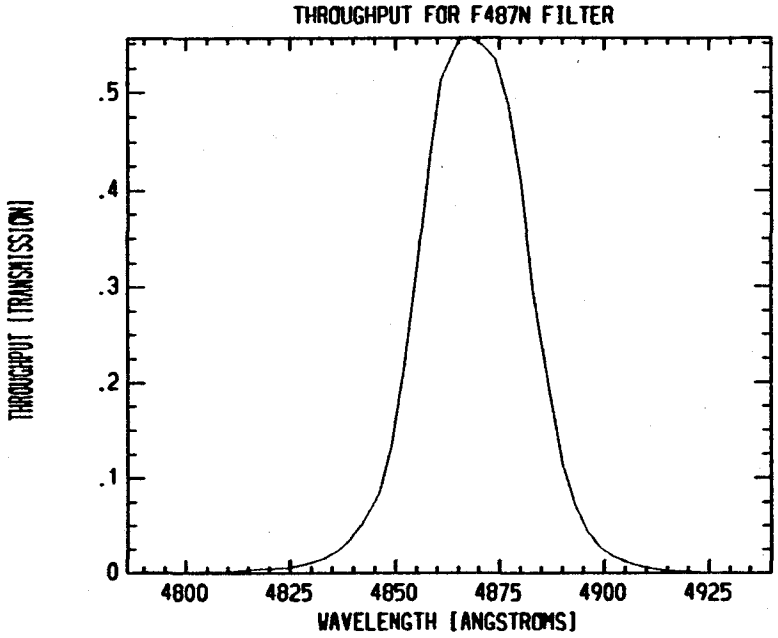
THROUGHPUT FOR F487N FILTER
THROUGHPUT [TRANSMISSION]
0
.1
.2
.3
.4
.5
4800
4825
4850
4875
4900
4925
WAVELENGTH [ANGSTROMS]

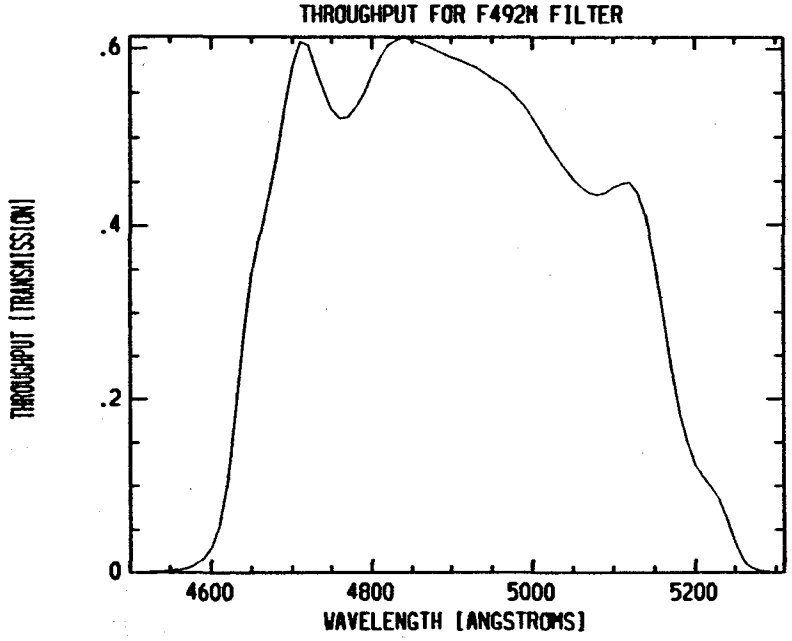
THROUGHPUT FOR F492N FILTER
THROUGHPUT [TRANSMISSION]
0
.2
.4
.6
4600
4800
5000
5200
WAVELENGTH [ANGSTROMS]

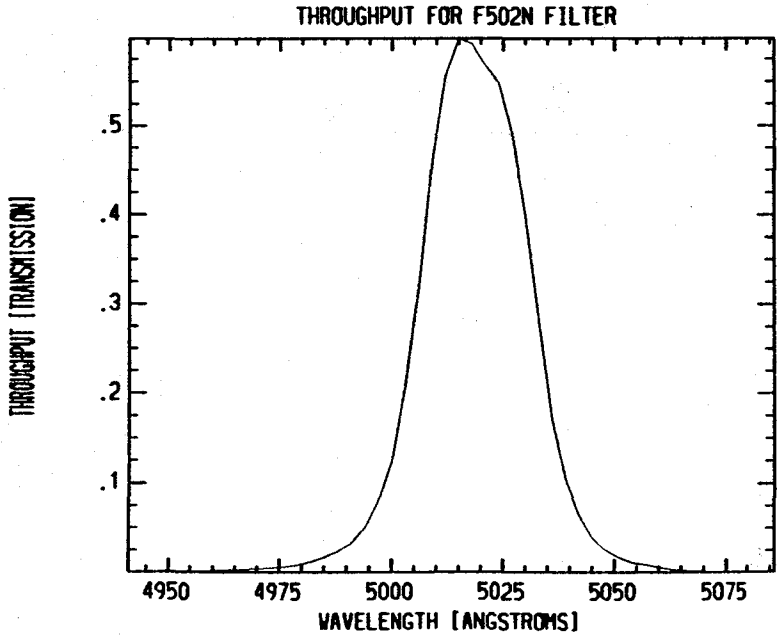
THROUGHPUT FOR F502N FILTER
THROUGHPUT [TRANSMISSION]
.1
.2
.3
.4
.5
4950
4975
5000
5025
5050
5075
WAVELENGTH [ANGSTROMS]

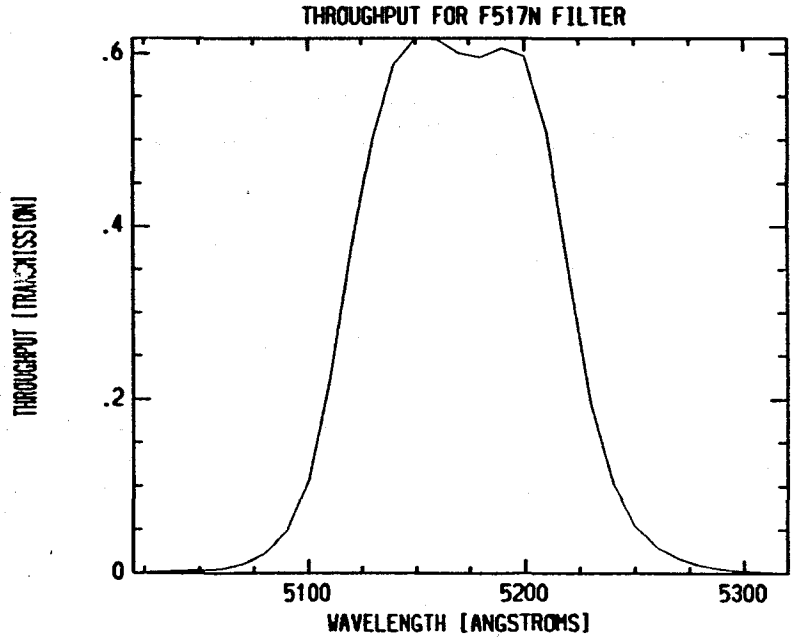
THROUGHPUT FOR F517N FILTER
THROUGHPUT [TRANSMISSION]
0
.2
.4
.6
5100
5200
5300
WAVELENGTH [ANGSTROMS]

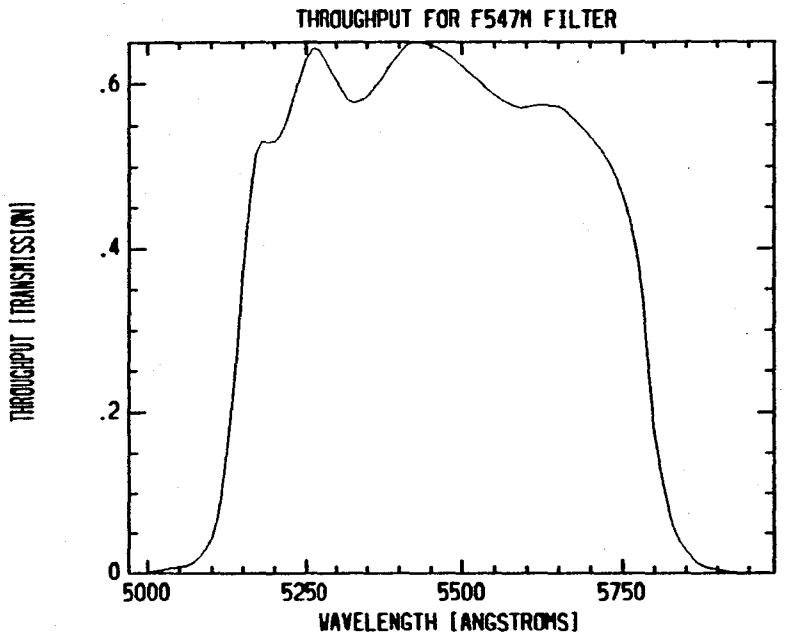
THROUGHPUT FOR F547M FILTER
THROUGHPUT [TRANSMISSION]
.6
.4
.2
0
5000
5250
5500
5750
WAVELENGTH [ANGSTROMS]

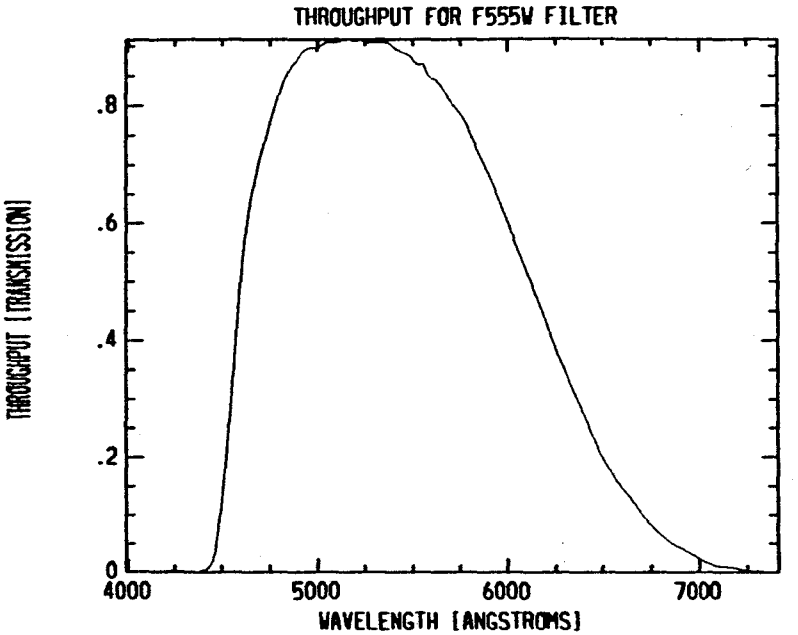
THROUGHPUT FOR F555W FILTER
THROUGHPUT [TRANSMISSION]
.8
.6
.4
.2
0
4000
5000
6000
7000
WAVELENGTH [ANGSTROMS]

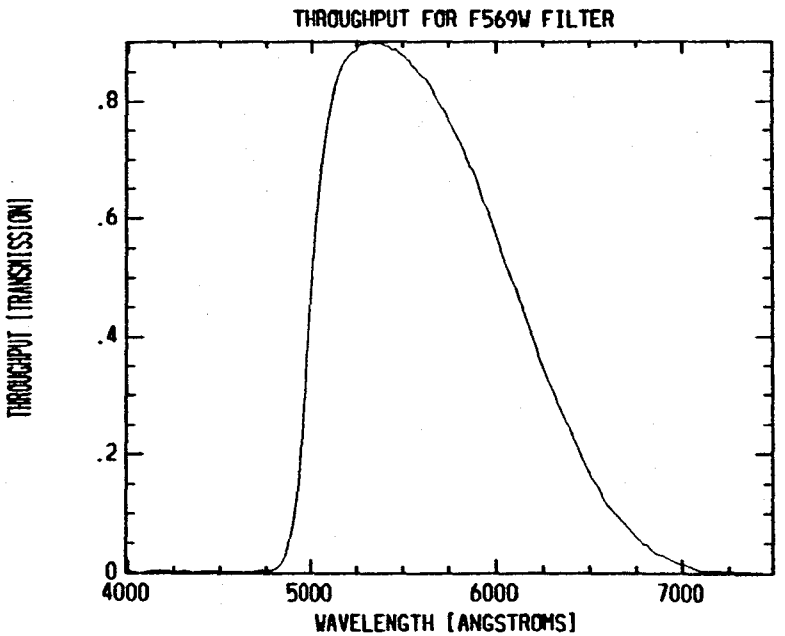
THROUGHPUT FOR F569W FILTER
THROUGHPUT [TRANSMISSION]
.8
.6
.4
.2
0
4000
5000
6000
7000
WAVELENGTH [ANGSTROMS]

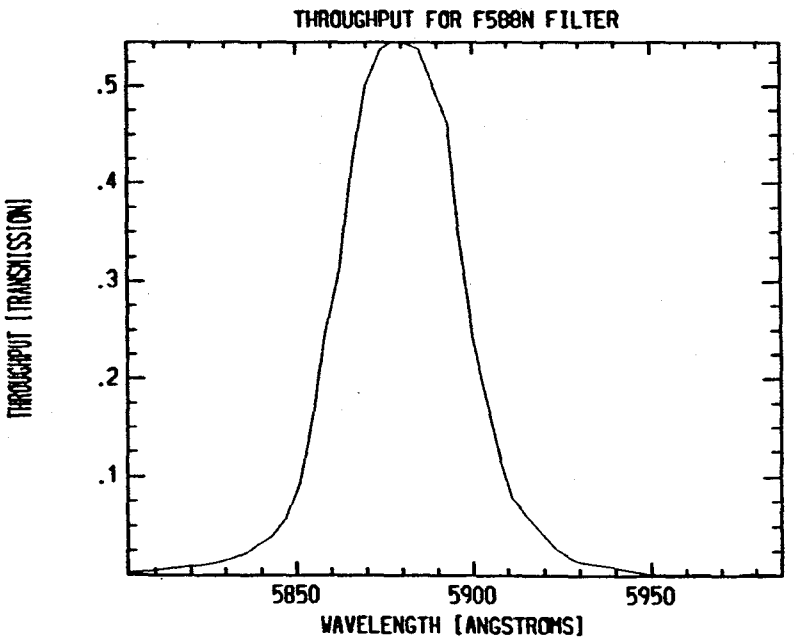
THROUGHPUT FOR F588N FILTER
THROUGHPUT [TRANSMISSION]
.5
.4
.3
.2
.1
5850
5900
5950
WAVELENGTH [ANGSTROMS]

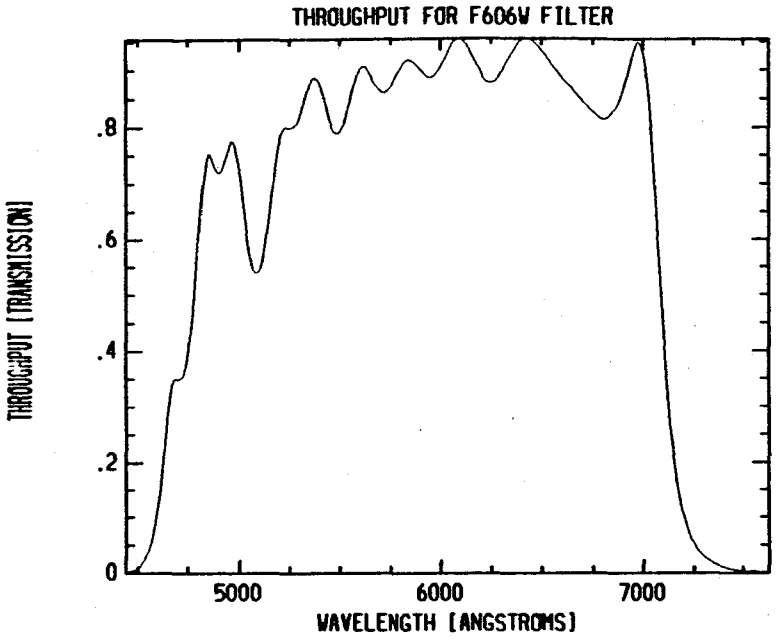
THROUGHPUT FOR F606W FILTER
THROUGHPUT [TRANSMISSION]
0
.2
.4
.6
.8
5000
6000
7000
WAVELENGTH [ANGSTROMS]

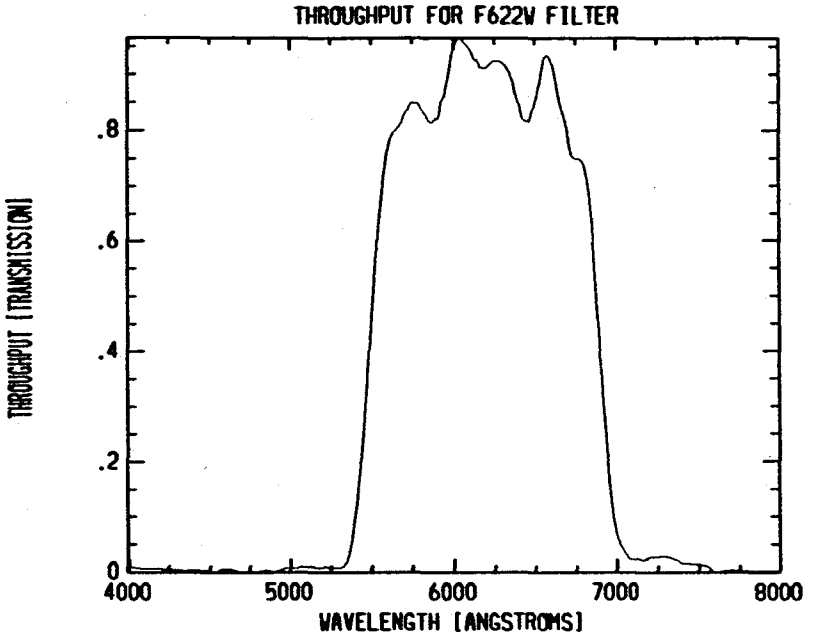
THROUGHPUT FOR F622W FILTER
THROUGHPUT [TRANSMISSION]
0
.2
.4
.6
.8
4000
5000
6000
7000
8000
WAVELENGTH [ANGSTROMS]

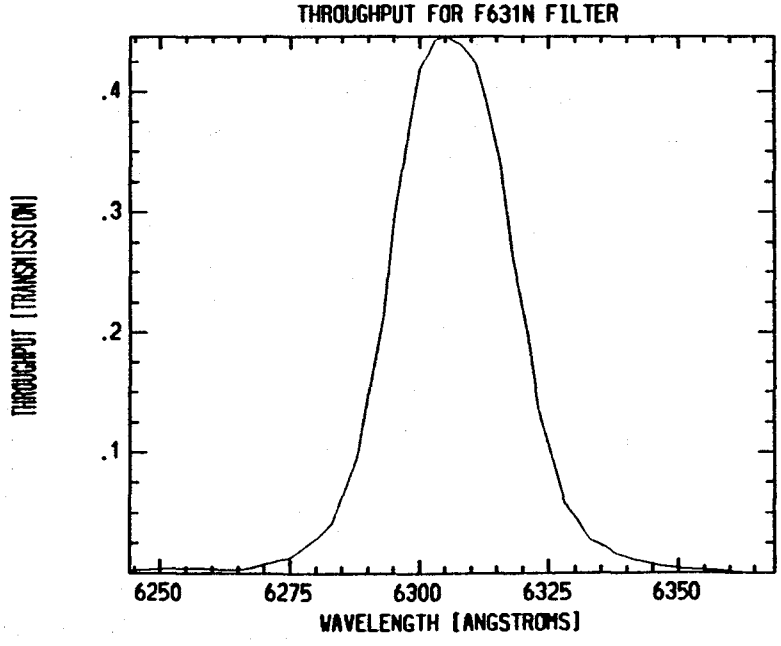
THROUGHPUT FOR F631N FILTER
THROUGHPUT [TRANSMISSION]
.1
.2
.3
.4
6250
6275
6300
6325
6350
WAVELENGTH [ANGSTROMS]

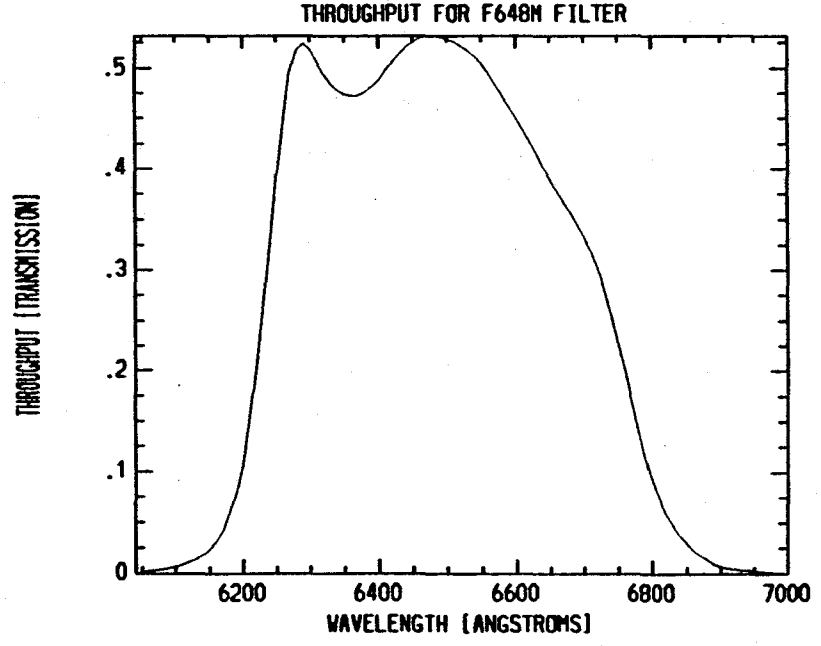
THROUGHPUT FOR F648M FILTER
THROUGHPUT [TRANSMISSION]
0
.1
.2
.3
.4
.5
6200
6400
6600
6800
7000
WAVELENGTH [ANGSTROMS]

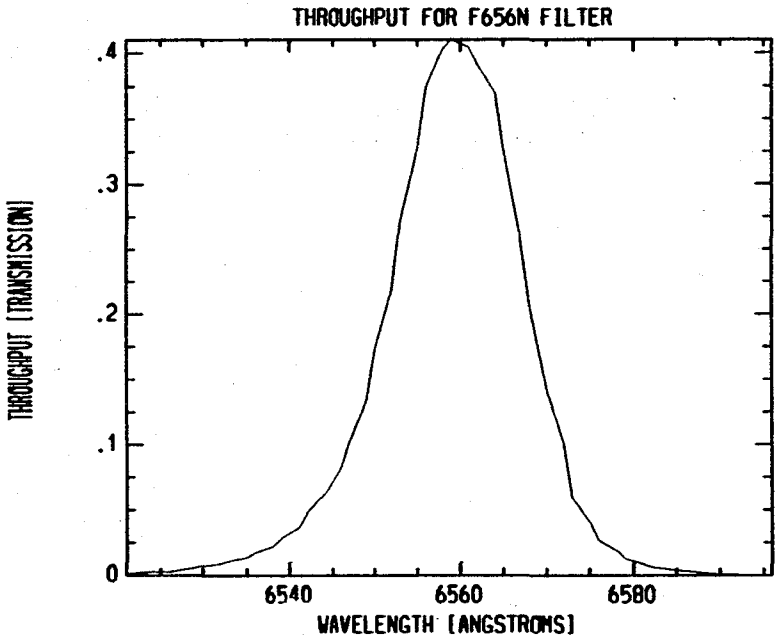
THROUGHPUT FOR F656N FILTER
THROUGHPUT [TRANSMISSION]
.4
.3
.2
.1
0
6540
6560
6580
WAVELENGTH [ANGSTROMS]

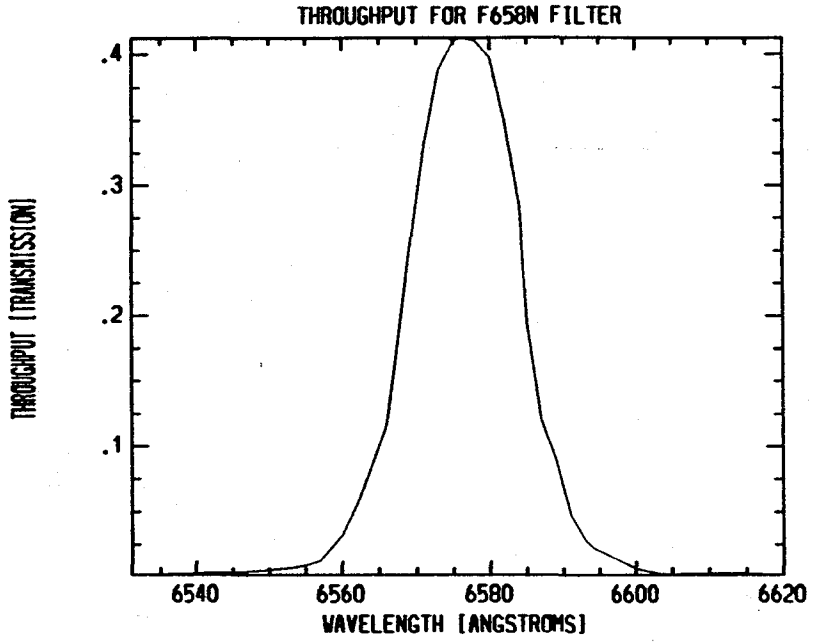
THROUGHPUT FOR F658N FILTER
THROUGHPUT [TRANSMISSION]
.4
.3
.2
.1
6540
6560
6580
6600
6620
WAVELENGTH [ANGSTROMS]

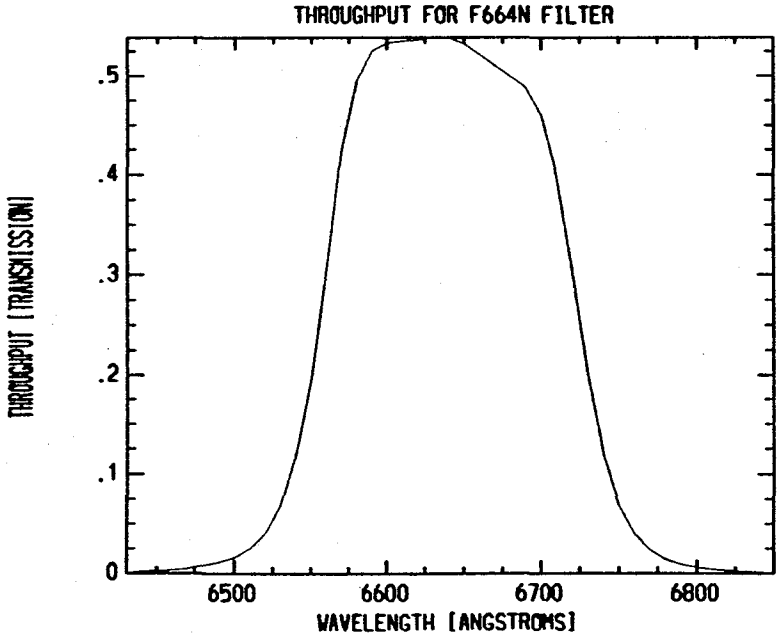
THROUGHPUT FOR F664N FILTER
THROUGHPUT [TRANSMISSION]
.5
.4
.3
.2
.1
0
6500
6600
6700
6800
WAVELENGTH [ANGSTROMS]

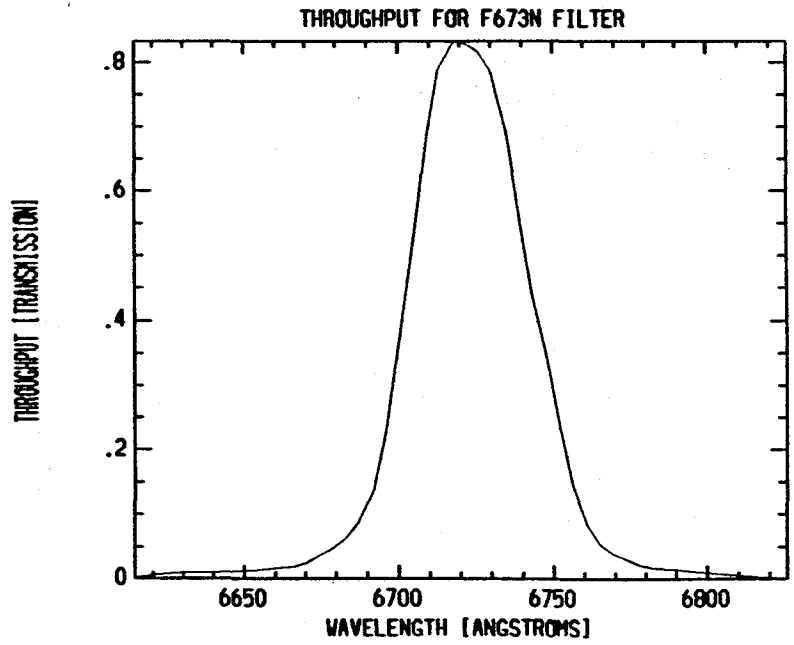
THROUGHPUT FOR F673N FILTER
THROUGHPUT [TRANSMISSION]
.8
.6
.4
.2
0
6650
6700
6750
6800
WAVELENGTH [ANGSTROMS]

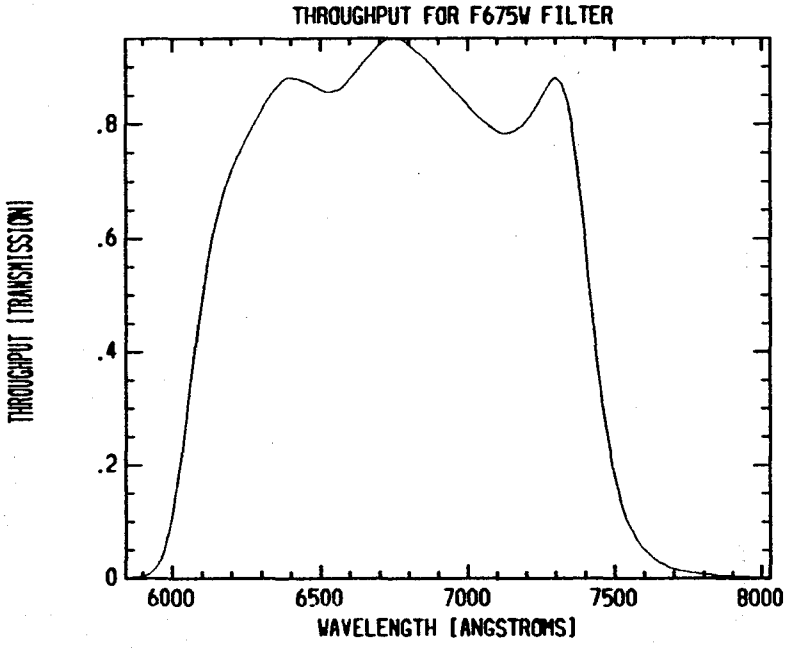
THROUGHPUT FOR F675W FILTER
THROUGHPUT [TRANSMISSION]
0
.2
.4
.6
.8
6000
6500
7000
7500
8000
WAVELENGTH [ANGSTROMS]

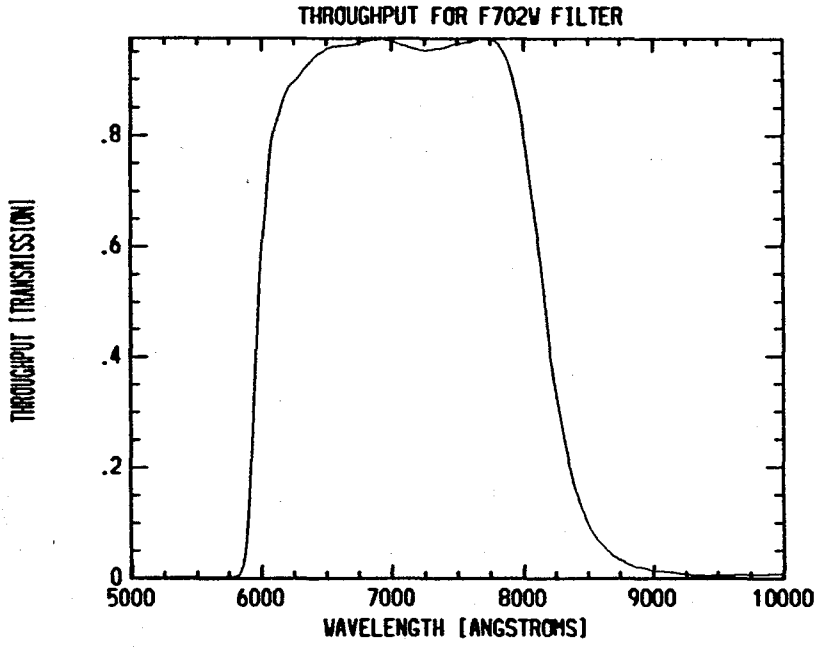
THROUGHPUT FOR F702W FILTER
THROUGHPUT [TRANSMISSION]
0
.2
.4
.6
.8
5000
6000
7000
8000
9000
10000
WAVELENGTH [ANGSTROMS]

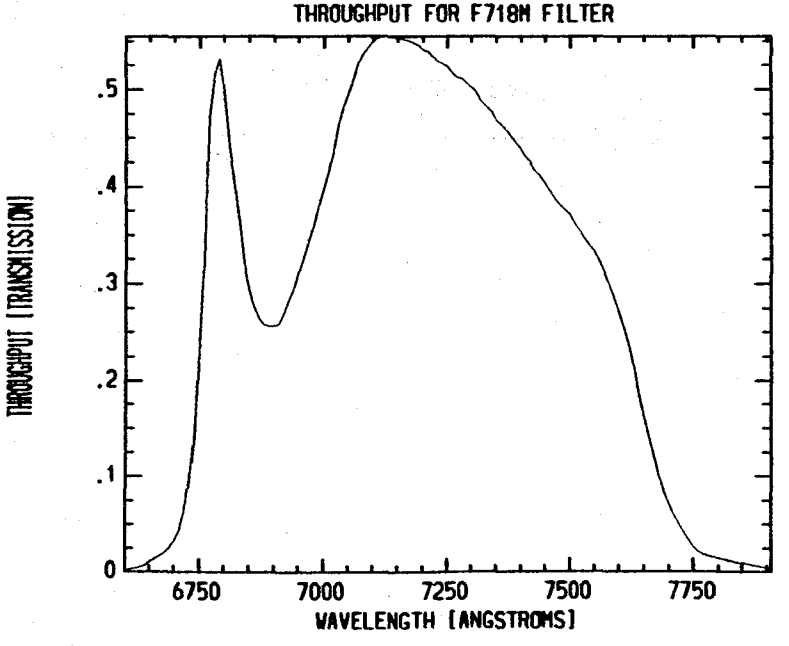
THROUGHPUT FOR F718M FILTER
THROUGHPUT [TRANSMISSION]
0
.1
.2
.3
.4
.5
6750
7000
7250
7500
7750
WAVELENGTH [ANGSTROMS]

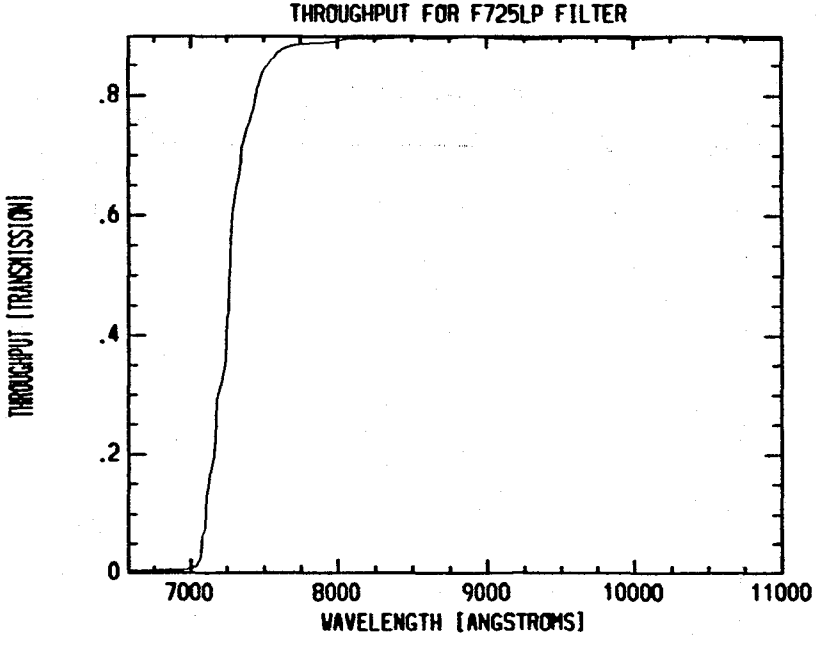
THROUGHPUT FOR F725LP FILTER
THROUGHPUT [TRANSMISSION]
0
.2
.4
.6
.8
7000
8000
9000
10000
11000
WAVELENGTH [ANGSTROMS]

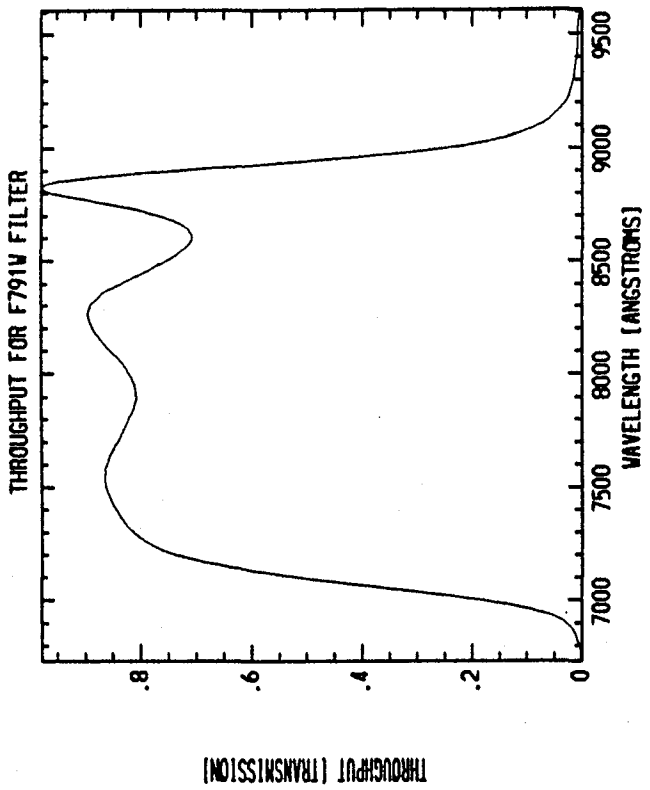
THROUGHPUT FOR F791W FILTER
THROUGHPUT [TRANSMISSION]
WAVELENGTH [ANGSTROMS]
0
.2
.4
.6
.8
7000
7500
8000
8500
9000
9500

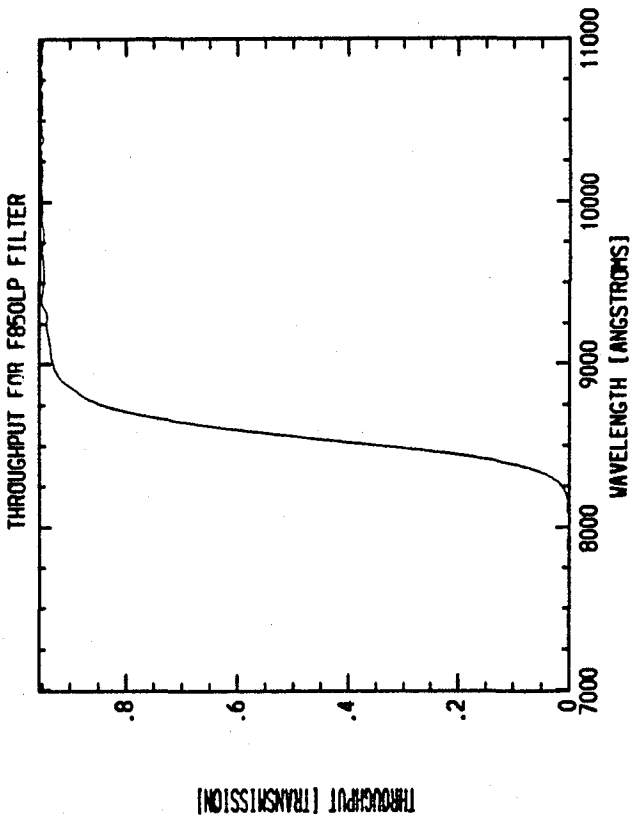
THROUGHPUT FOR F850LP FILTER
THROUGHPUT [TRANSMISSION]
WAVELENGTH [ANGSTROMS]
0
.2
.4
.6
.8
7000
8000
9000
10000
11000

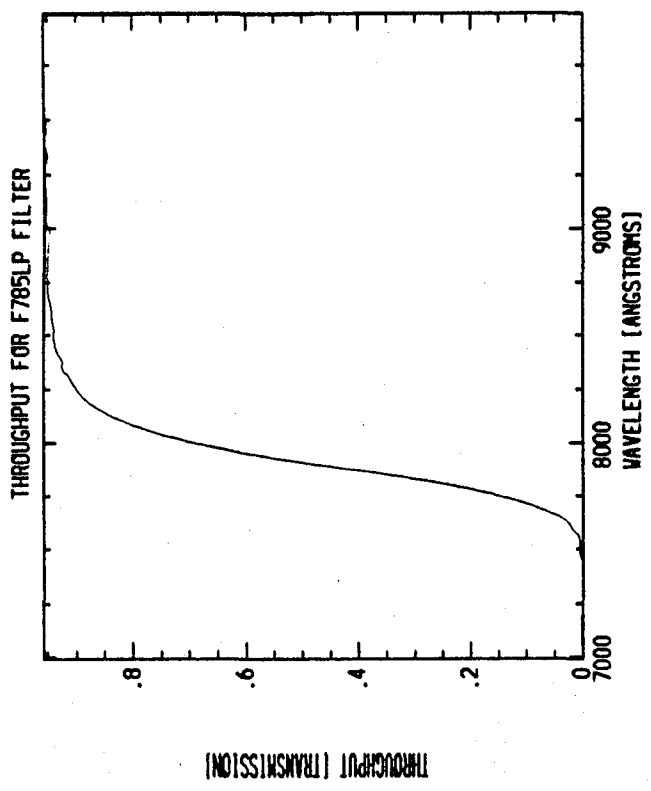
THROUGHPUT FOR F785LP FILTER
THROUGHPUT [TRANSMISSION]
WAVELENGTH [ANGSTROMS]
0
.2
.4
.6
.8
7000
8000
9000

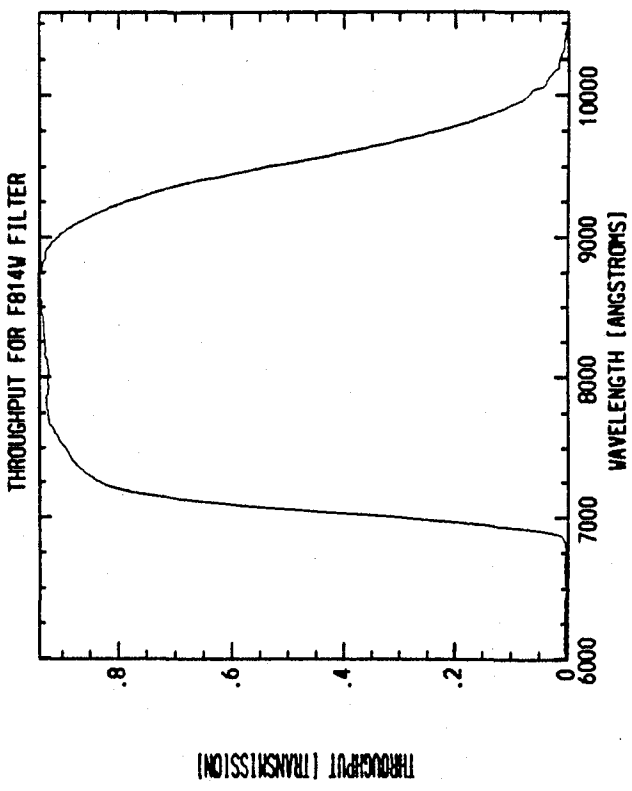
THROUGHPUT FOR F814W FILTER
THROUGHPUT [TRANSMISSION]
WAVELENGTH [ANGSTROMS]
0
.2
.4
.6
.8
6000
7000
8000
9000
10000

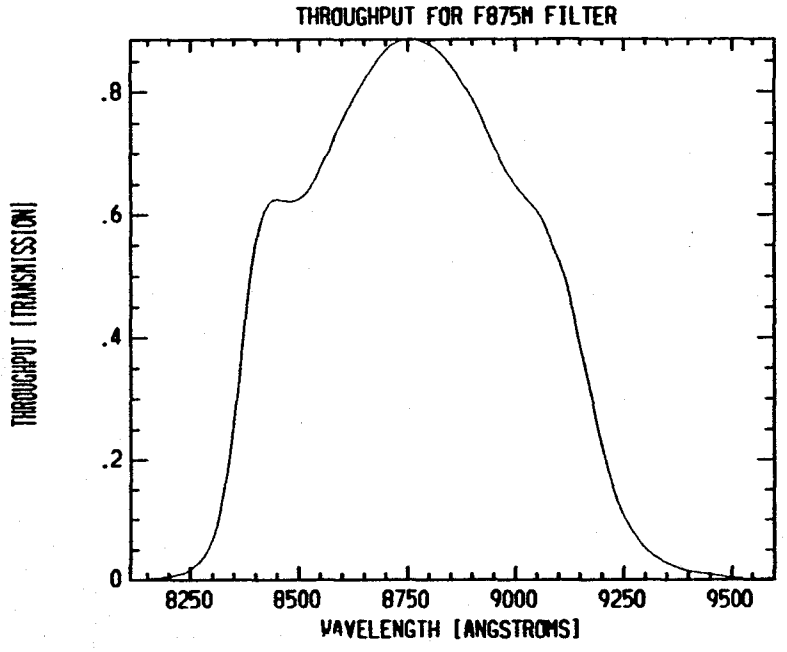
THROUGHPUT FOR F875M FILTER
THROUGHPUT [TRANSMISSION]
0
.2
.4
.6
.8
8250
8500
8750
9000
9250
9500
WAVELENGTH [ANGSTROMS]

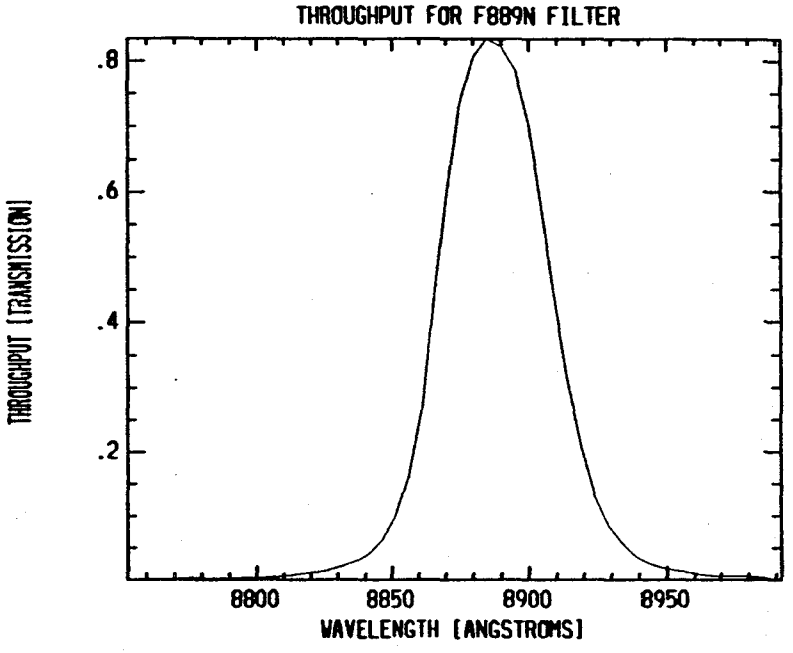
THROUGHPUT FOR F889N FILTER
THROUGHPUT [TRANSMISSION]
.2
.4
.6
.8
8800
8850
8900
8950
WAVELENGTH [ANGSTROMS]

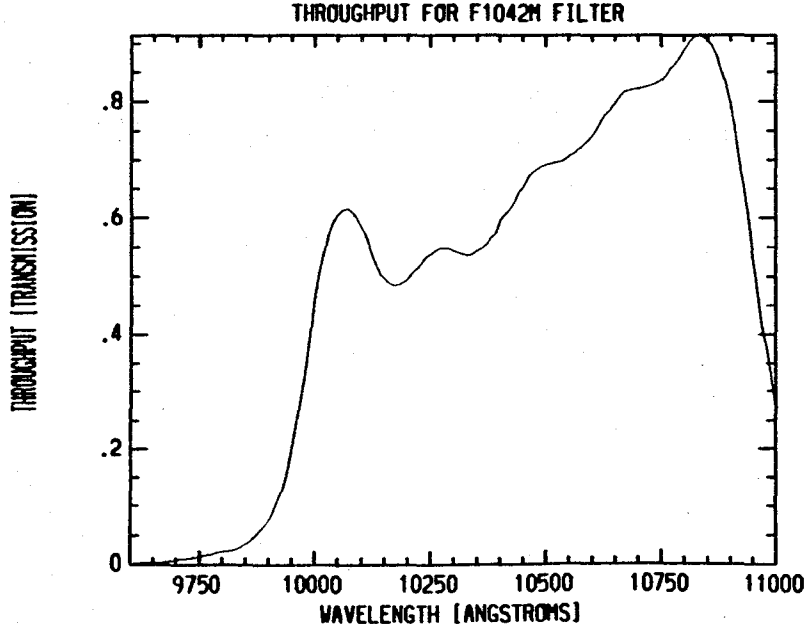
THROUGHPUT FOR F1042M FILTER
THROUGHPUT [TRANSMISSION]
0
.2
.4
.6
.8
9750
10000
10250
10500
10750
11000
WAVELENGTH [ANGSTROMS]

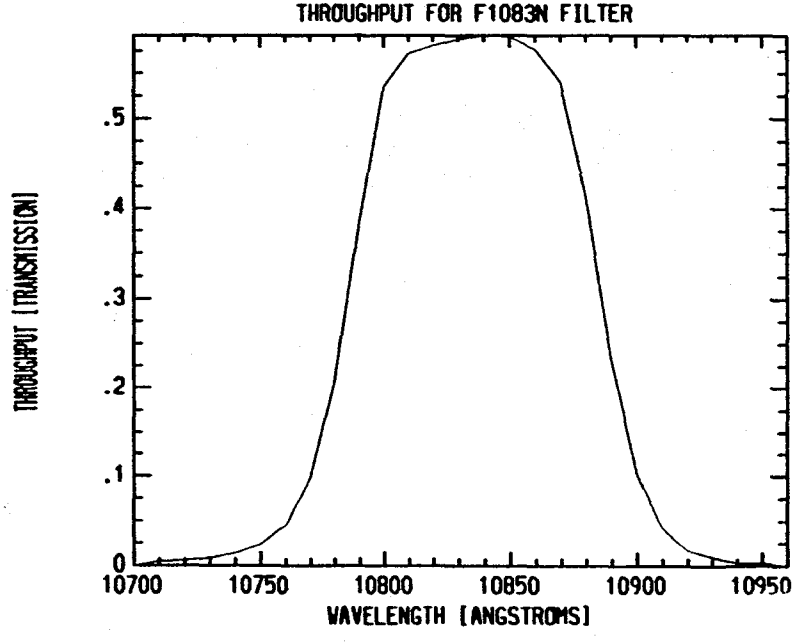
THROUGHPUT FOR F1083N FILTER
THROUGHPUT [TRANSMISSION]
0
.1
.2
.3
.4
.5
10700
10750
10800
10850
10900
10950
WAVELENGTH [ANGSTROMS]

Figure 3.2.3

The next 20 pages show the effiency curves for each WF/PC filter, including the OTA, WF/PC optics, and CCD QE. The coding for each camera head is as follows:

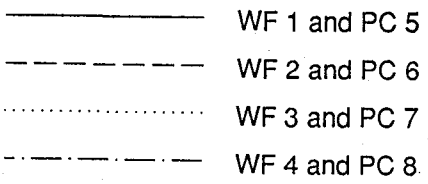

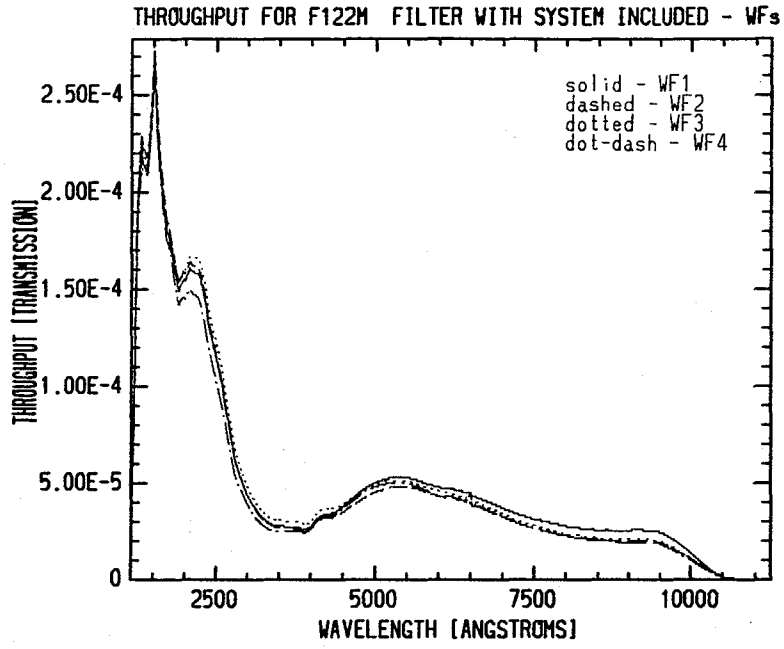
THROUGHPUT FOR F122M FILTER WITH SYSTEM INCLUDED - WFs
solid - WF1
dashed - WF2
dotted - WF3
dot-dash - WF4
THROUGHPUT [TRANSMISSION]
2.50E-4
2.00E-4
1.50E-4
1.00E-4
5.00E-5
0
2500
5000
7500
10000
WAVELENGTH [ANGSTROMS]

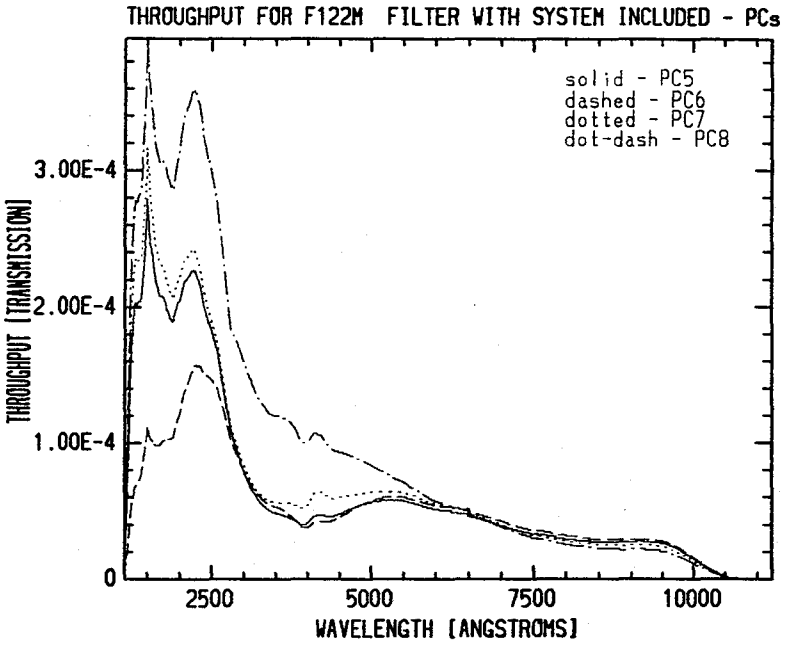
THROUGHPUT FOR F122M FILTER WITH SYSTEM INCLUDED - PCs
solid - PC5
dashed - PC6
dotted - PC7
dot-dash - PC8
THROUGHPUT [TRANSMISSION]
3.00E-4
2.00E-4
1.00E-4
0
2500
5000
7500
10000
WAVELENGTH [ANGSTROMS]

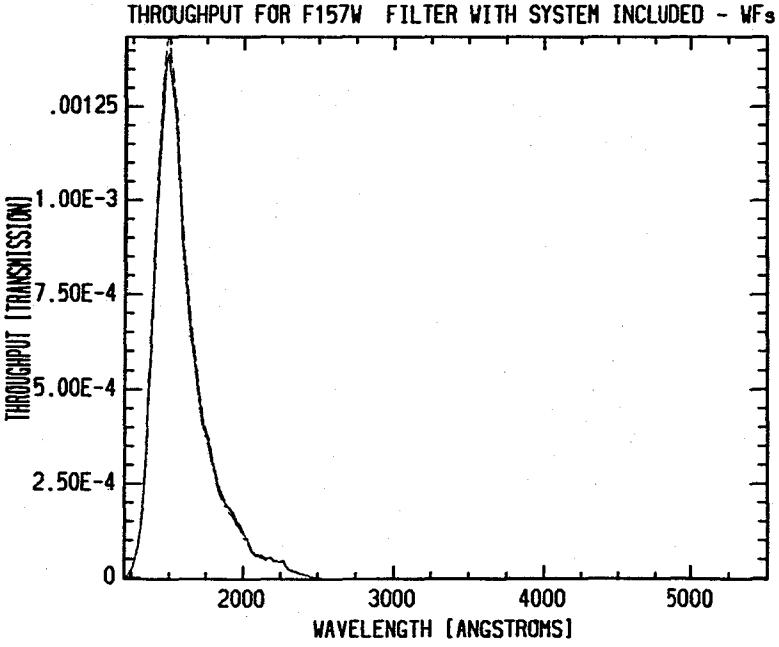
THROUGHPUT FOR F157W FILTER WITH SYSTEM INCLUDED - WFs
THROUGHPUT [TRANSMISSION]
.00125
1.00E-3
7.50E-4
5.00E-4
2.50E-4
0
2000
3000
4000
5000
WAVELENGTH [ANGSTROMS]

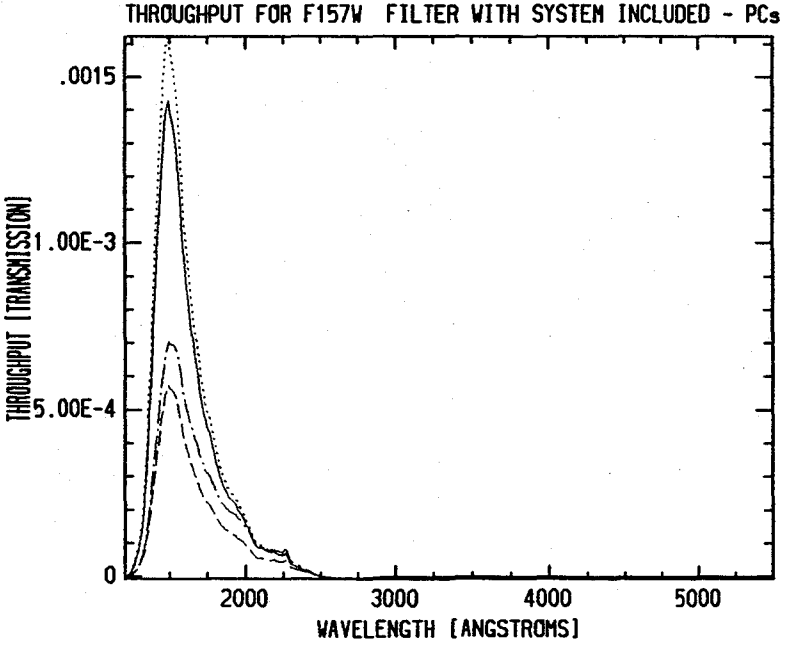
THROUGHPUT FOR F157W FILTER WITH SYSTEM INCLUDED - PCs
THROUGHPUT [TRANSMISSION]
.0015
1.00E-3
5.00E-4
0
2000
3000
4000
5000
WAVELENGTH [ANGSTROMS]

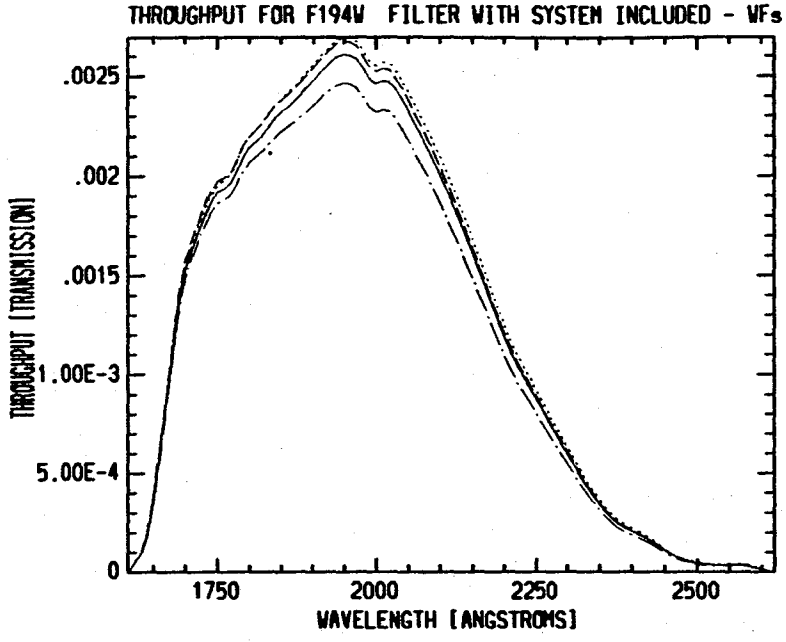
THROUGHPUT FOR F194W FILTER WITH SYSTEM INCLUDED - WFs
THROUGHPUT [TRANSMISSION]
.0025
.002
.0015
1.00E-3
5.00E-4
0
1750
2000
2250
2500
WAVELENGTH [ANGSTROMS]

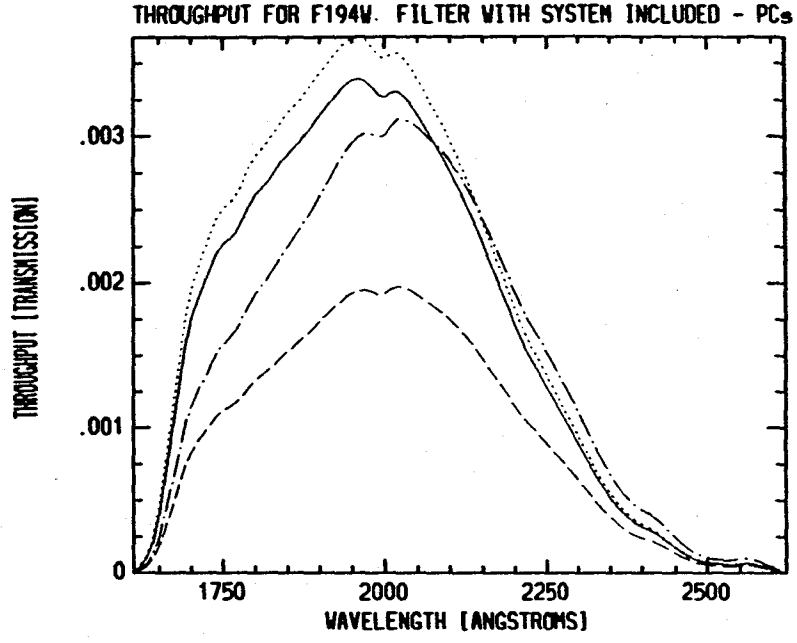
THROUGHPUT FOR F194W FILTER WITH SYSTEM INCLUDED - PCs
THROUGHPUT [TRANSMISSION]
.003
.002
.001
0
1750
2000
2250
2500
WAVELENGTH [ANGSTROMS]

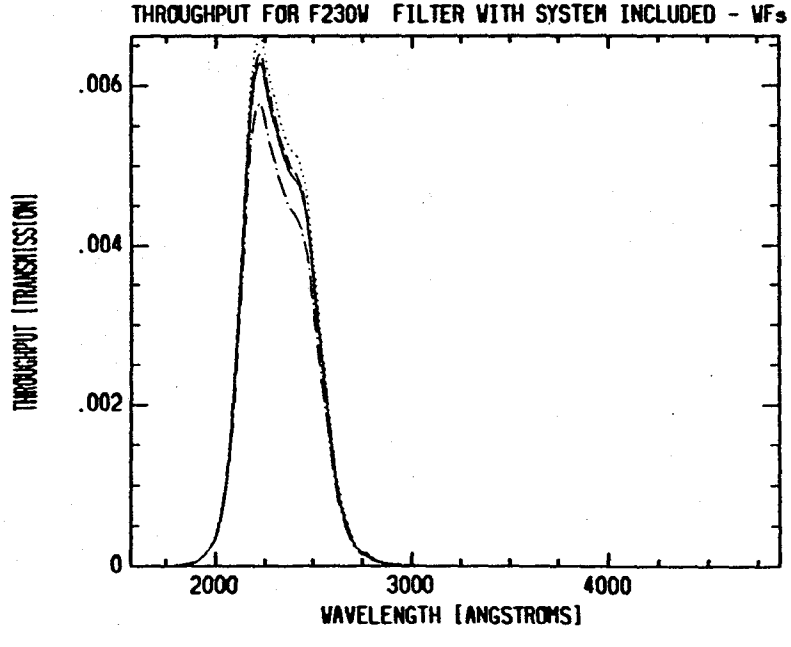
THROUGHPUT FOR F230W FILTER WITH SYSTEM INCLUDED - WFs
THROUGHPUT [TRANSMISSION]
.006
.004
.002
0
2000
3000
4000
WAVELENGTH [ANGSTROMS]

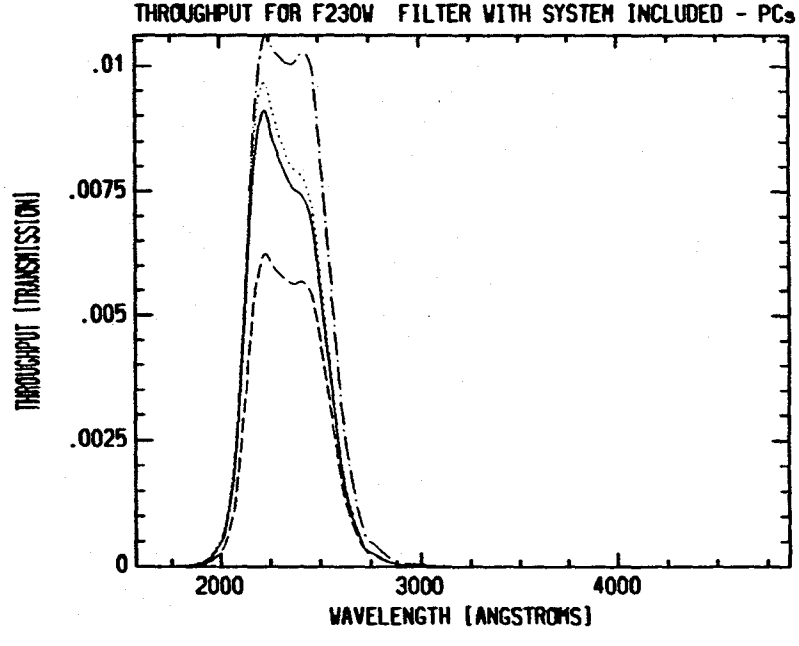
THROUGHPUT FOR F230W FILTER WITH SYSTEM INCLUDED - PCs
THROUGHPUT [TRANSMISSION]
.01
.0075
.005
.0025
0
2000
3000
4000
WAVELENGTH [ANGSTROMS]

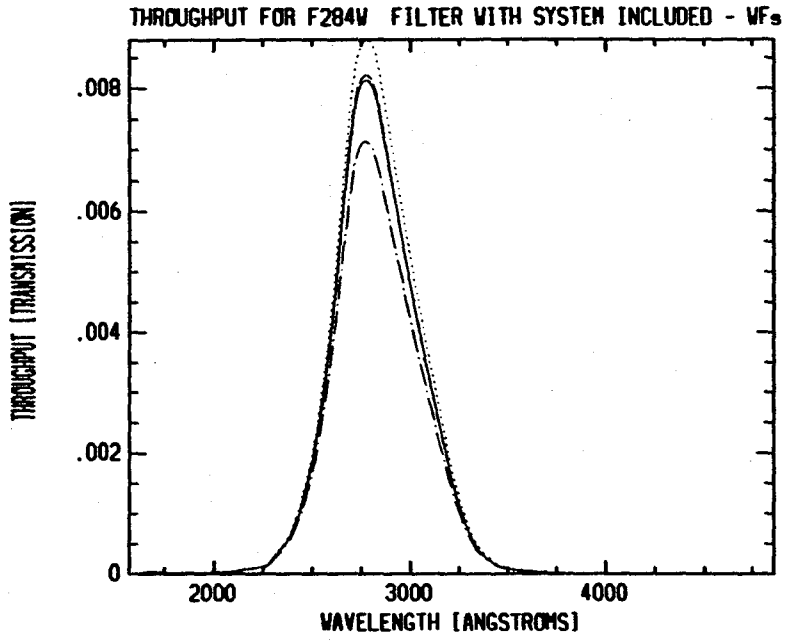
THROUGHPUT FOR F284W FILTER WITH SYSTEM INCLUDED - WFs
THROUGHPUT [TRANSMISSION]
.008
.006
.004
.002
0
2000
3000
4000
WAVELENGTH [ANGSTROMS]

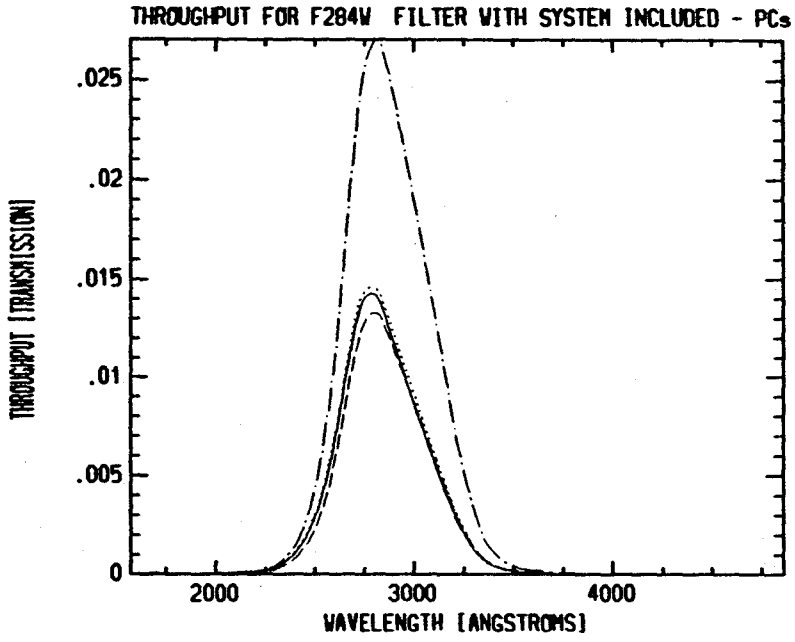
THROUGHPUT FOR F284W FILTER WITH SYSTEM INCLUDED - PCs
THROUGHPUT [TRANSMISSION]
.025
.02
.015
.01
.005
0
2000
3000
4000
WAVELENGTH [ANGSTROMS]

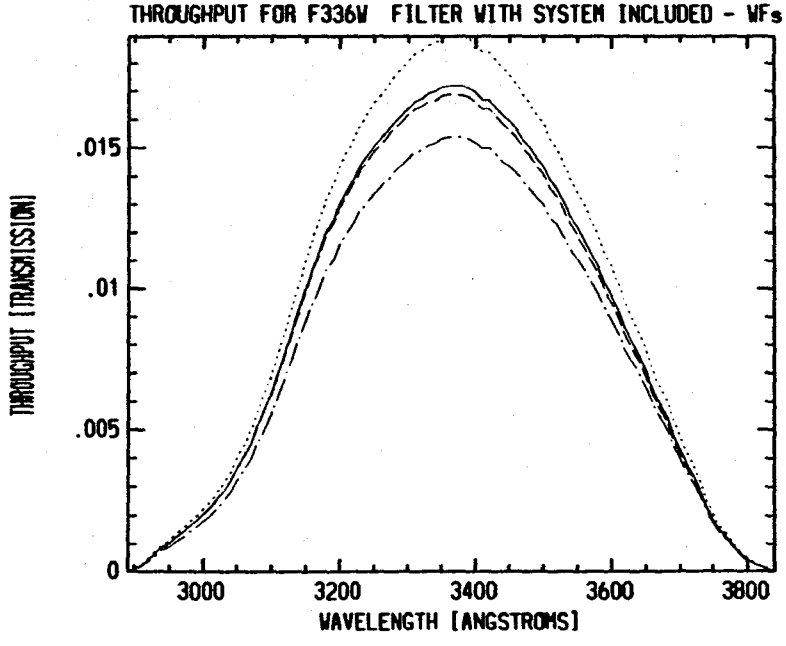
THROUGHPUT FOR F336W FILTER WITH SYSTEM INCLUDED - WFs
THROUGHPUT [TRANSMISSION]
.015
.01
.005
0
3000
3200
3400
3600
3800
WAVELENGTH [ANGSTROMS]

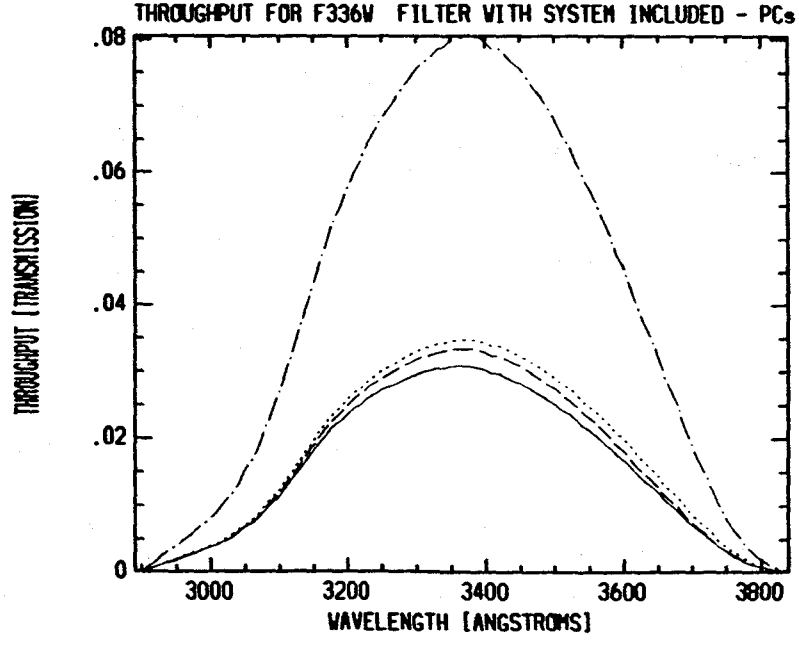
THROUGHPUT FOR F336W FILTER WITH SYSTEM INCLUDED - PCs
THROUGHPUT [TRANSMISSION]
.08
.06
.04
.02
0
3000
3200
3400
3600
3800
WAVELENGTH [ANGSTROMS]

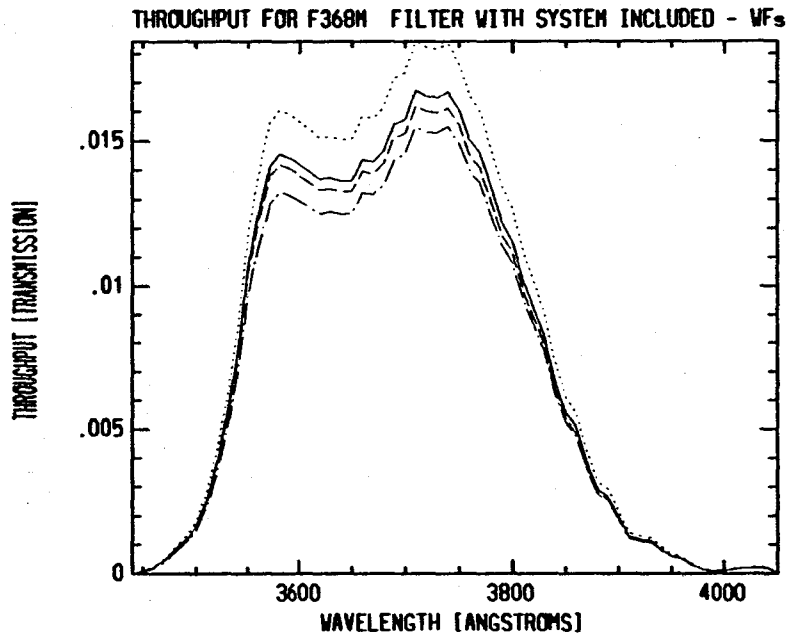
THROUGHPUT FOR F368M FILTER WITH SYSTEM INCLUDED - WFs
THROUGHPUT [TRANSMISSION]
.015
.01
.005
0
3600
3800
4000
WAVELENGTH [ANGSTROMS]

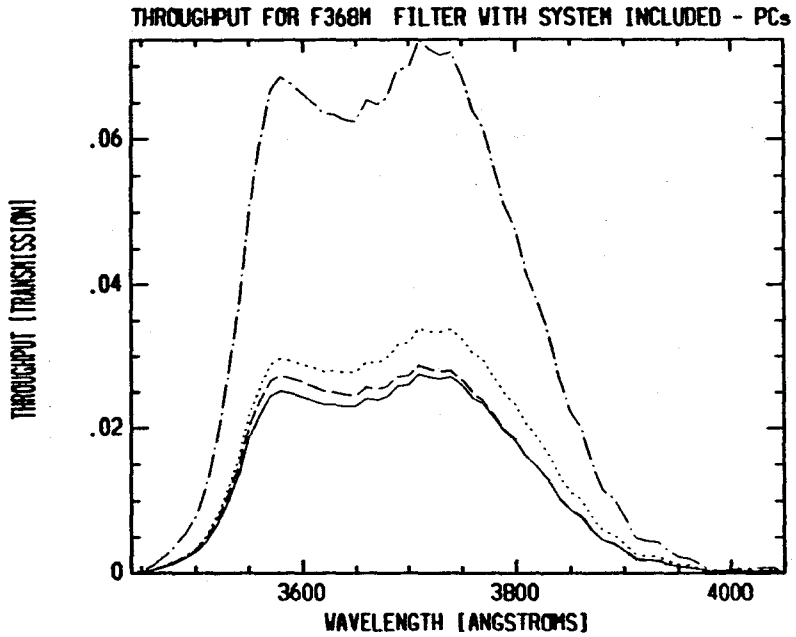
THROUGHPUT FOR F368M FILTER WITH SYSTEM INCLUDED - PCs
THROUGHPUT [TRANSMISSION]
.06
.04
.02
0
3600
3800
4000
WAVELENGTH [ANGSTROMS]

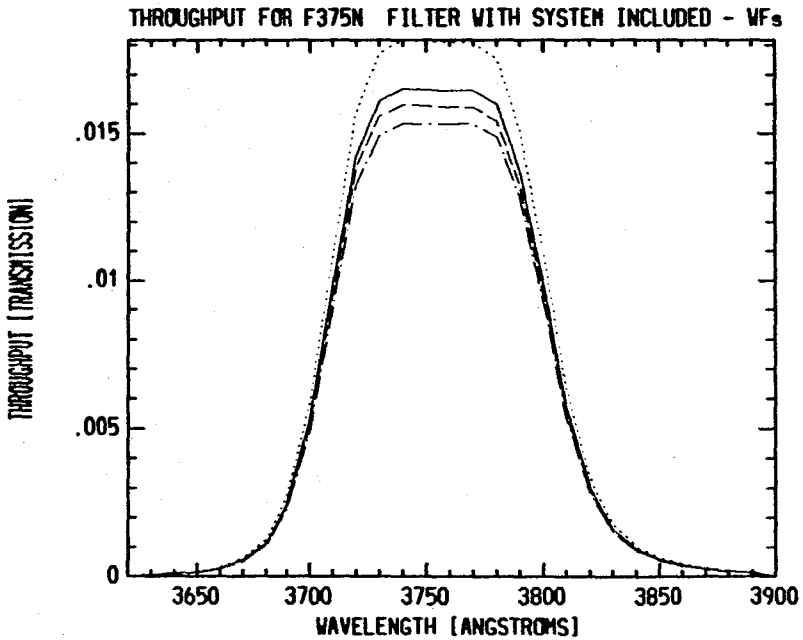
THROUGHPUT FOR F375N FILTER WITH SYSTEM INCLUDED - WFs
THROUGHPUT [TRANSMISSION]
.015
.01
.005
0
3650
3700
3750
3800
3850
3900
WAVELENGTH [ANGSTROMS]

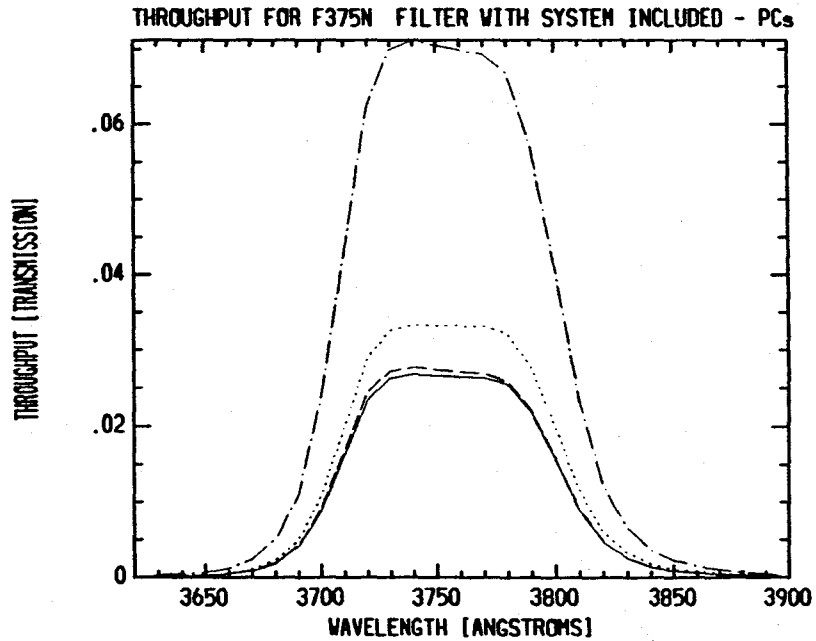
THROUGHPUT FOR F375N FILTER WITH SYSTEM INCLUDED - PCs
THROUGHPUT [TRANSMISSION]
.06
.04
.02
0
3650
3700
3750
3800
3850
3900
WAVELENGTH [ANGSTROMS]

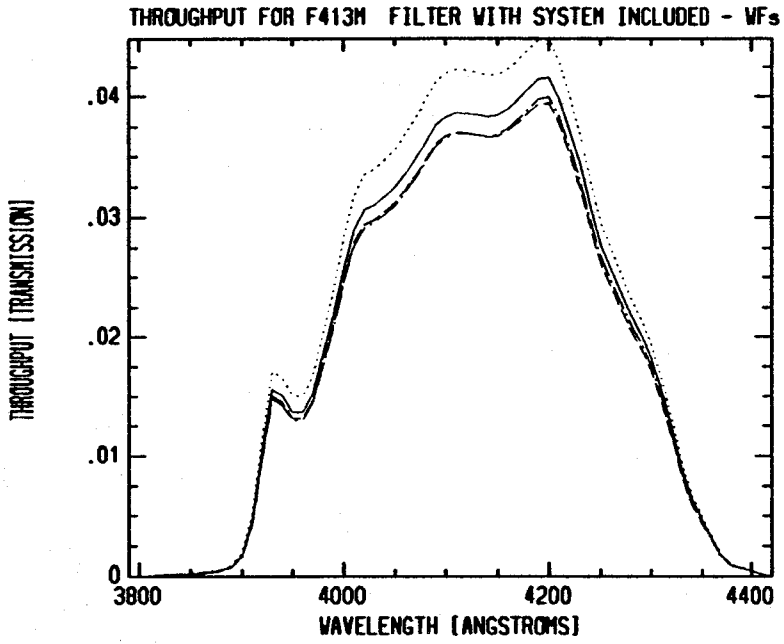
THROUGHPUT FOR F413M FILTER WITH SYSTEM INCLUDED - WFs
THROUGHPUT [TRANSMISSION]
.04
.03
.02
.01
0
3800
4000
4200
4400
WAVELENGTH [ANGSTROMS]

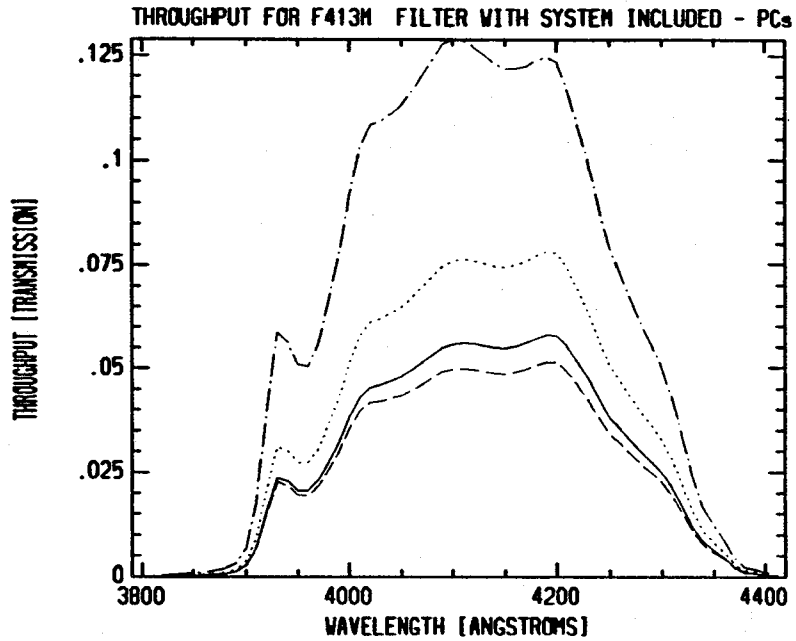
THROUGHPUT FOR F413M FILTER WITH SYSTEM INCLUDED - PCs
THROUGHPUT [TRANSMISSION]
.125
.1
.075
.05
.025
0
3800
4000
4200
4400
WAVELENGTH [ANGSTROMS]

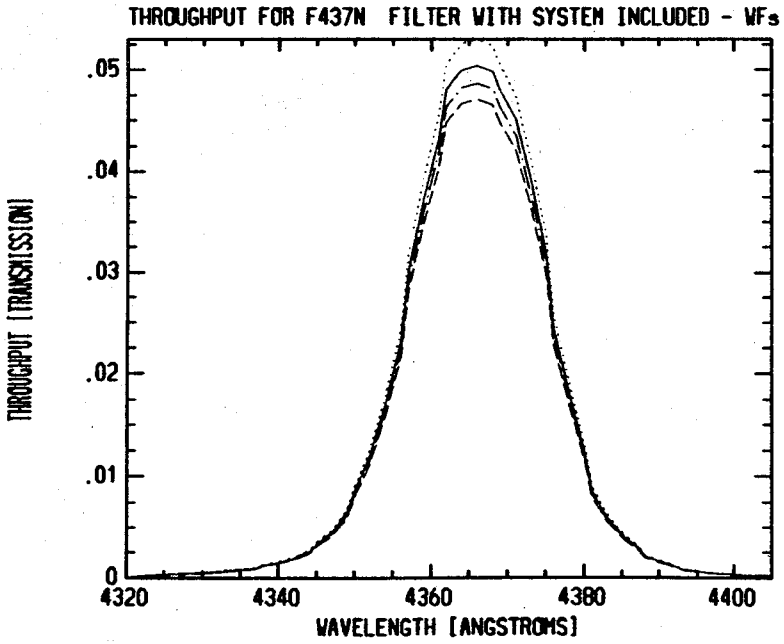
THROUGHPUT FOR F437N FILTER WITH SYSTEM INCLUDED - WFs
THROUGHPUT [TRANSMISSION]
.05
.04
.03
.02
.01
0
4320
4340
4360
4380
4400
WAVELENGTH [ANGSTROMS]

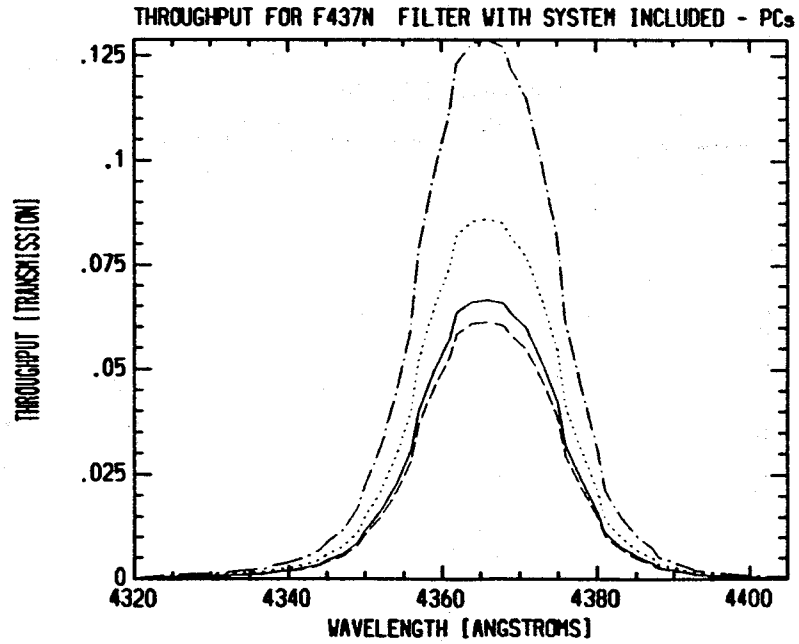
THROUGHPUT FOR F437N FILTER WITH SYSTEM INCLUDED - PCs
THROUGHPUT [TRANSMISSION]
.125
.1
.075
.05
.025
0
4320
4340
4360
4380
4400
WAVELENGTH [ANGSTROMS]

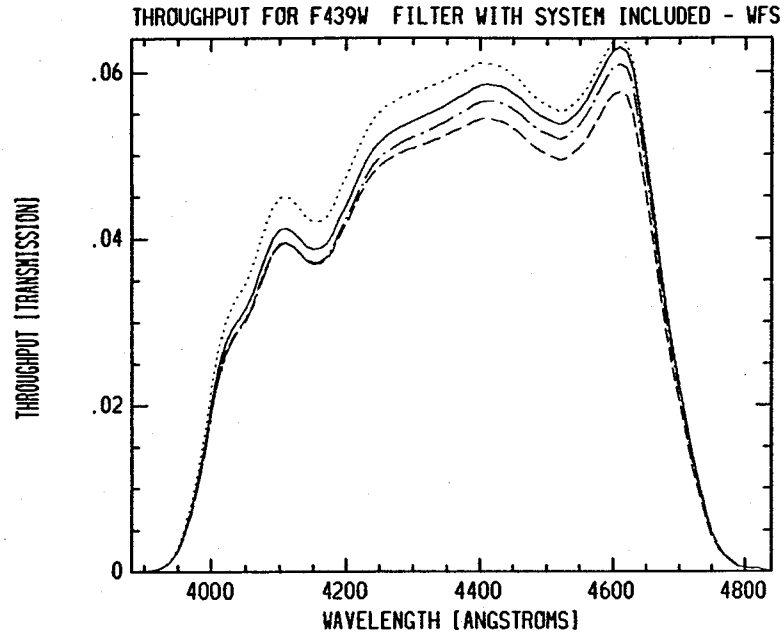
THROUGHPUT FOR F439W FILTER WITH SYSTEM INCLUDED - WFS
THROUGHPUT [TRANSMISSION]
.06
.04
.02
0
4000
4200
4400
4600
4800
WAVELENGTH [ANGSTROMS]

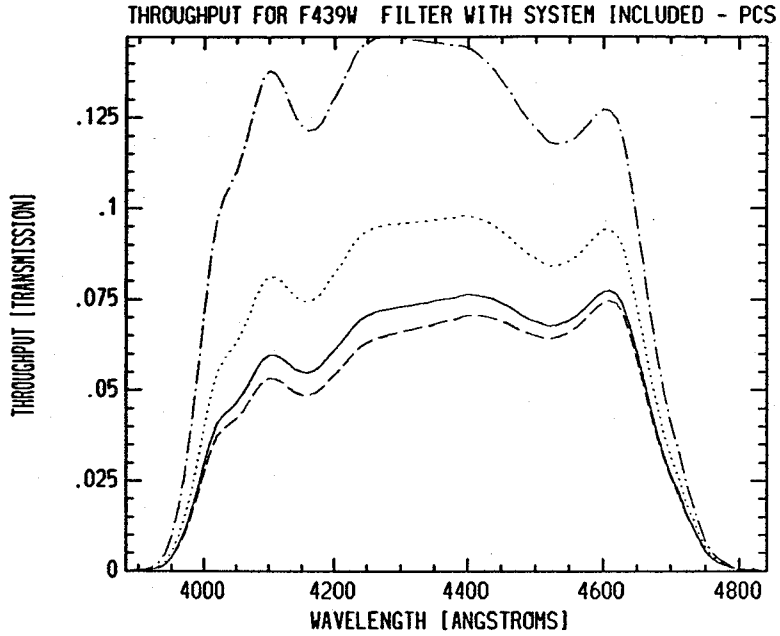
THROUGHPUT FOR F439W FILTER WITH SYSTEM INCLUDED - PCS
THROUGHPUT [TRANSMISSION]
.125
.1
.075
.05
.025
0
4000
4200
4400
4600
4800
WAVELENGTH [ANGSTROMS]

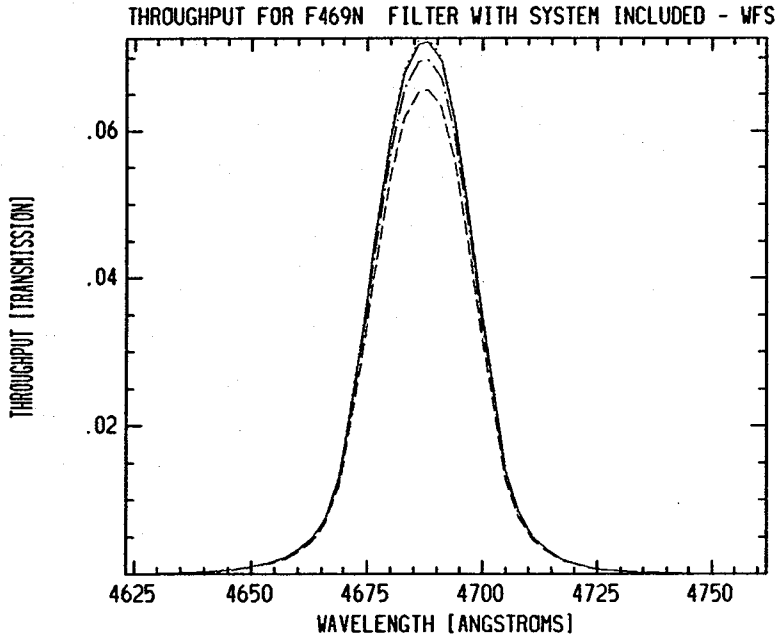
THROUGHPUT FOR F469N FILTER WITH SYSTEM INCLUDED - WFS
THROUGHPUT [TRANSMISSION]
.06
.04
.02
4625
4650
4675
4700
4725
4750
WAVELENGTH [ANGSTROMS]

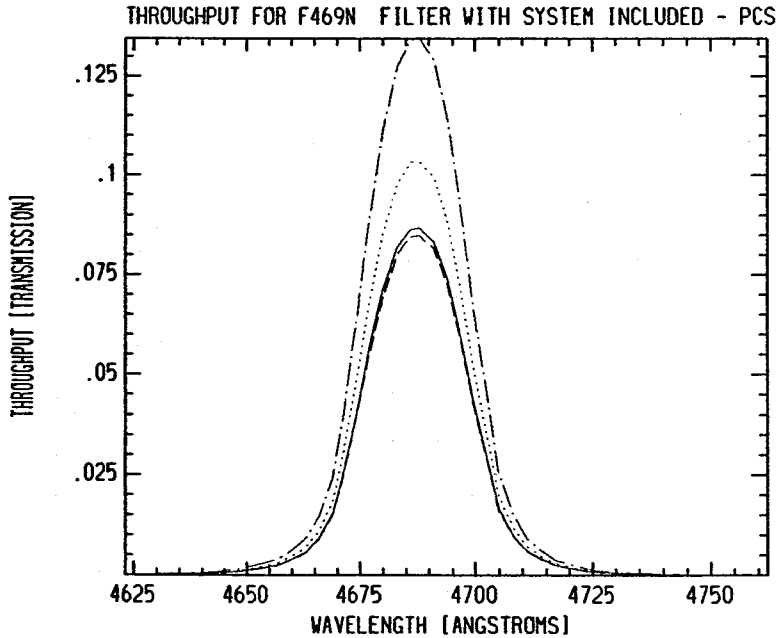
THROUGHPUT FOR F469N FILTER WITH SYSTEM INCLUDED - PCS
THROUGHPUT [TRANSMISSION]
.125
.1
.075
.05
.025
4625
4650
4675
4700
4725
4750
WAVELENGTH [ANGSTROMS]

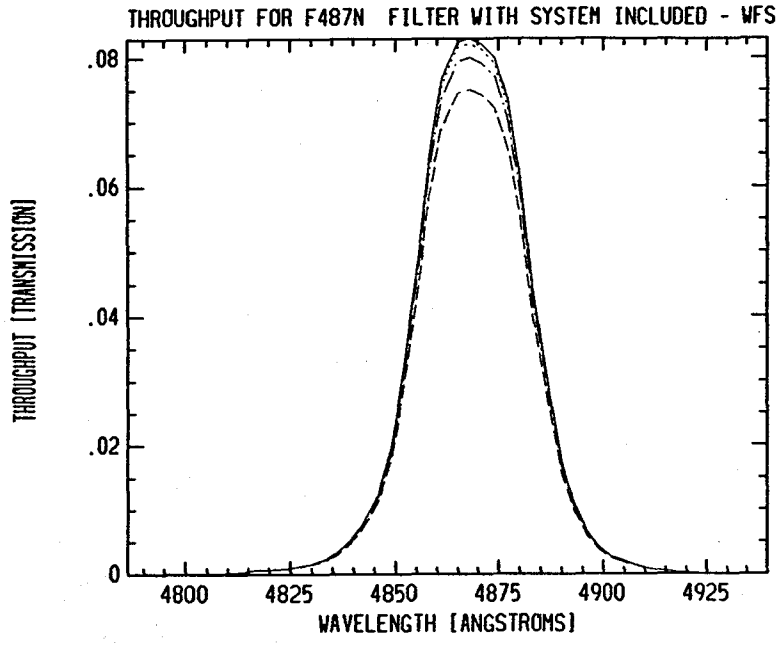
THROUGHPUT FOR F487N FILTER WITH SYSTEM INCLUDED - WFS
THROUGHPUT [TRANSMISSION]
.08
.06
.04
.02
0
4800
4825
4850
4875
4900
4925
WAVELENGTH [ANGSTROMS]

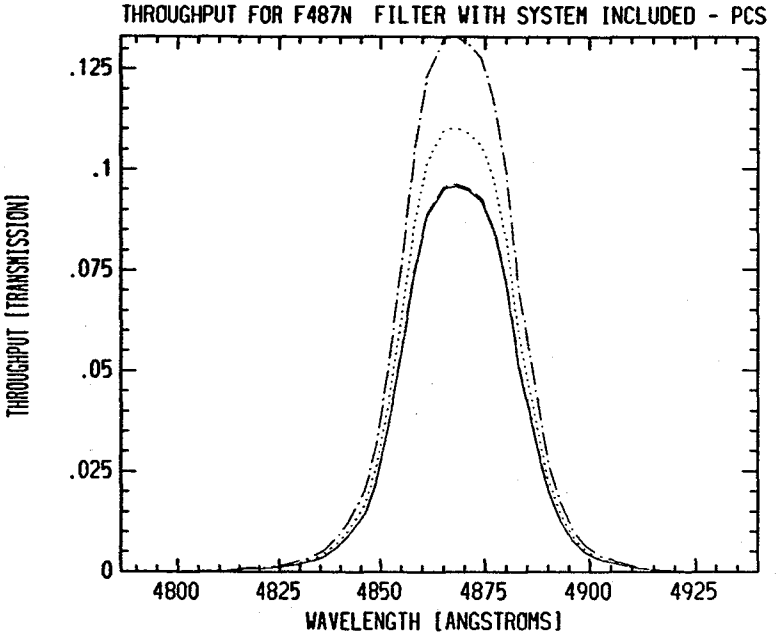
THROUGHPUT FOR F487N FILTER WITH SYSTEM INCLUDED - PCS
THROUGHPUT [TRANSMISSION]
.125
.1
.075
.05
.025
0
4800
4825
4850
4875
4900
4925
WAVELENGTH [ANGSTROMS]

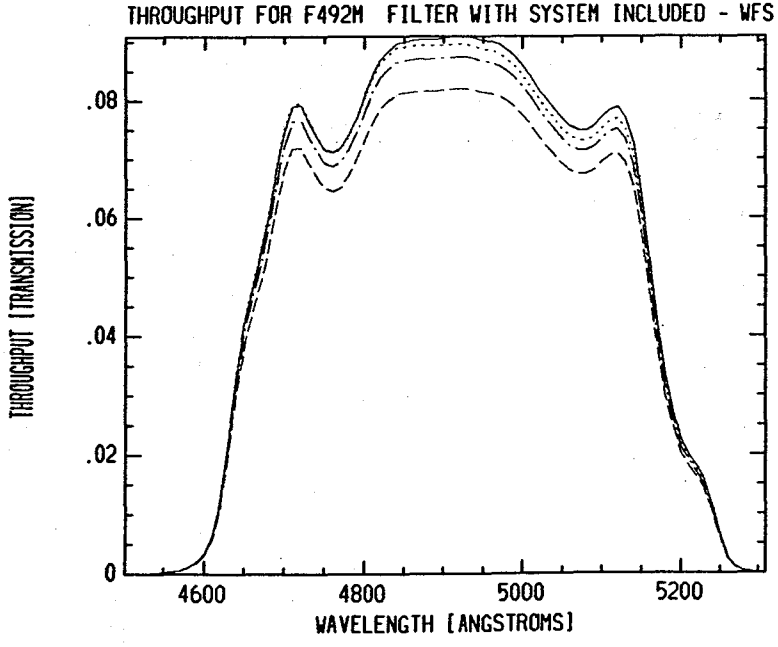
THROUGHPUT FOR F492M FILTER WITH SYSTEM INCLUDED - WFS
THROUGHPUT [TRANSMISSION]
.08
.06
.04
.02
0
4600
4800
5000
5200
WAVELENGTH [ANGSTROMS]

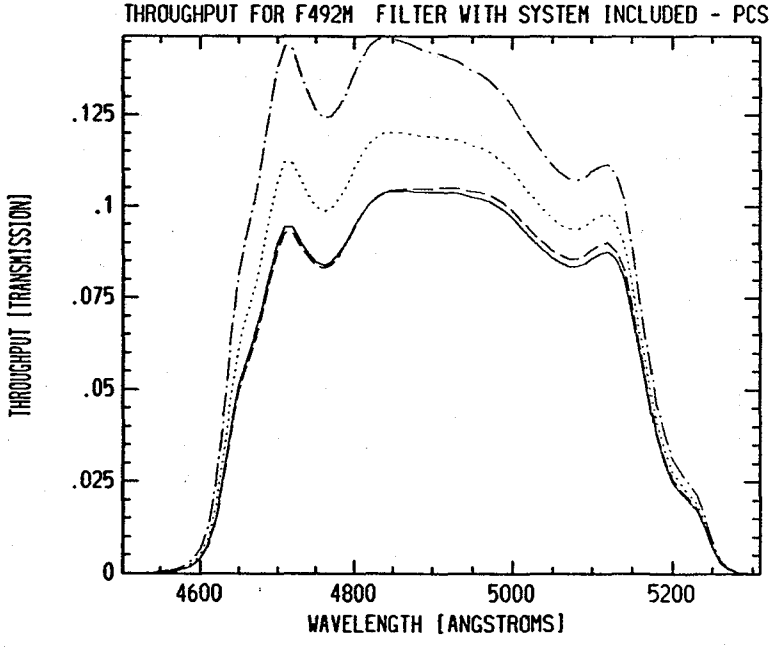
THROUGHPUT FOR F492M FILTER WITH SYSTEM INCLUDED - PCS
THROUGHPUT [TRANSMISSION]
.125
.1
.075
.05
.025
0
4600
4800
5000
5200
WAVELENGTH [ANGSTROMS]

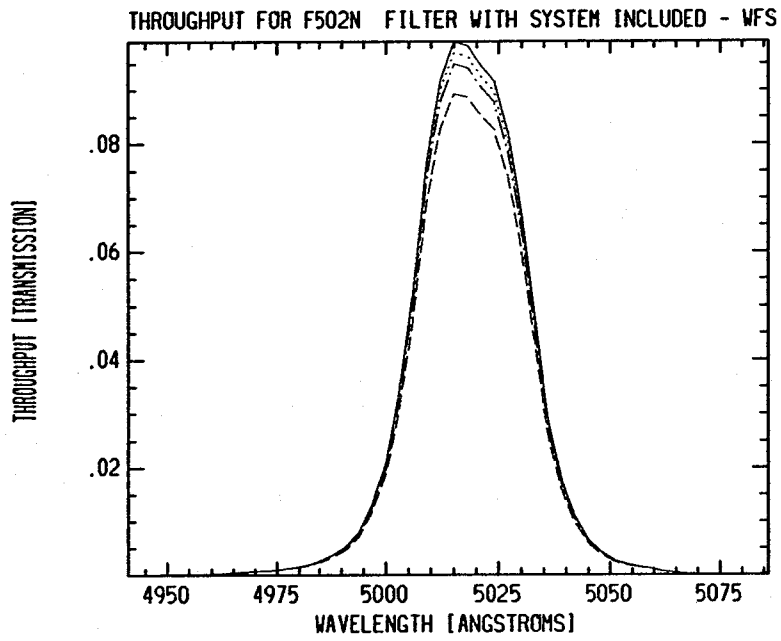
THROUGHPUT FOR F502N FILTER WITH SYSTEM INCLUDED - WFS
THROUGHPUT [TRANSMISSION]
.08
.06
.04
.02
4950
4975
5000
5025
5050
5075
WAVELENGTH [ANGSTROMS]

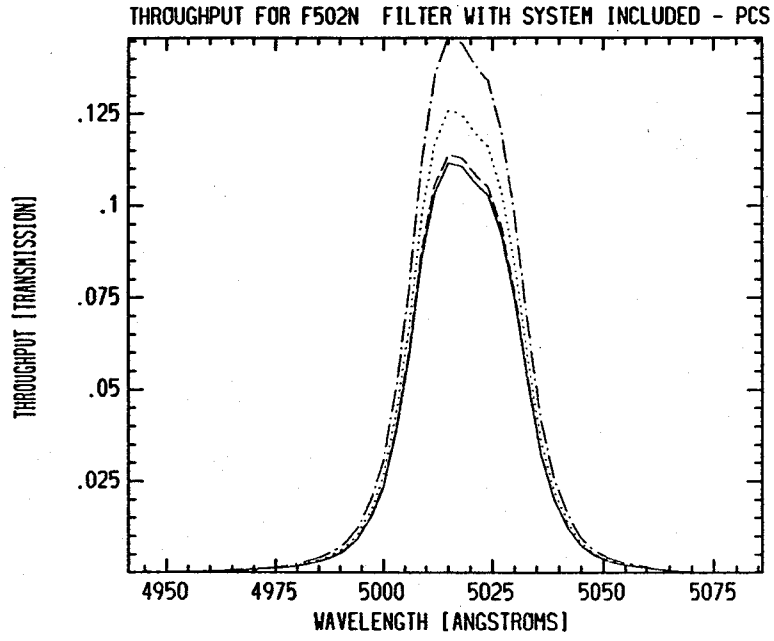
THROUGHPUT FOR F502N FILTER WITH SYSTEM INCLUDED - PCS
THROUGHPUT [TRANSMISSION]
.125
.1
.075
.05
.025
4950
4975
5000
5025
5050
5075
WAVELENGTH [ANGSTROMS]

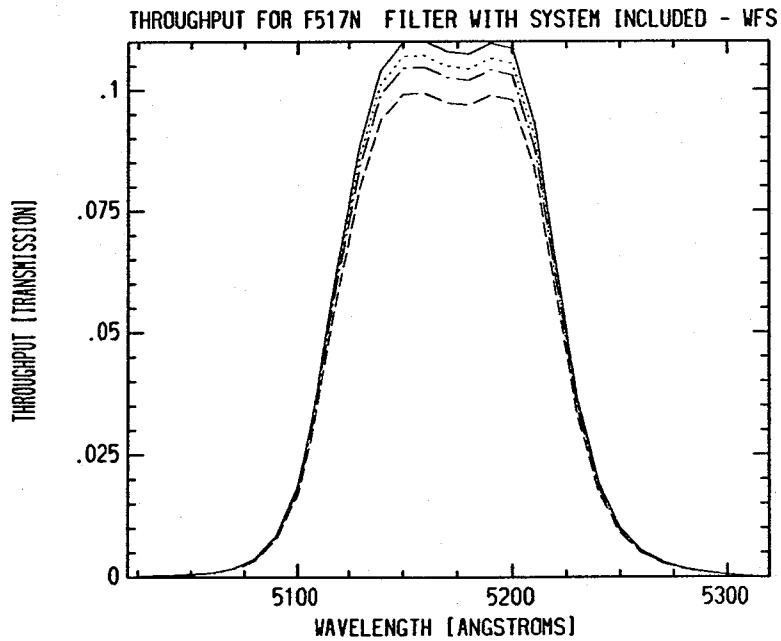
THROUGHPUT FOR F517N FILTER WITH SYSTEM INCLUDED - WFS
THROUGHPUT [TRANSMISSION]
.1
.075
.05
.025
0
5100
5200
5300
WAVELENGTH [ANGSTROMS]

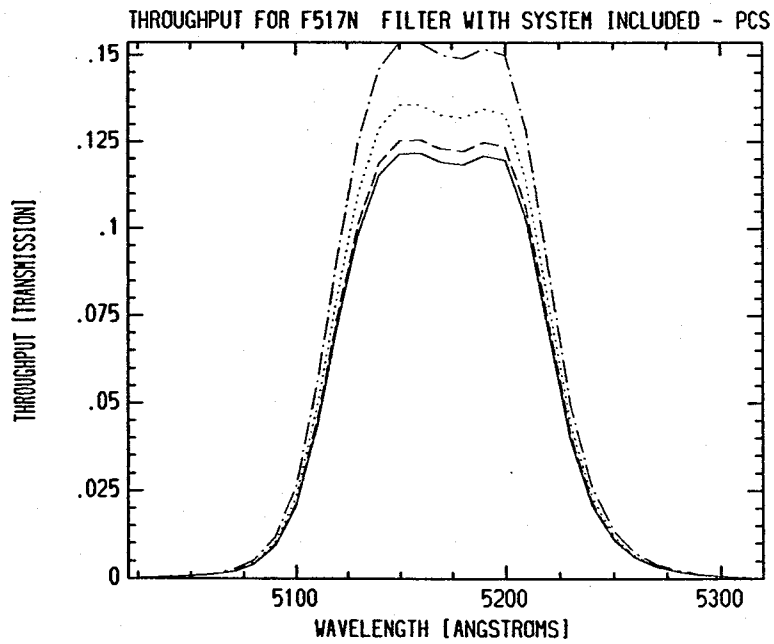
THROUGHPUT FOR F517N FILTER WITH SYSTEM INCLUDED - PCS
THROUGHPUT [TRANSMISSION]
.15
.125
.1
.075
.05
.025
0
5100
5200
5300
WAVELENGTH [ANGSTROMS]

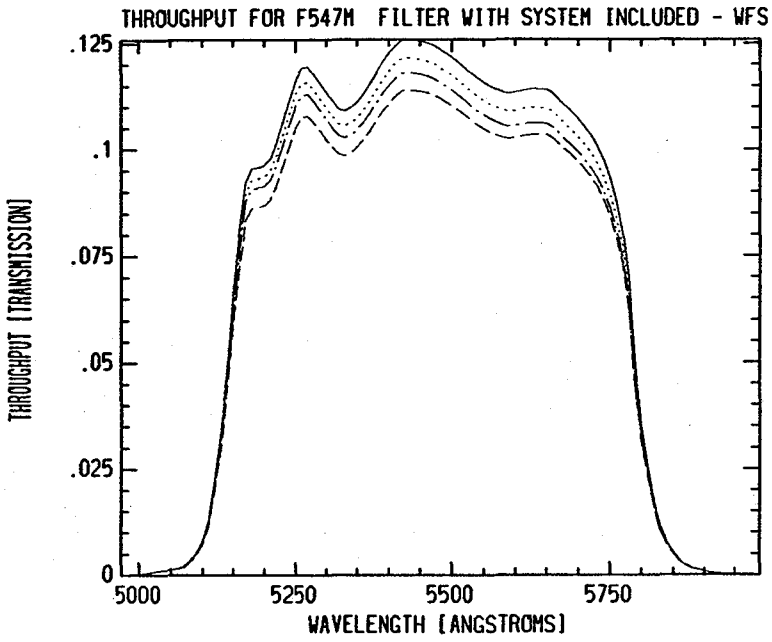
THROUGHPUT FOR F547M FILTER WITH SYSTEM INCLUDED - WFS
THROUGHPUT [TRANSMISSION]
.125
.1
.075
.05
.025
0
5000
5250
5500
5750
WAVELENGTH [ANGSTROMS]

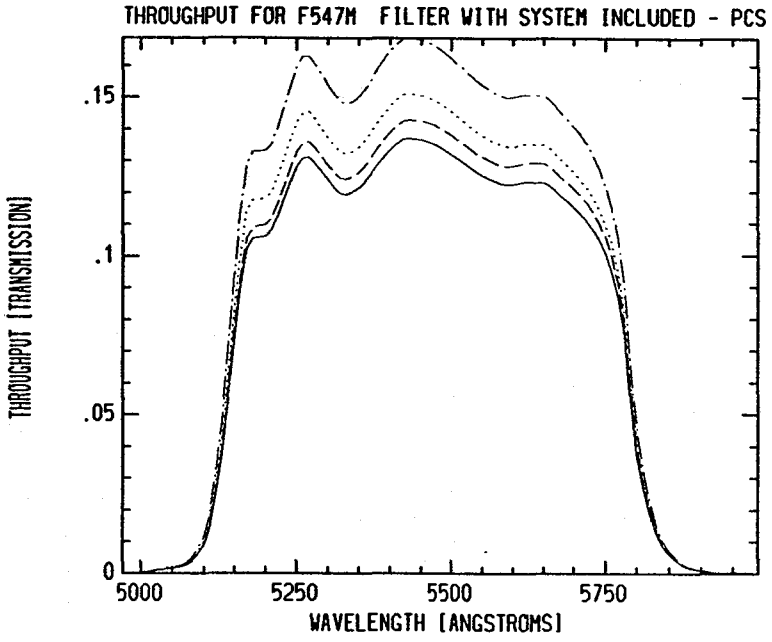
THROUGHPUT FOR F547M FILTER WITH SYSTEM INCLUDED - PCS
THROUGHPUT [TRANSMISSION]
.15
.1
.05
0
5000
5250
5500
5750
WAVELENGTH [ANGSTROMS]

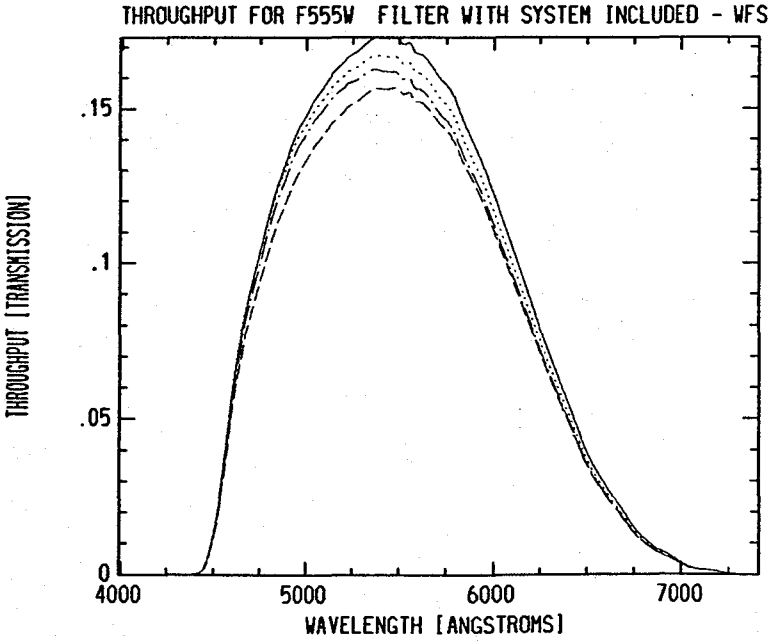
THROUGHPUT FOR F555W FILTER WITH SYSTEM INCLUDED - WFS
THROUGHPUT [TRANSMISSION]
.15
.1
.05
0
4000
5000
6000
7000
WAVELENGTH [ANGSTROMS]

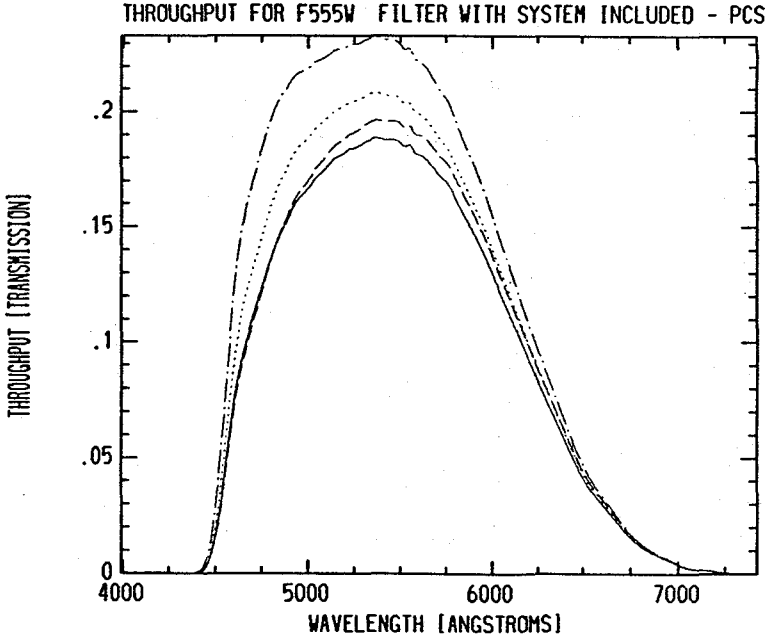
THROUGHPUT FOR F555W FILTER WITH SYSTEM INCLUDED - PCS
THROUGHPUT [TRANSMISSION]
.2
.15
.1
.05
0
4000
5000
6000
7000
WAVELENGTH [ANGSTROMS]

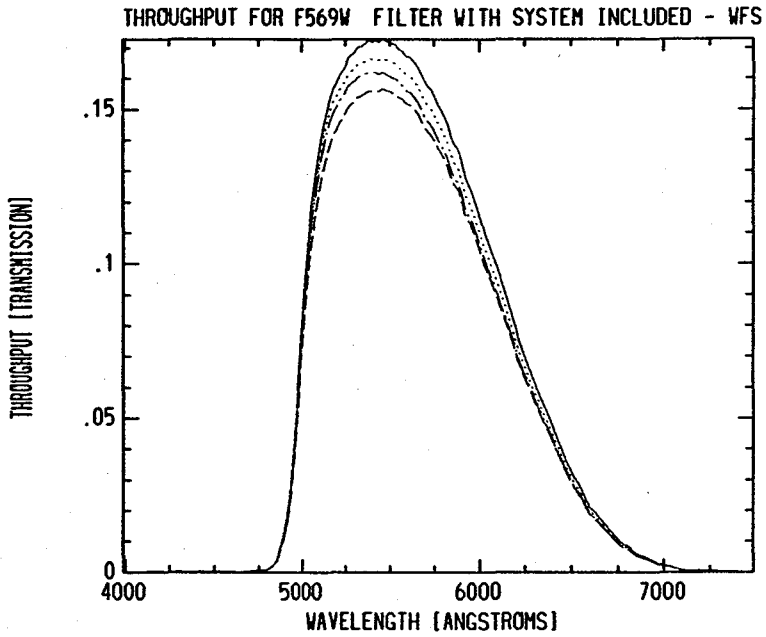
THROUGHPUT FOR F569W FILTER WITH SYSTEM INCLUDED - WFS
THROUGHPUT [TRANSMISSION]
.15
.1
.05
0
4000
5000
6000
7000
WAVELENGTH [ANGSTROMS]

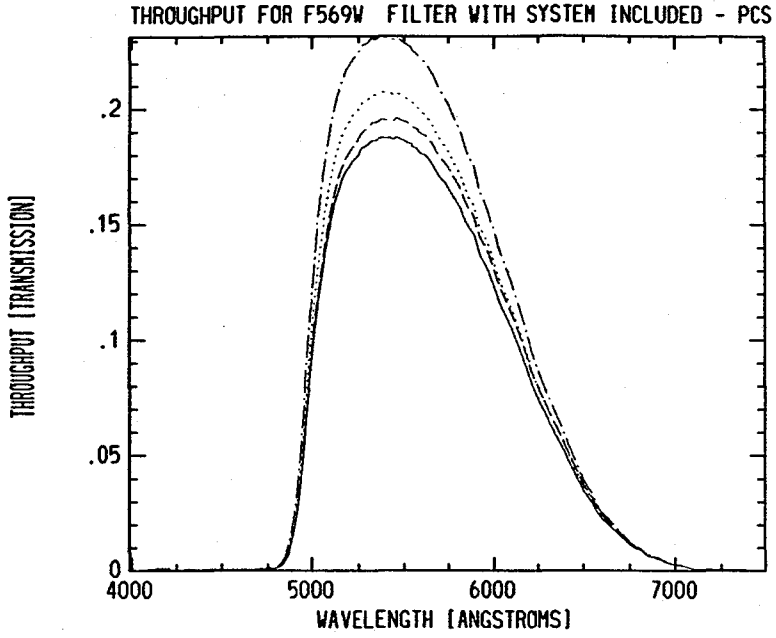
THROUGHPUT FOR F569W FILTER WITH SYSTEM INCLUDED - PCS
THROUGHPUT [TRANSMISSION]
.2
.15
.1
.05
0
4000
5000
6000
7000
WAVELENGTH [ANGSTROMS]

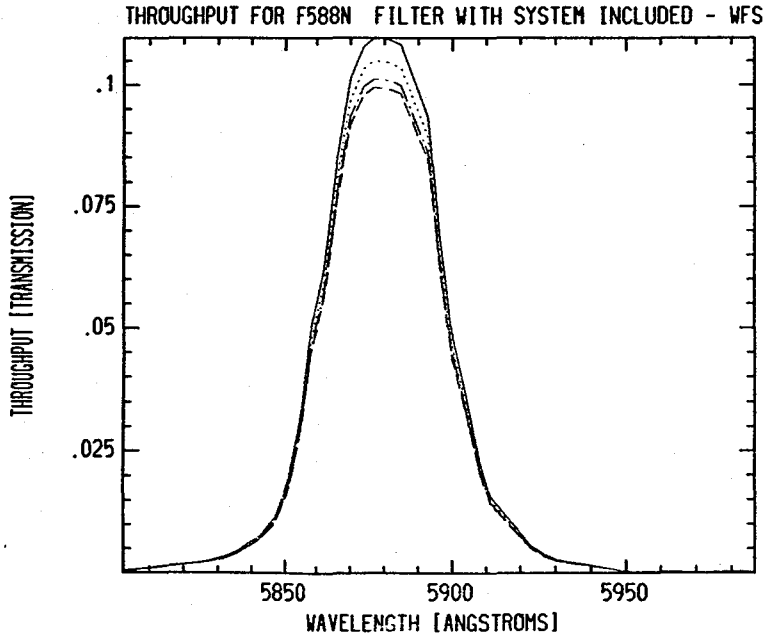
THROUGHPUT FOR F588N FILTER WITH SYSTEM INCLUDED - WFS
THROUGHPUT [TRANSMISSION]
.1
.075
.05
.025
5850
5900
5950
WAVELENGTH [ANGSTROMS]

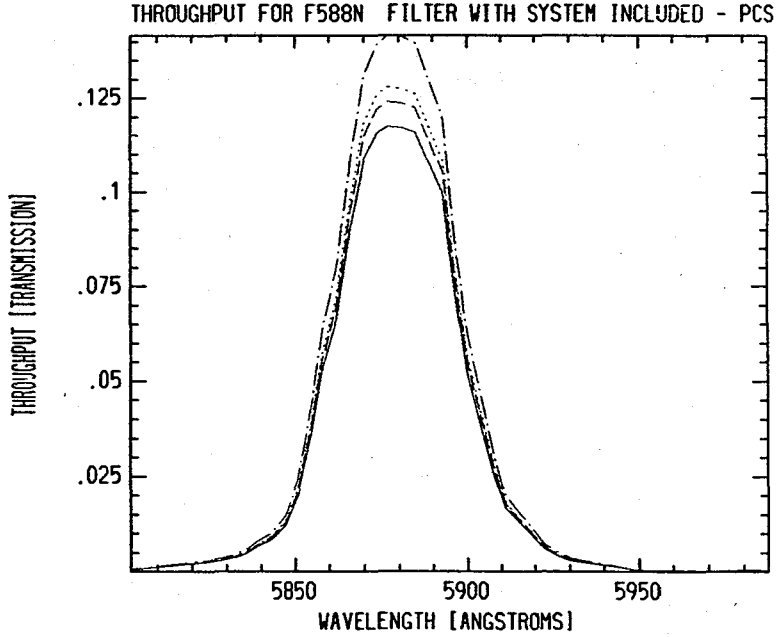
THROUGHPUT FOR F588N FILTER WITH SYSTEM INCLUDED - PCS
THROUGHPUT [TRANSMISSION]
.125
.1
.075
.05
.025
5850
5900
5950
WAVELENGTH [ANGSTROMS]

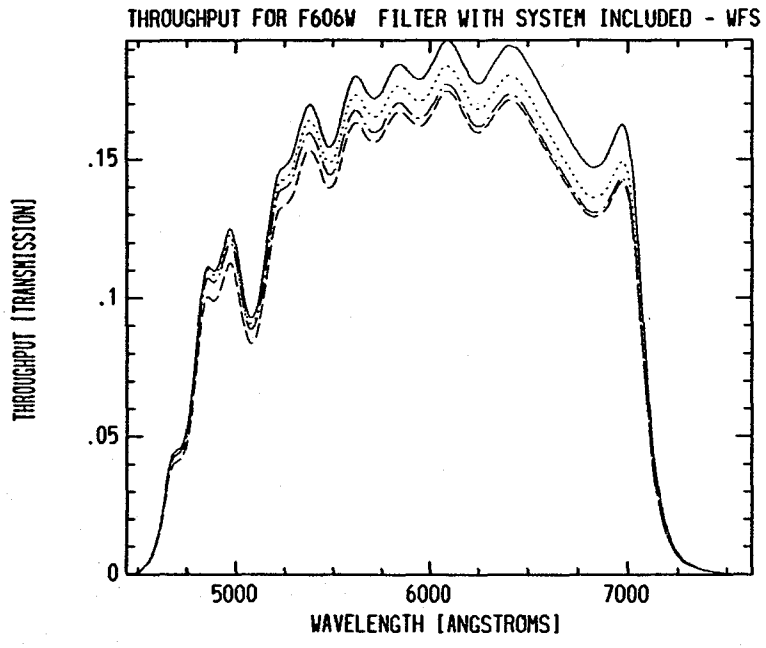
THROUGHPUT FOR F606W FILTER WITH SYSTEM INCLUDED - WFS
THROUGHPUT [TRANSMISSION]
0
.05
.1
.15
5000
6000
7000
WAVELENGTH [ANGSTROMS]

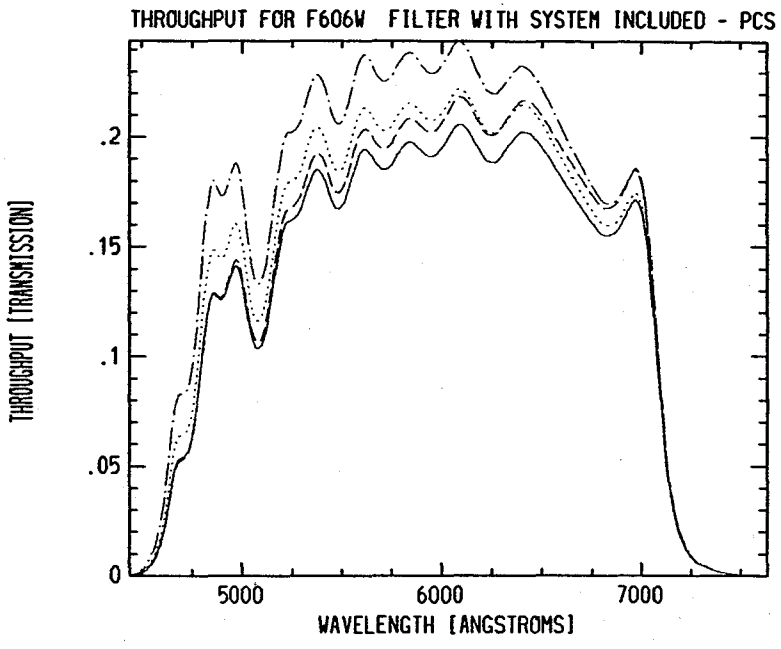
THROUGHPUT FOR F606W FILTER WITH SYSTEM INCLUDED - PCS
THROUGHPUT [TRANSMISSION]
0
.05
.1
.15
.2
5000
6000
7000
WAVELENGTH [ANGSTROMS]

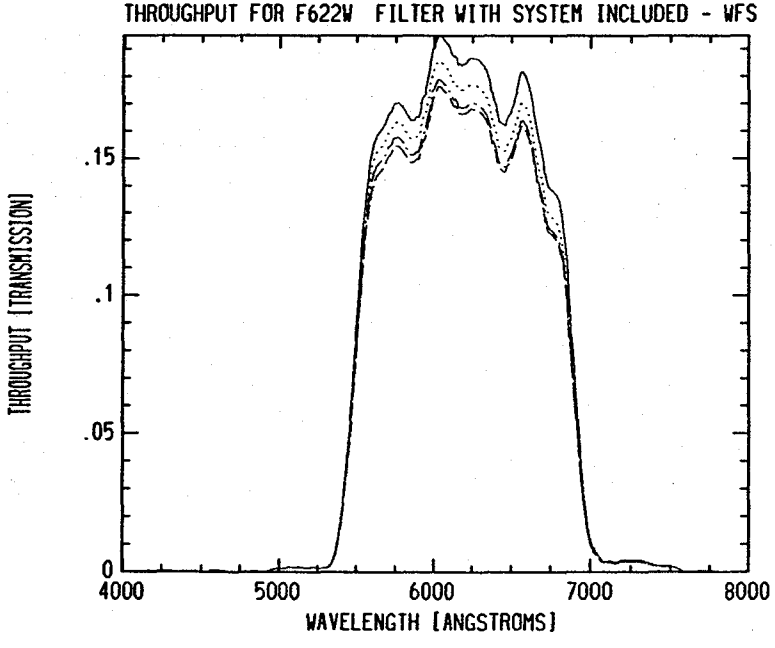
THROUGHPUT FOR F622W FILTER WITH SYSTEM INCLUDED - WFS
THROUGHPUT [TRANSMISSION]
0
.05
.1
.15
4000
5000
6000
7000
8000
WAVELENGTH [ANGSTROMS]

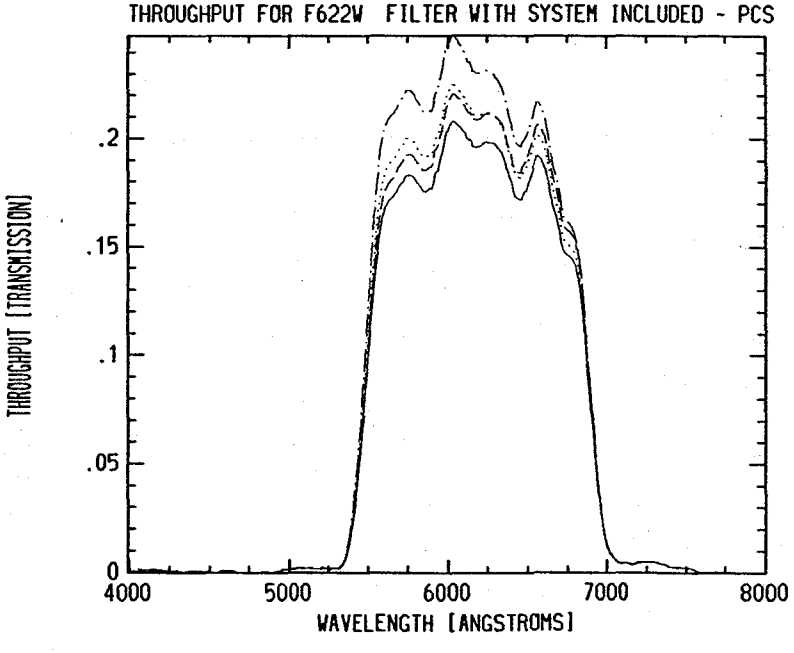
THROUGHPUT FOR F622W FILTER WITH SYSTEM INCLUDED - PCS
THROUGHPUT [TRANSMISSION]
0
.05
.1
.15
.2
4000
5000
6000
7000
8000
WAVELENGTH [ANGSTROMS]

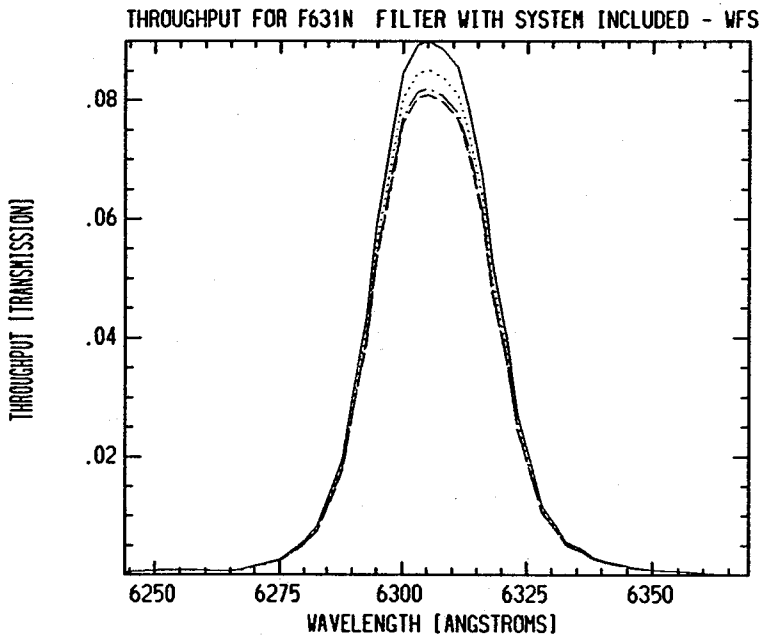
THROUGHPUT FOR F631N FILTER WITH SYSTEM INCLUDED - WFS
THROUGHPUT [TRANSMISSION]
.08
.06
.04
.02
6250
6275
6300
6325
6350
WAVELENGTH [ANGSTROMS]

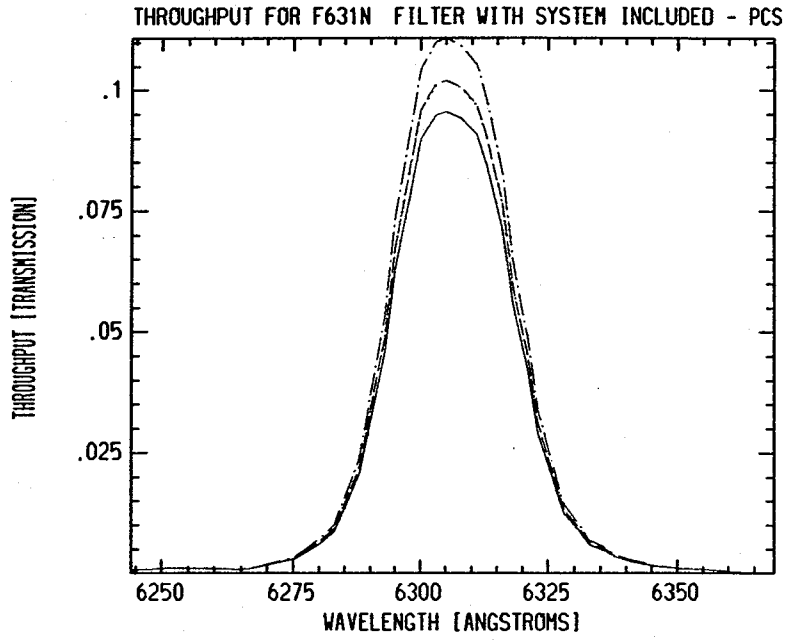
THROUGHPUT FOR F631N FILTER WITH SYSTEM INCLUDED - PCS
THROUGHPUT [TRANSMISSION]
.1
.075
.05
.025
6250
6275
6300
6325
6350
WAVELENGTH [ANGSTROMS]

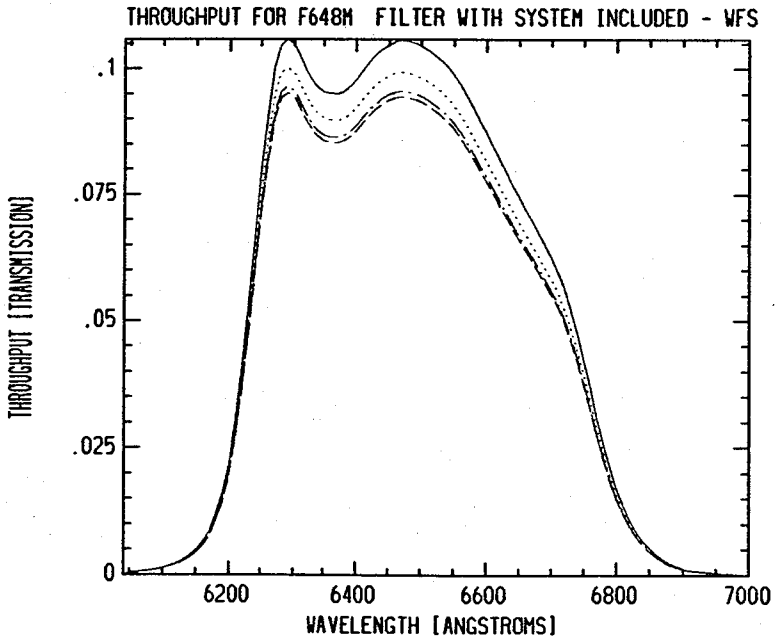
THROUGHPUT FOR F648M FILTER WITH SYSTEM INCLUDED - WFS
THROUGHPUT [TRANSMISSION]
.1
.075
.05
.025
0
6200
6400
6600
6800
7000
WAVELENGTH [ANGSTROMS]

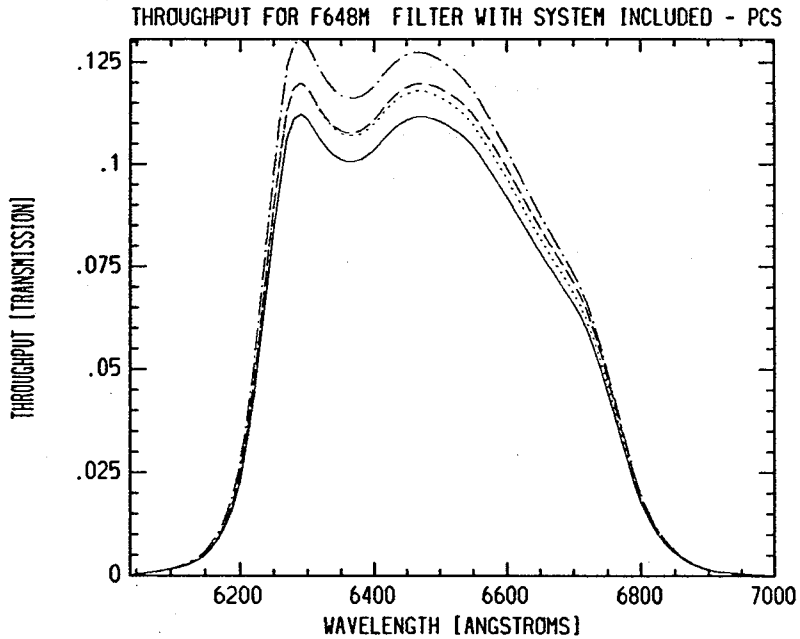
THROUGHPUT FOR F648M FILTER WITH SYSTEM INCLUDED - PCS
THROUGHPUT [TRANSMISSION]
.125
.1
.075
.05
.025
0
6200
6400
6600
6800
7000
WAVELENGTH [ANGSTROMS]

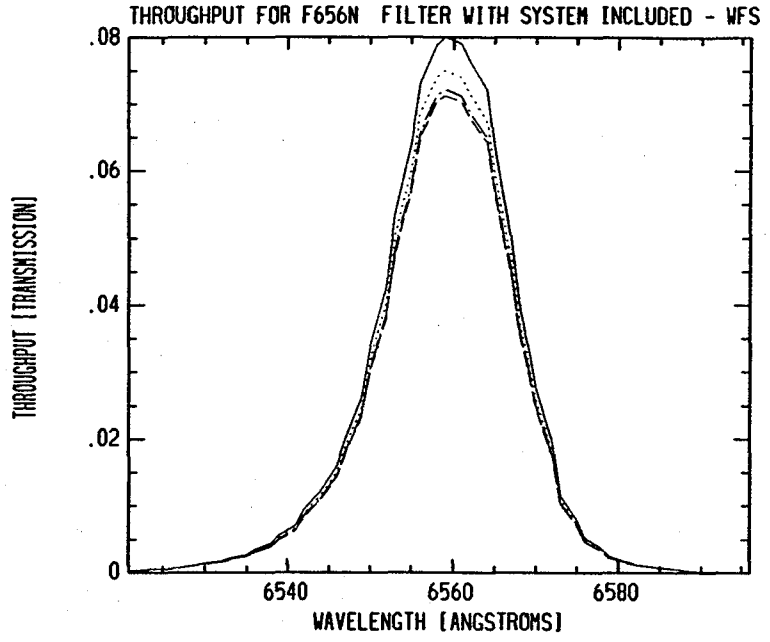
THROUGHPUT FOR F656N FILTER WITH SYSTEM INCLUDED - WFS
THROUGHPUT [TRANSMISSION]
.08
.06
.04
.02
0
6540
6560
6580
WAVELENGTH [ANGSTROMS]

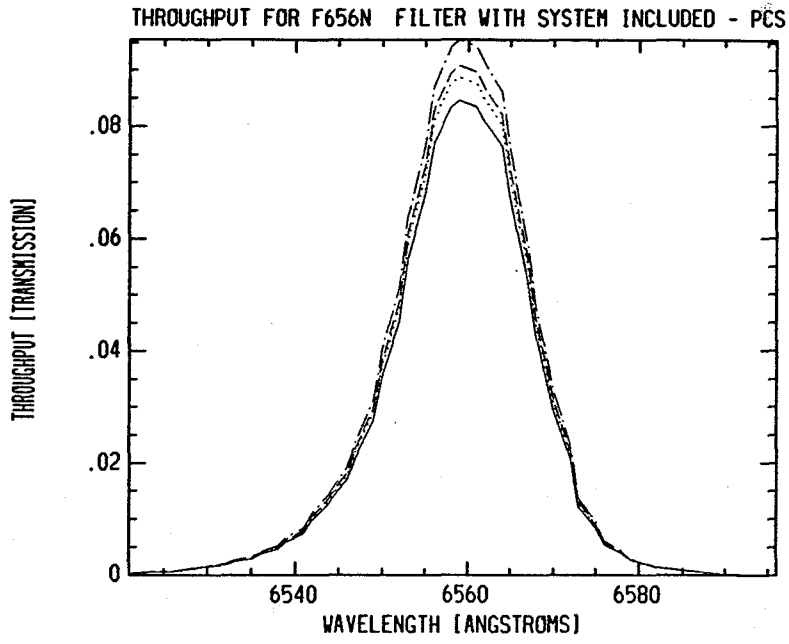
THROUGHPUT FOR F656N FILTER WITH SYSTEM INCLUDED - PCS
THROUGHPUT [TRANSMISSION]
.08
.06
.04
.02
0
6540
6560
6580
WAVELENGTH [ANGSTROMS]

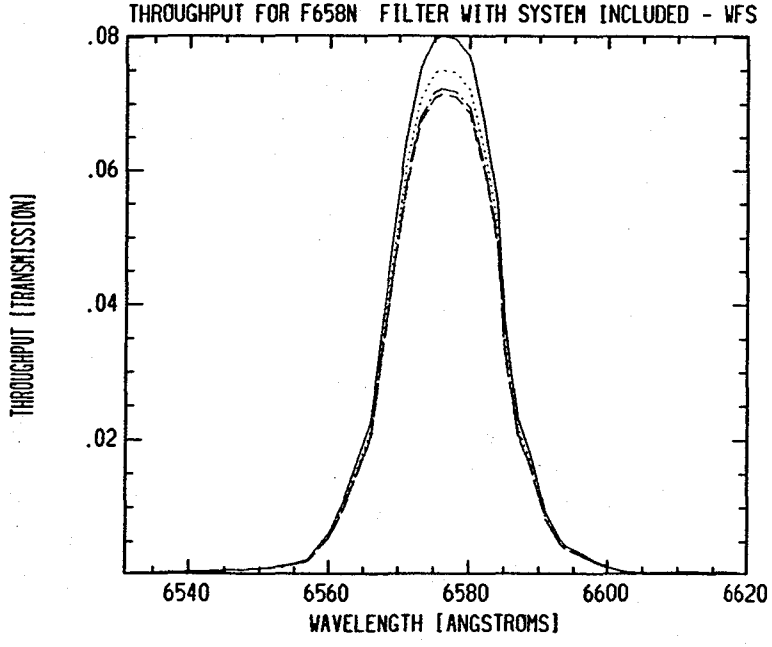
THROUGHPUT FOR F658N FILTER WITH SYSTEM INCLUDED - WFS
THROUGHPUT [TRANSMISSION]
.08
.06
.04
.02
6540
6560
6580
6600
6620
WAVELENGTH [ANGSTROMS]

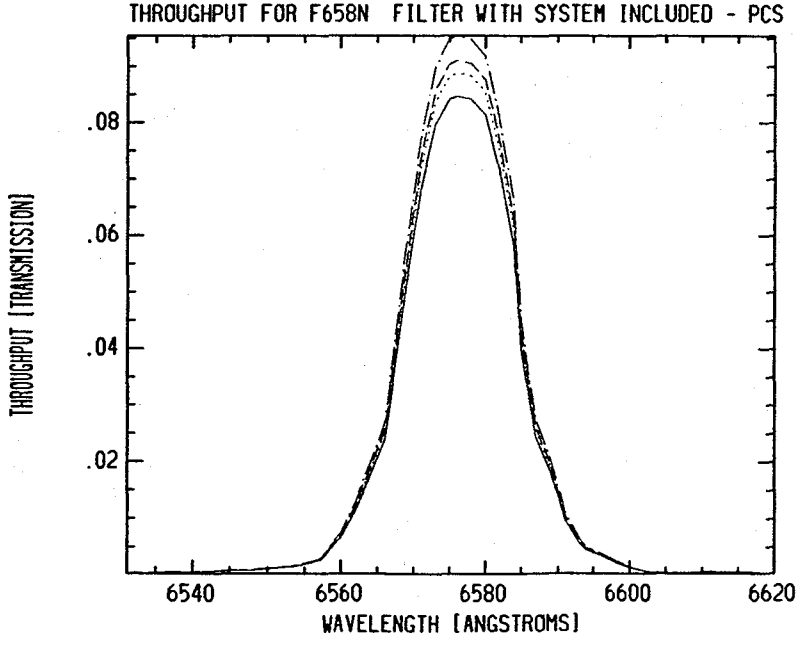
THROUGHPUT FOR F658N FILTER WITH SYSTEM INCLUDED - PCS
THROUGHPUT [TRANSMISSION]
.08
.06
.04
.02
6540
6560
6580
6600
6620
WAVELENGTH [ANGSTROMS]

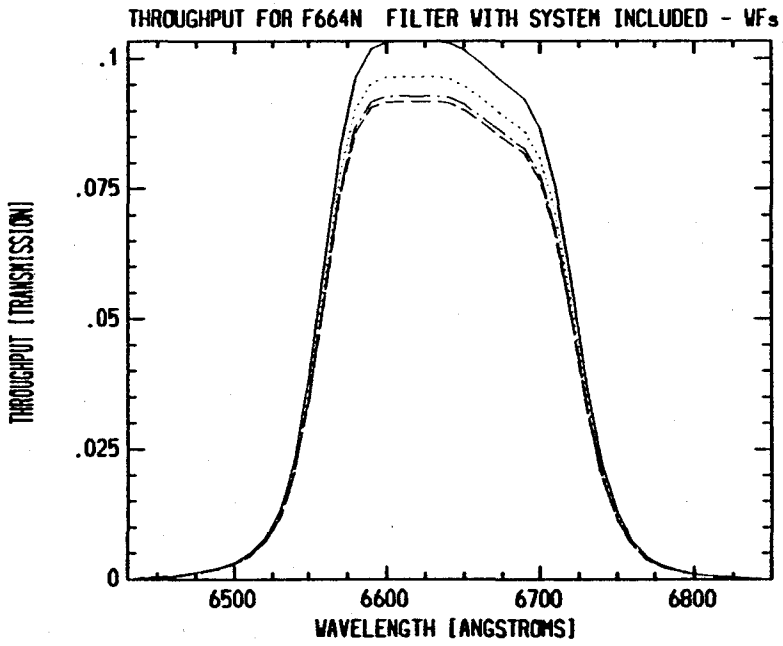
THROUGHPUT FOR F664N FILTER WITH SYSTEM INCLUDED - WFs
THROUGHPUT [TRANSMISSION]
.1
.075
.05
.025
0
6500
6600
6700
6800
WAVELENGTH [ANGSTROMS]

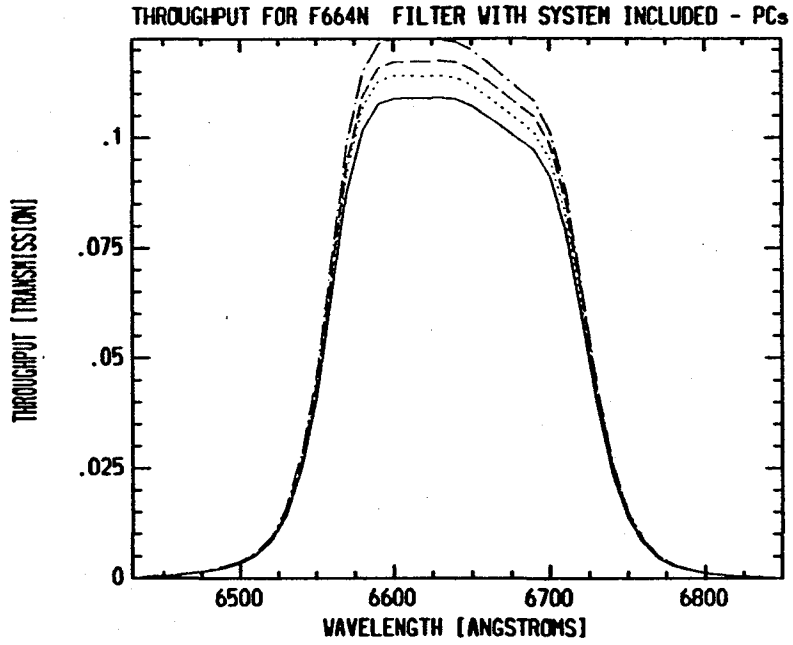
THROUGHPUT FOR F664N FILTER WITH SYSTEM INCLUDED - PCs
THROUGHPUT [TRANSMISSION]
.1
.075
.05
.025
0
6500
6600
6700
6800
WAVELENGTH [ANGSTROMS]

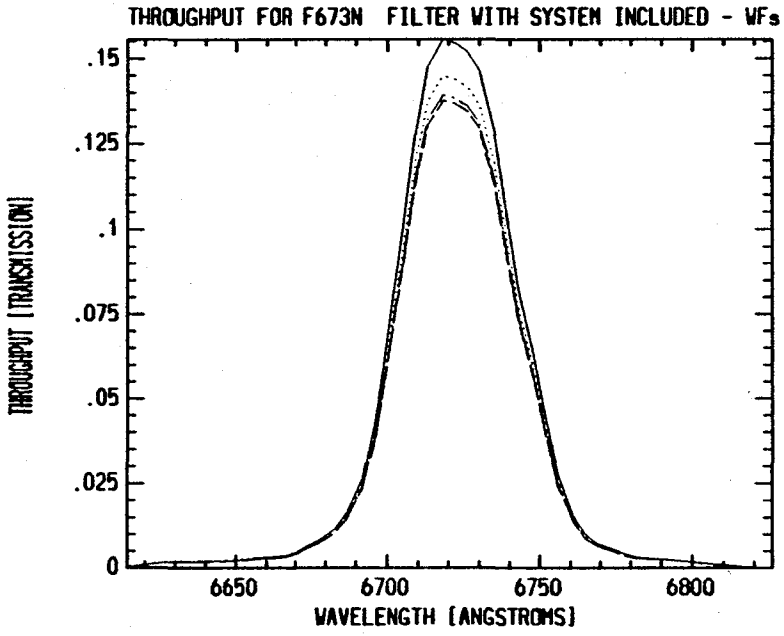
THROUGHPUT FOR F673N FILTER WITH SYSTEM INCLUDED - WFs
THROUGHPUT [TRANSMISSION]
.15
.125
.1
.075
.05
.025
0
6650
6700
6750
6800
WAVELENGTH [ANGSTROMS]

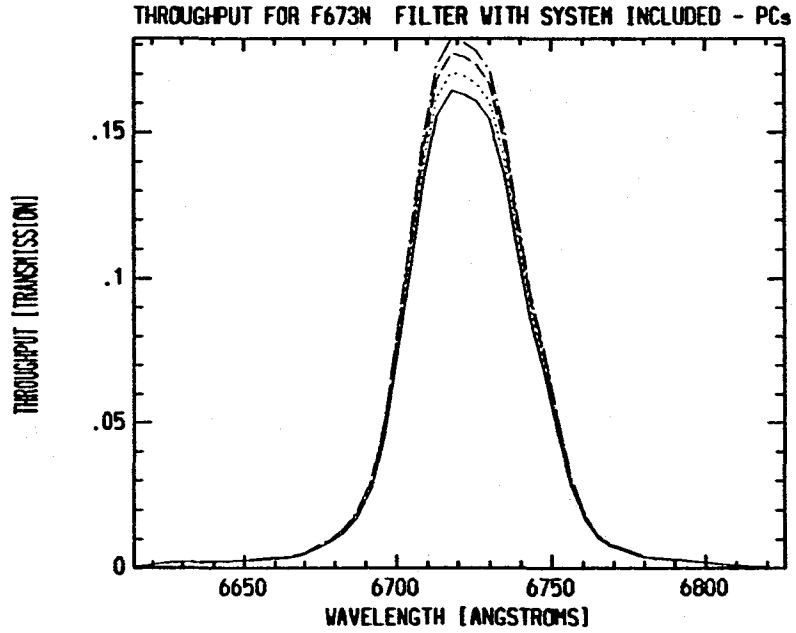
THROUGHPUT FOR F673N FILTER WITH SYSTEM INCLUDED - PCs
THROUGHPUT [TRANSMISSION]
.15
.1
.05
0
6650
6700
6750
6800
WAVELENGTH [ANGSTROMS]

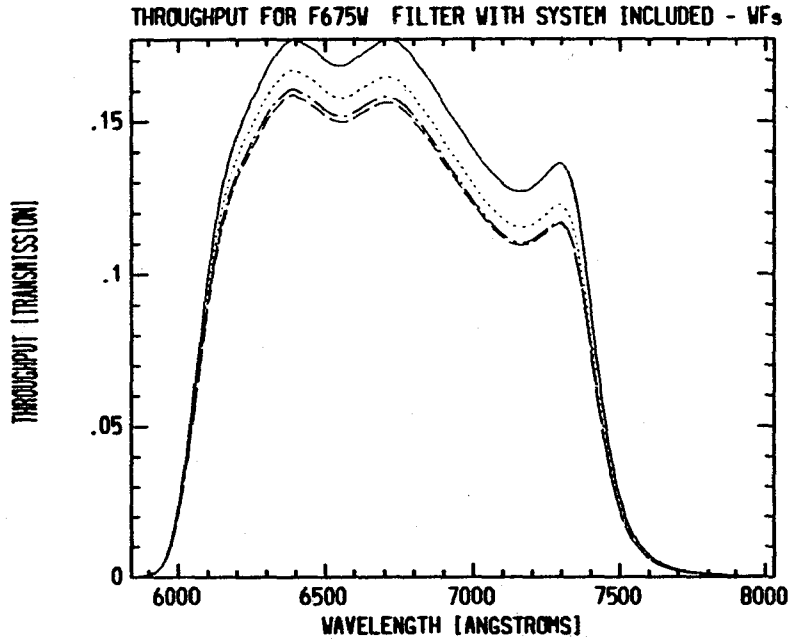
THROUGHPUT FOR F675W FILTER WITH SYSTEM INCLUDED - WFs
THROUGHPUT [TRANSMISSION]
0
.05
.1
.15
6000
6500
7000
7500
8000
WAVELENGTH [ANGSTROMS]

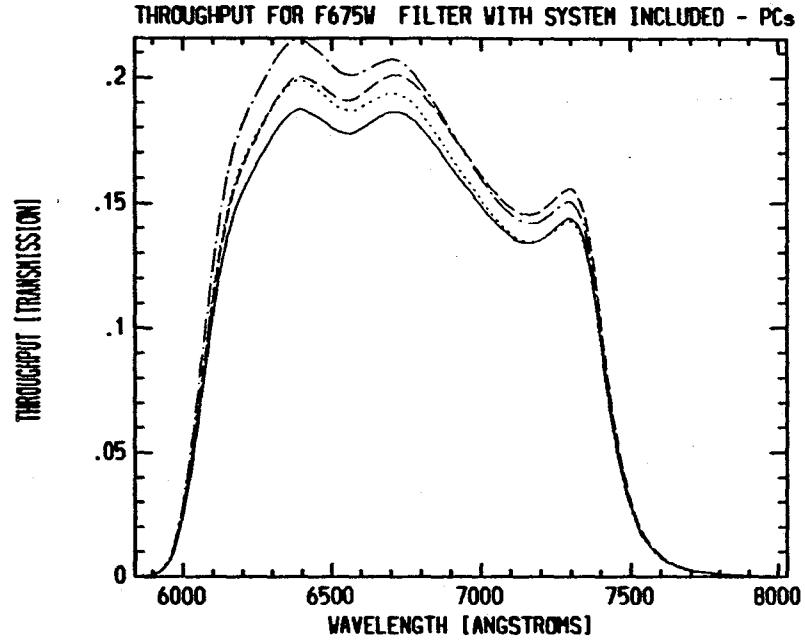
THROUGHPUT FOR F675W FILTER WITH SYSTEM INCLUDED - PCs
THROUGHPUT [TRANSMISSION]
0
.05
.1
.15
.2
6000
6500
7000
7500
8000
WAVELENGTH [ANGSTROMS]

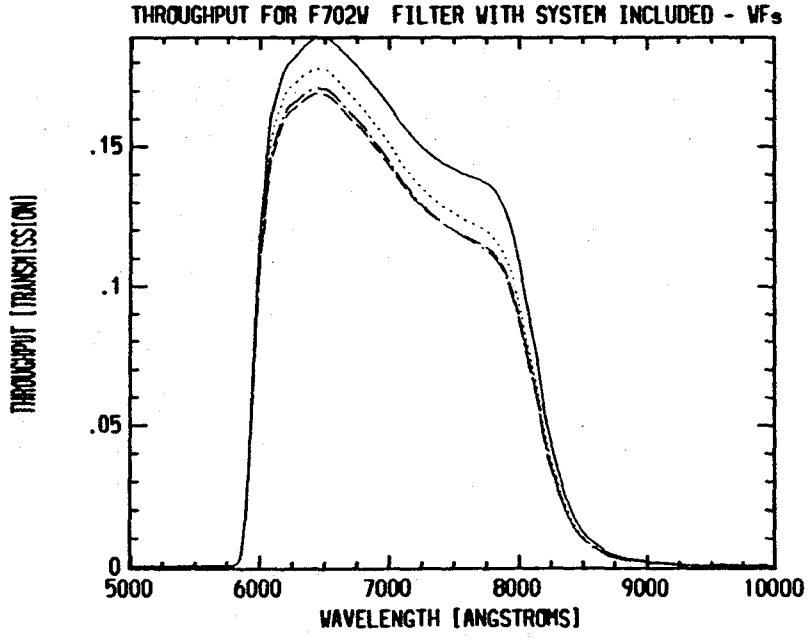
THROUGHPUT FOR F702W FILTER WITH SYSTEM INCLUDED - WFs
THROUGHPUT [TRANSMISSION]
0
.05
.1
.15
5000
6000
7000
8000
9000
10000
WAVELENGTH [ANGSTROMS]

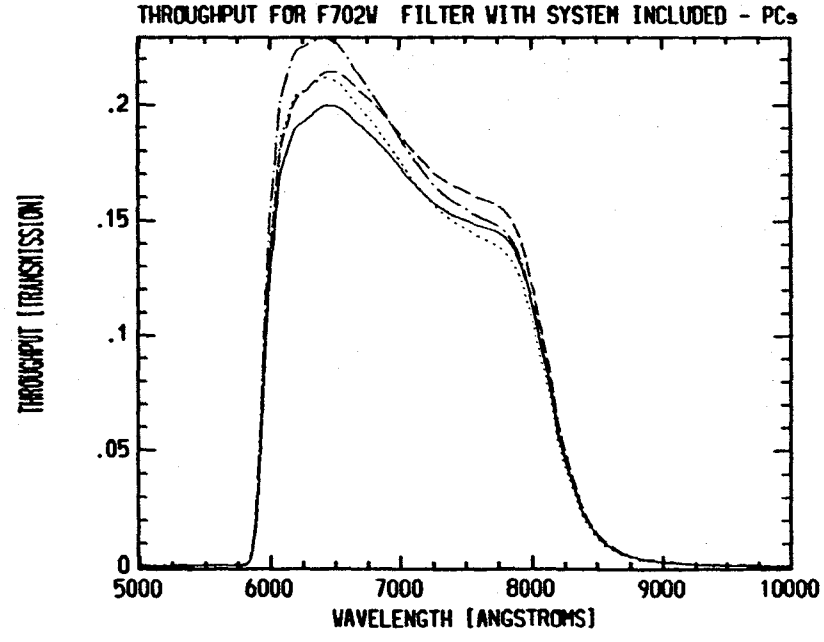
THROUGHPUT FOR F702W FILTER WITH SYSTEM INCLUDED - PCs
THROUGHPUT [TRANSMISSION]
0
.05
.1
.15
.2
5000
6000
7000
8000
9000
10000
WAVELENGTH [ANGSTROMS]

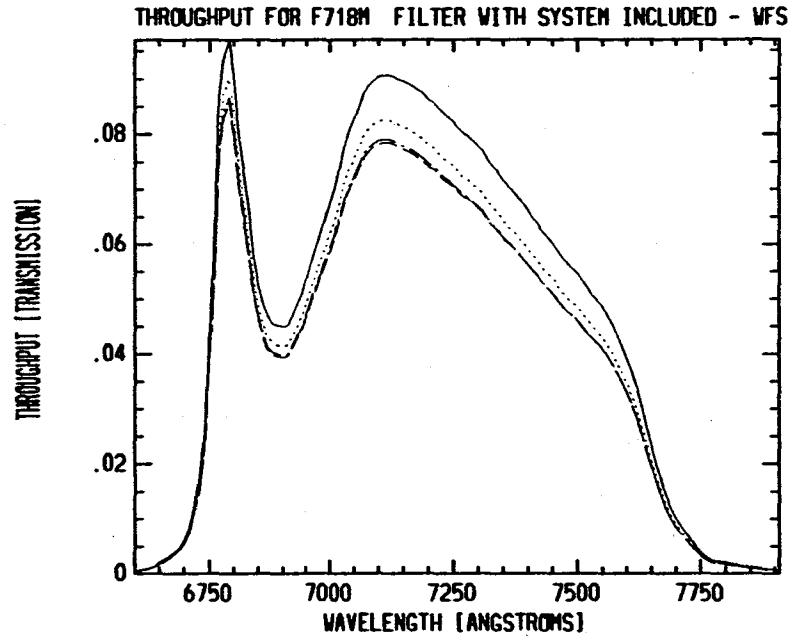
THROUGHPUT FOR F718M FILTER WITH SYSTEM INCLUDED - WFS
THROUGHPUT [TRANSMISSION]
.08
.06
.04
.02
0
6750
7000
7250
7500
7750
WAVELENGTH [ANGSTROMS]

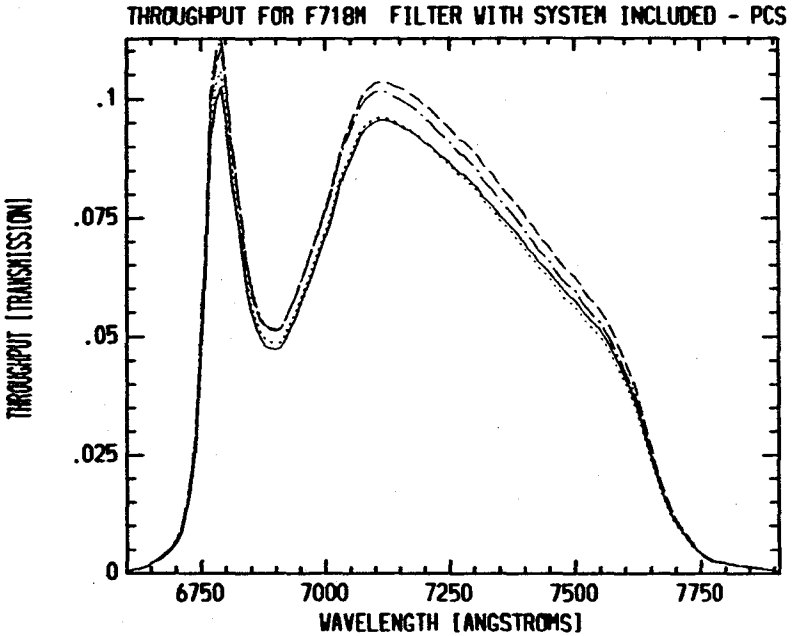
THROUGHPUT FOR F718M FILTER WITH SYSTEM INCLUDED - PCS
THROUGHPUT [TRANSMISSION]
.1
.075
.05
.025
0
6750
7000
7250
7500
7750
WAVELENGTH [ANGSTROMS]

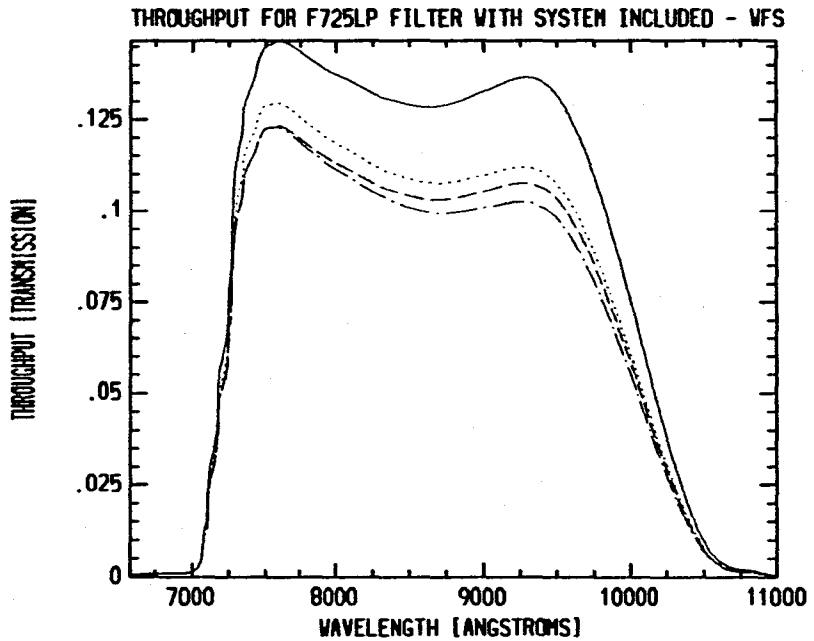
THROUGHPUT FOR F725LP FILTER WITH SYSTEM INCLUDED - WFS
THROUGHPUT [TRANSMISSION]
.125
.1
.075
.05
.025
0
7000
8000
9000
10000
11000
WAVELENGTH [ANGSTROMS]

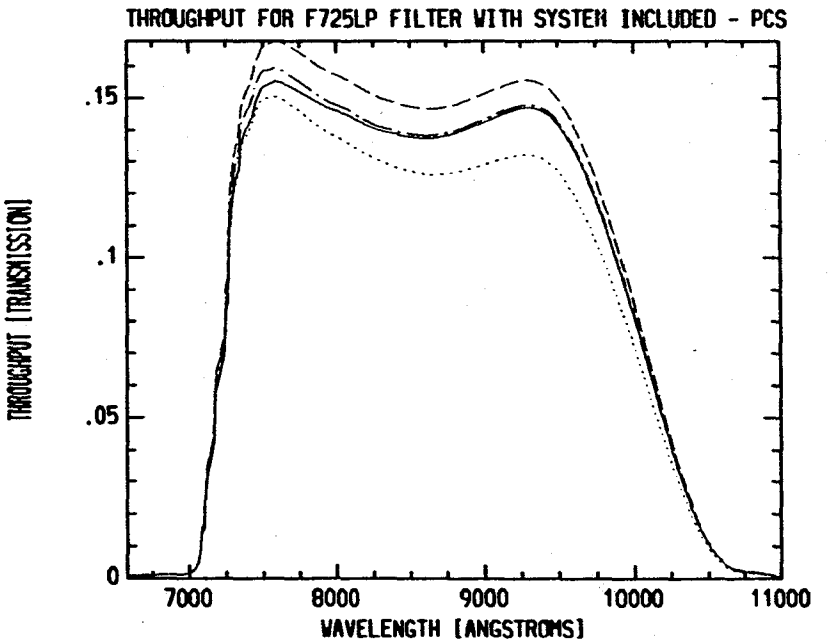
THROUGHPUT FOR F725LP FILTER WITH SYSTEM INCLUDED - PCS
THROUGHPUT [TRANSMISSION]
.15
.1
.05
0
7000
8000
9000
10000
11000
WAVELENGTH [ANGSTROMS]

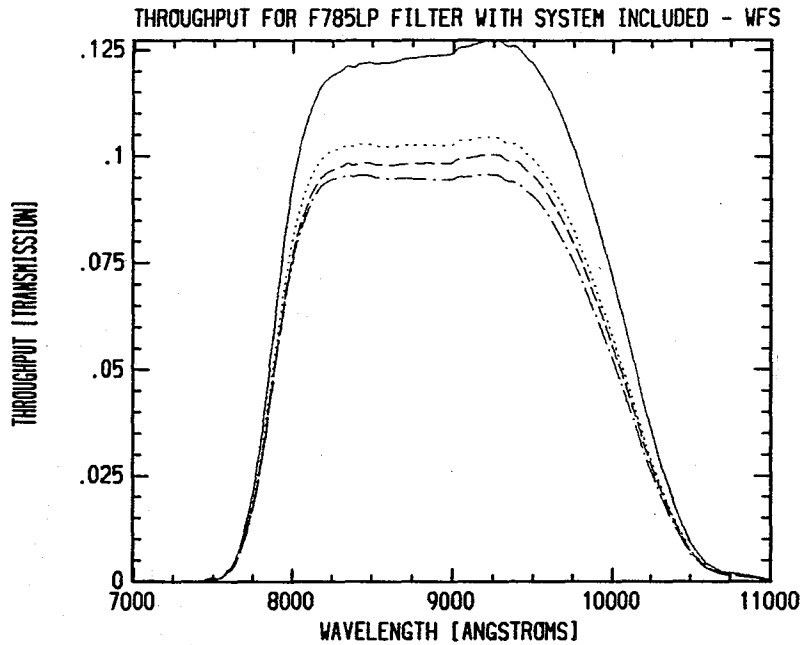
THROUGHPUT FOR F785LP FILTER WITH SYSTEM INCLUDED - WFS
THROUGHPUT [TRANSMISSION]
.125
.1
.075
.05
.025
0
7000
8000
9000
10000
11000
WAVELENGTH [ANGSTROMS]

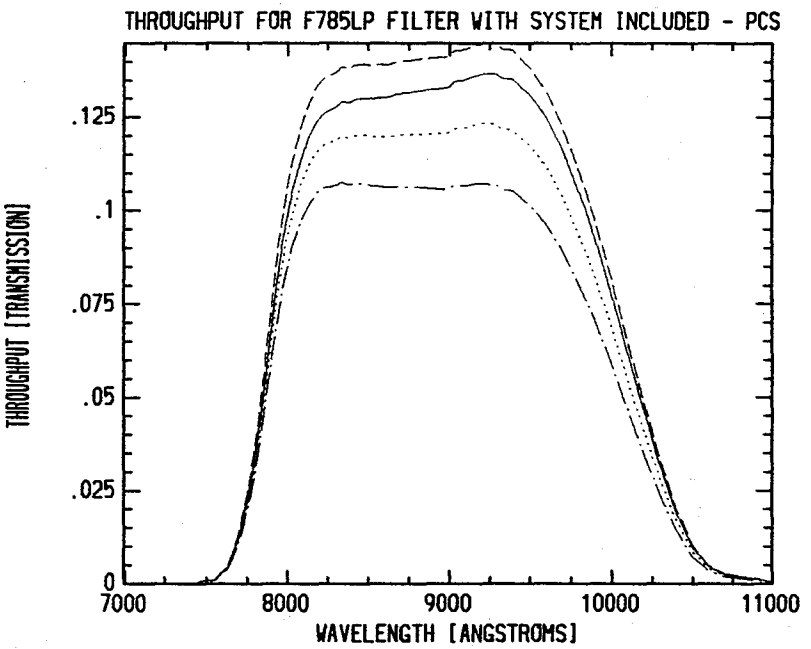
THROUGHPUT FOR F785LP FILTER WITH SYSTEM INCLUDED - PCS
THROUGHPUT [TRANSMISSION]
.125
.1
.075
.05
.025
0
7000
8000
9000
10000
11000
WAVELENGTH [ANGSTROMS]

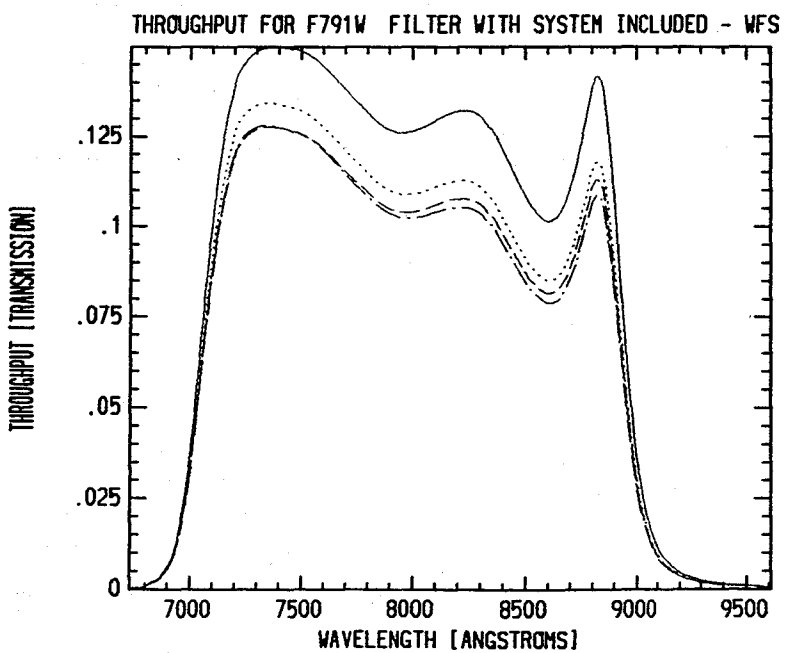
THROUGHPUT FOR F791W FILTER WITH SYSTEM INCLUDED - WFS
THROUGHPUT [TRANSMISSION]
.125
.1
.075
.05
.025
0
7000
7500
8000
8500
9000
9500
WAVELENGTH [ANGSTROMS]

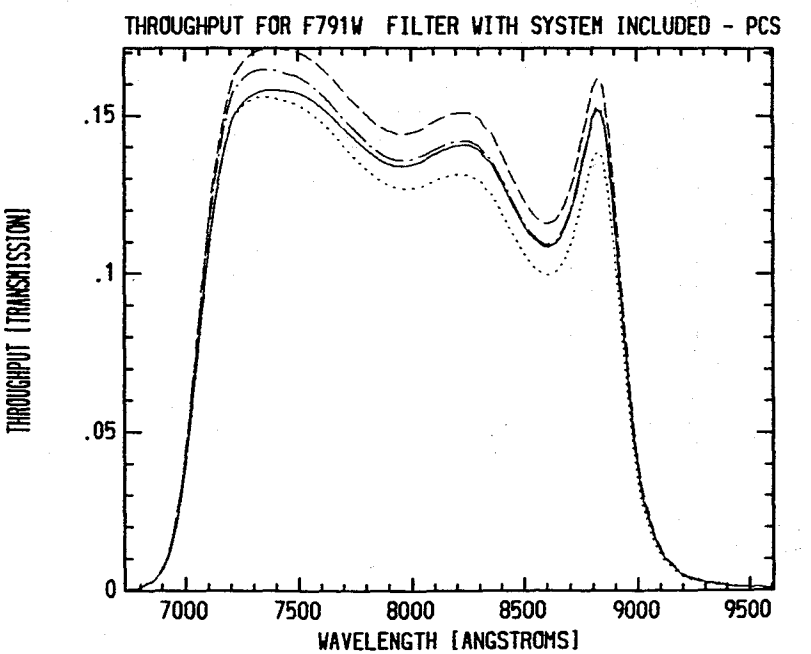
THROUGHPUT FOR F791W FILTER WITH SYSTEM INCLUDED - PCS
THROUGHPUT [TRANSMISSION]
.15
.1
.05
0
7000
7500
8000
8500
9000
9500
WAVELENGTH [ANGSTROMS]

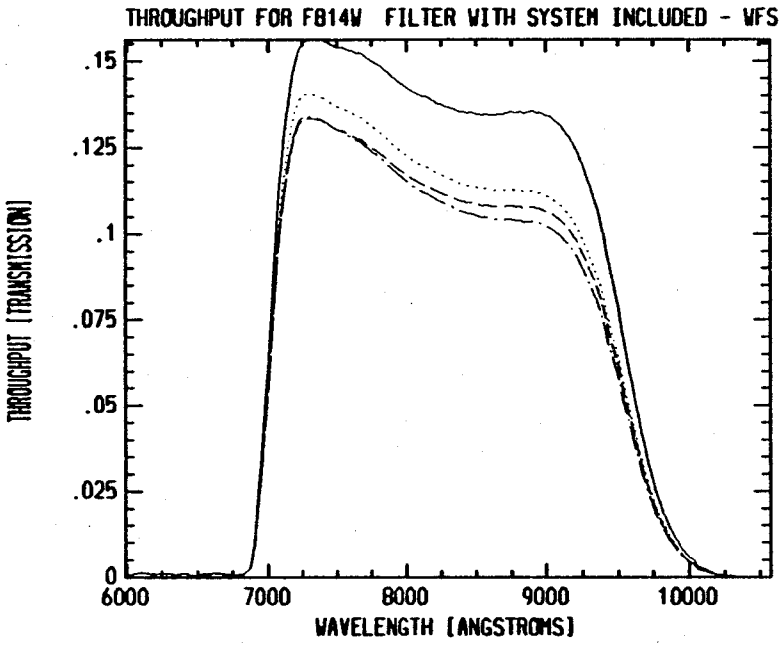
THROUGHPUT FOR F814W FILTER WITH SYSTEM INCLUDED - WFS
THROUGHPUT [TRANSMISSION]
.15
.125
.1
.075
.05
.025
0
6000
7000
8000
9000
10000
WAVELENGTH [ANGSTROMS]

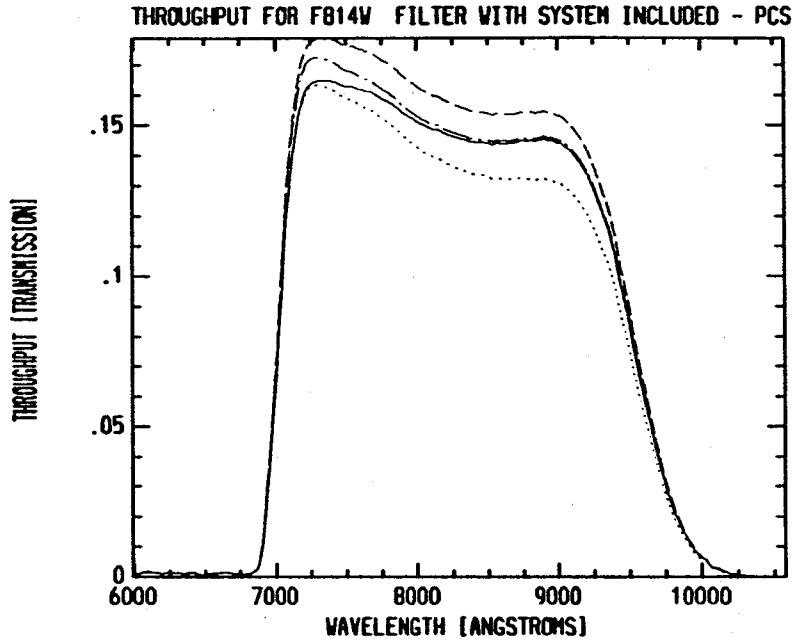
THROUGHPUT FOR F814W FILTER WITH SYSTEM INCLUDED - PCS
THROUGHPUT [TRANSMISSION]
.15
.1
.05
0
6000
7000
8000
9000
10000
WAVELENGTH [ANGSTROMS]

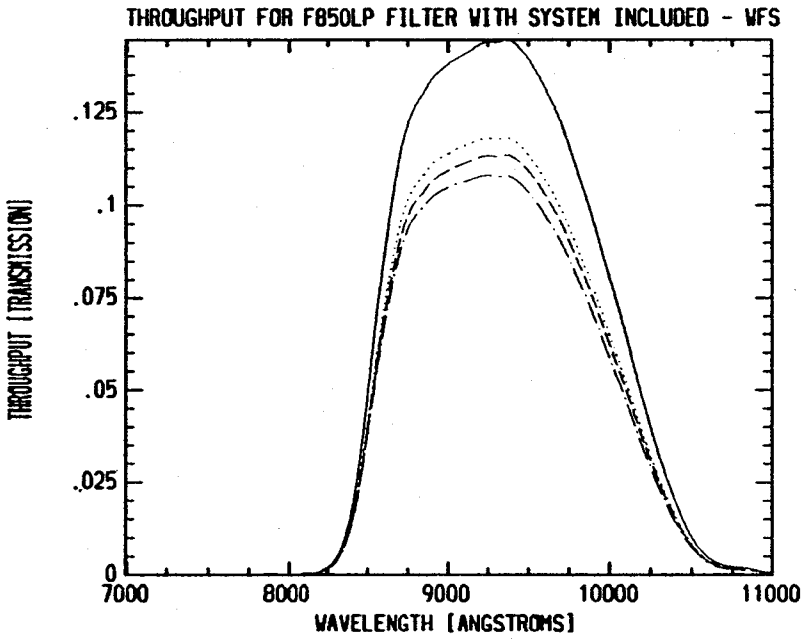
THROUGHPUT FOR F850LP FILTER WITH SYSTEM INCLUDED - WFS
THROUGHPUT [TRANSMISSION]
.125
.1
.075
.05
.025
0
7000
8000
9000
10000
11000
WAVELENGTH [ANGSTROMS]

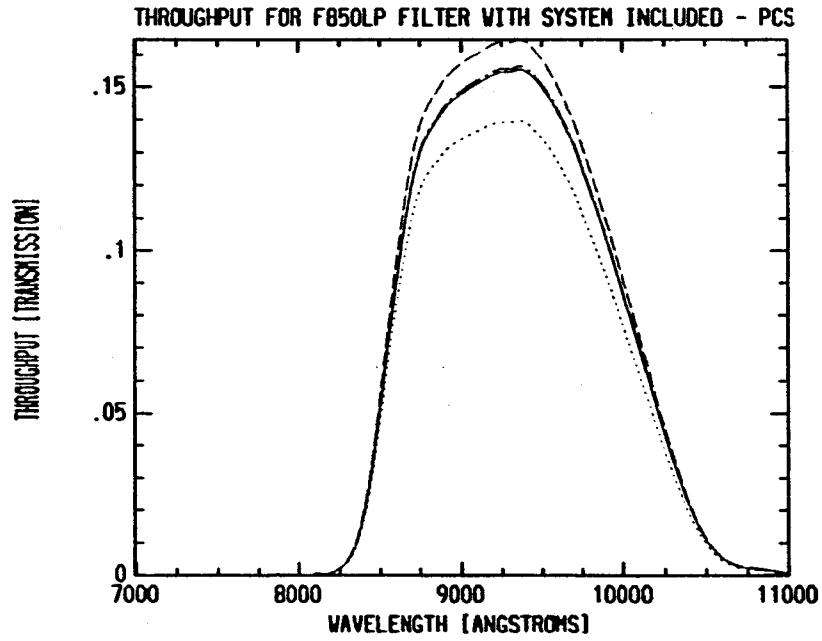
THROUGHPUT FOR F850LP FILTER WITH SYSTEM INCLUDED - PCS
THROUGHPUT [TRANSMISSION]
.15
.1
.05
0
7000
8000
9000
10000
11000
WAVELENGTH [ANGSTROMS]

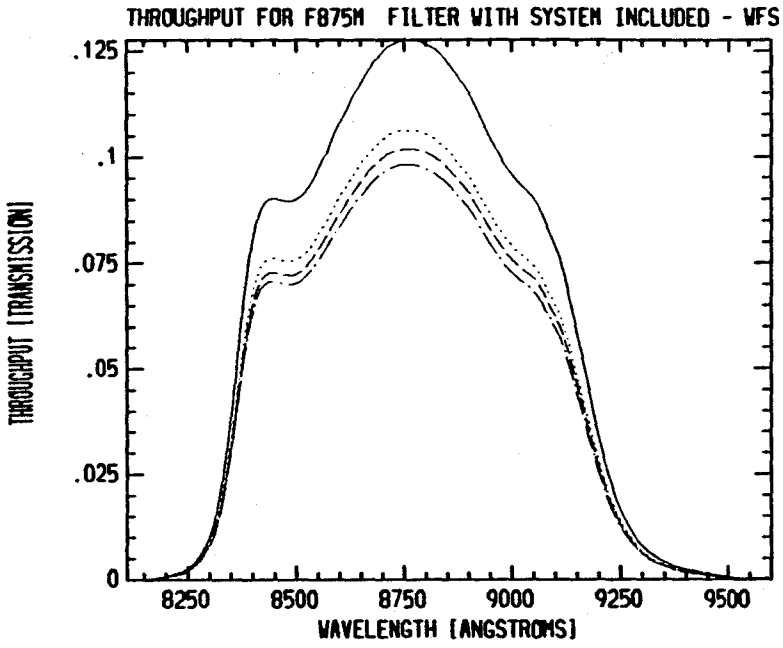
THROUGHPUT FOR F875M FILTER WITH SYSTEM INCLUDED - WFS
THROUGHPUT [TRANSMISSION]
.125
.1
.075
.05
.025
0
8250
8500
8750
9000
9250
9500
WAVELENGTH [ANGSTROMS]

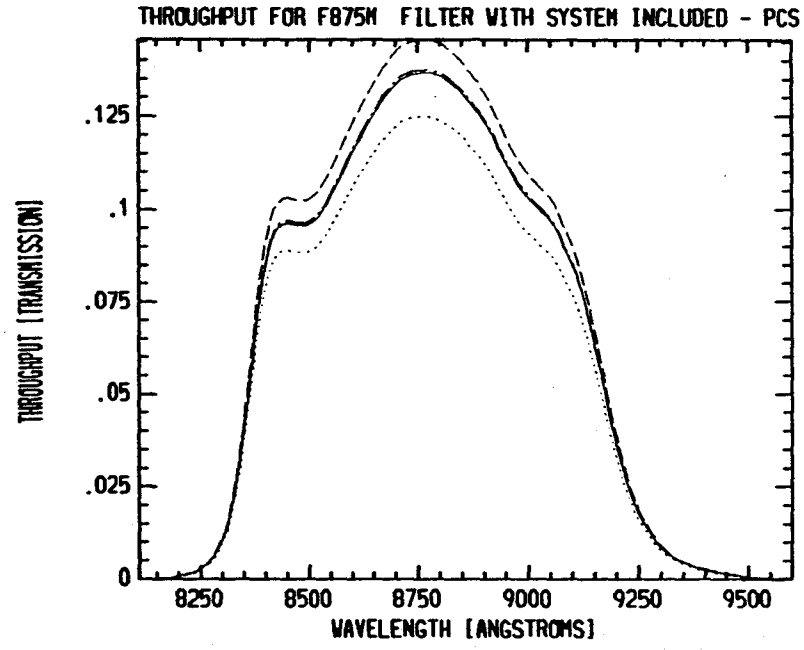
THROUGHPUT FOR F875M FILTER WITH SYSTEM INCLUDED - PCS
THROUGHPUT [TRANSMISSION]
.125
.1
.075
.05
.025
0
8250
8500
8750
9000
9250
9500
WAVELENGTH [ANGSTROMS]

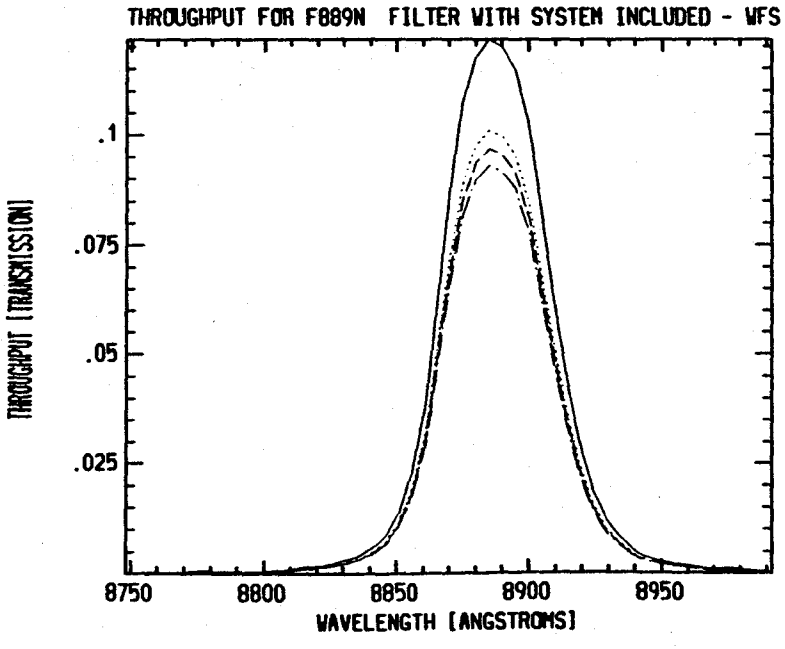
THROUGHPUT FOR F889N FILTER WITH SYSTEM INCLUDED - WFS
THROUGHPUT [TRANSMISSION]
.1
.075
.05
.025
8750
8800
8850
8900
8950
WAVELENGTH [ANGSTROMS]

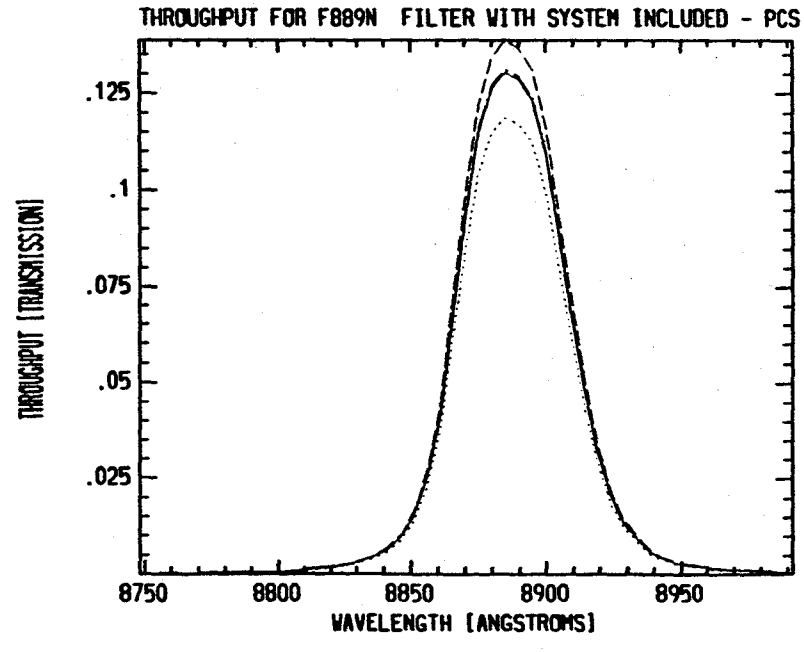
THROUGHPUT FOR F889N FILTER WITH SYSTEM INCLUDED - PCS
THROUGHPUT [TRANSMISSION]
.125
.1
.075
.05
.025
8750
8800
8850
8900
8950
WAVELENGTH [ANGSTROMS]

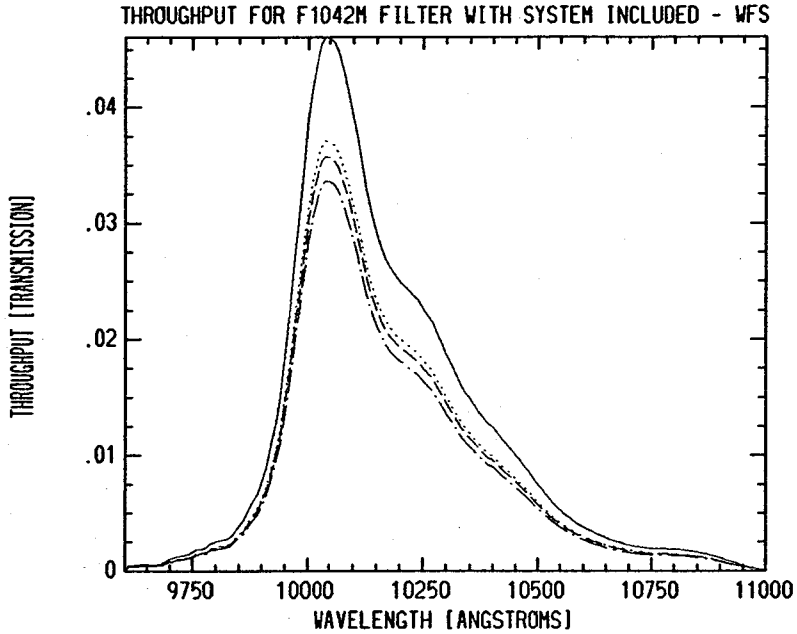
THROUGHPUT FOR F1042M FILTER WITH SYSTEM INCLUDED - WFS
THROUGHPUT [TRANSMISSION]
.04
.03
.02
.01
0
9750
10000
10250
10500
10750
11000
WAVELENGTH [ANGSTROMS]

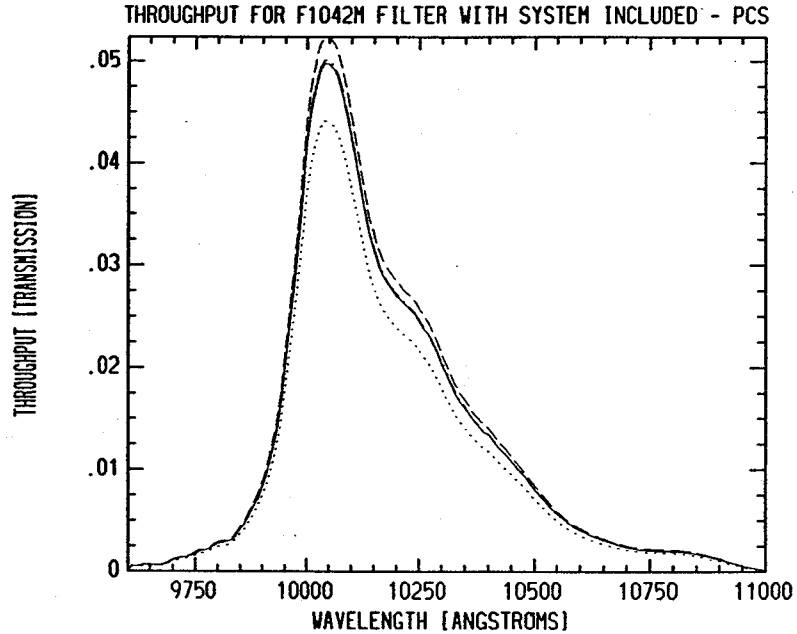
THROUGHPUT FOR F1042M FILTER WITH SYSTEM INCLUDED - PCS
THROUGHPUT [TRANSMISSION]
.05
.04
.03
.02
.01
0
9750
10000
10250
10500
10750
11000
WAVELENGTH [ANGSTROMS]

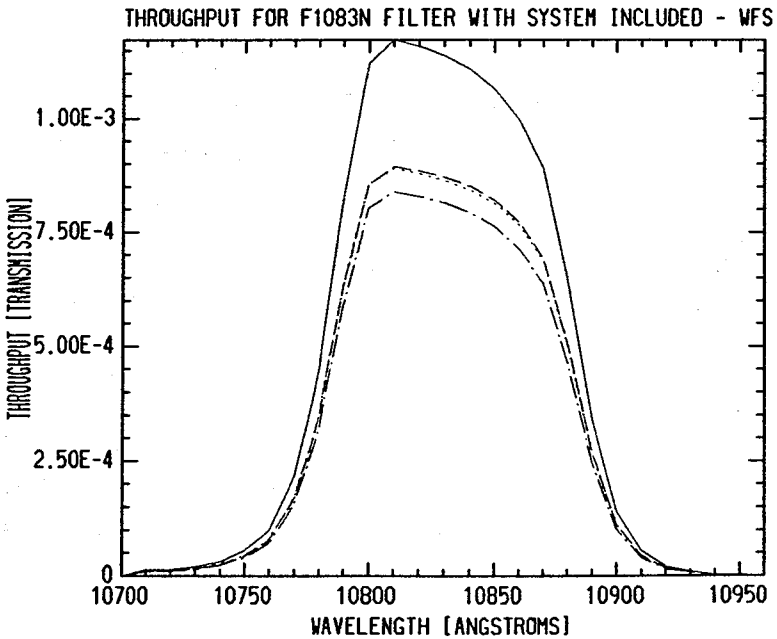
THROUGHPUT FOR F1083N FILTER WITH SYSTEM INCLUDED - WFS
THROUGHPUT [TRANSMISSION]
1.00E-3
7.50E-4
5.00E-4
2.50E-4
0
10700
10750
10800
10850
10900
10950
WAVELENGTH [ANGSTROMS]

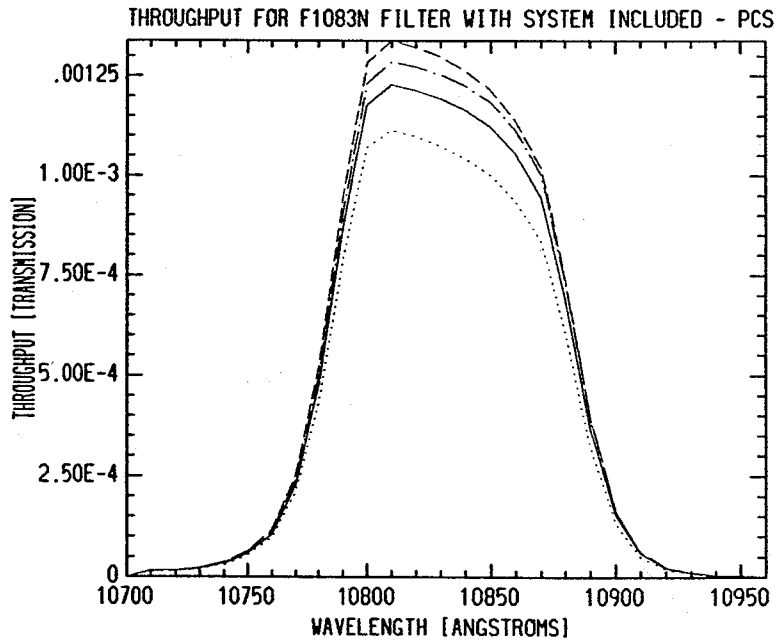
THROUGHPUT FOR F1083N FILTER WITH SYSTEM INCLUDED - PCS
THROUGHPUT [TRANSMISSION]
.00125
1.00E-3
7.50E-4
5.00E-4
2.50E-4
0
10700
10750
10800
10850
10900
10950
WAVELENGTH [ANGSTROMS]

Figure 3.2.5
Transmission curves for the gratings, including blaze envelopes

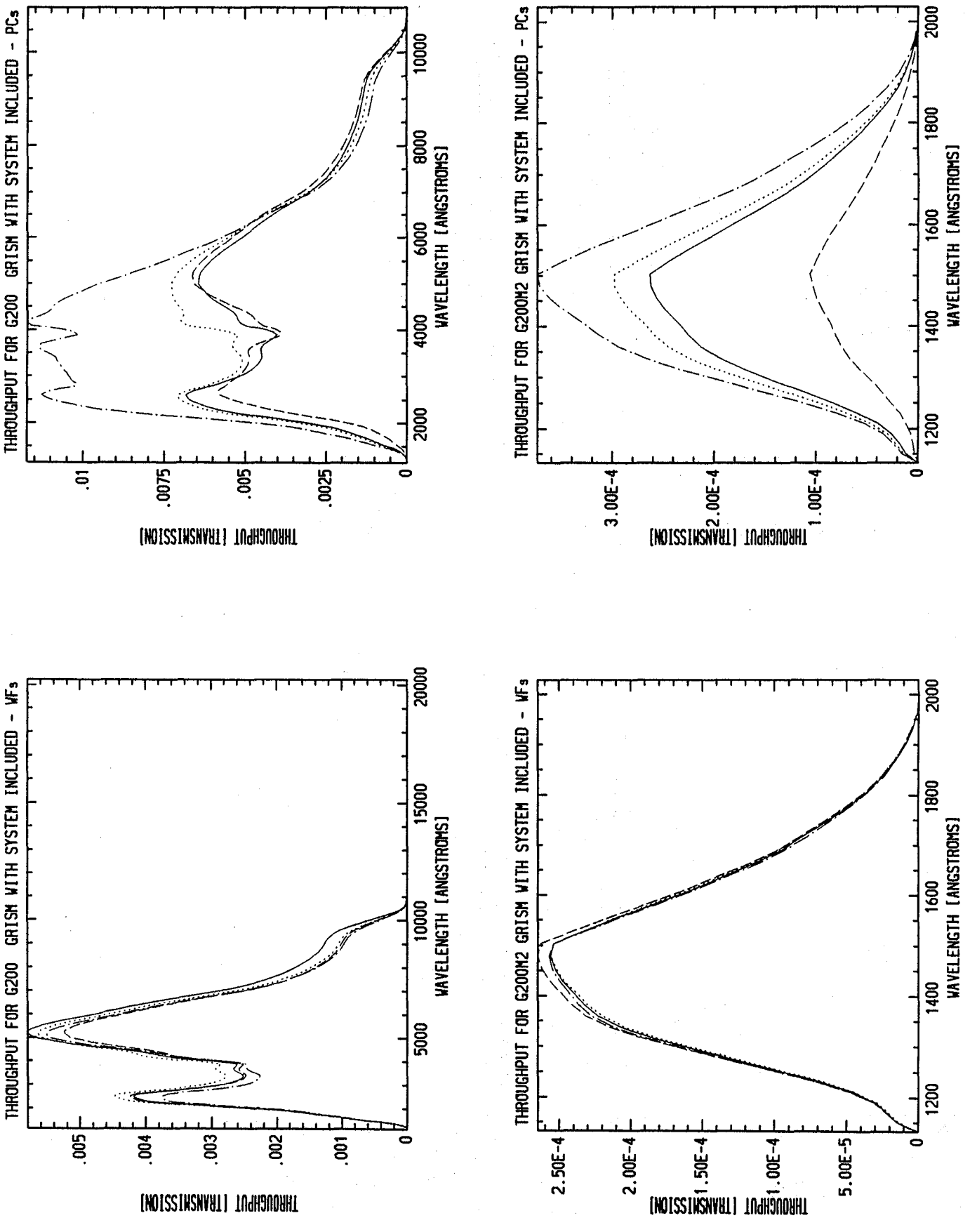

Figure 3.2.5
Transmission curves for the gratings, including blaze envelopes

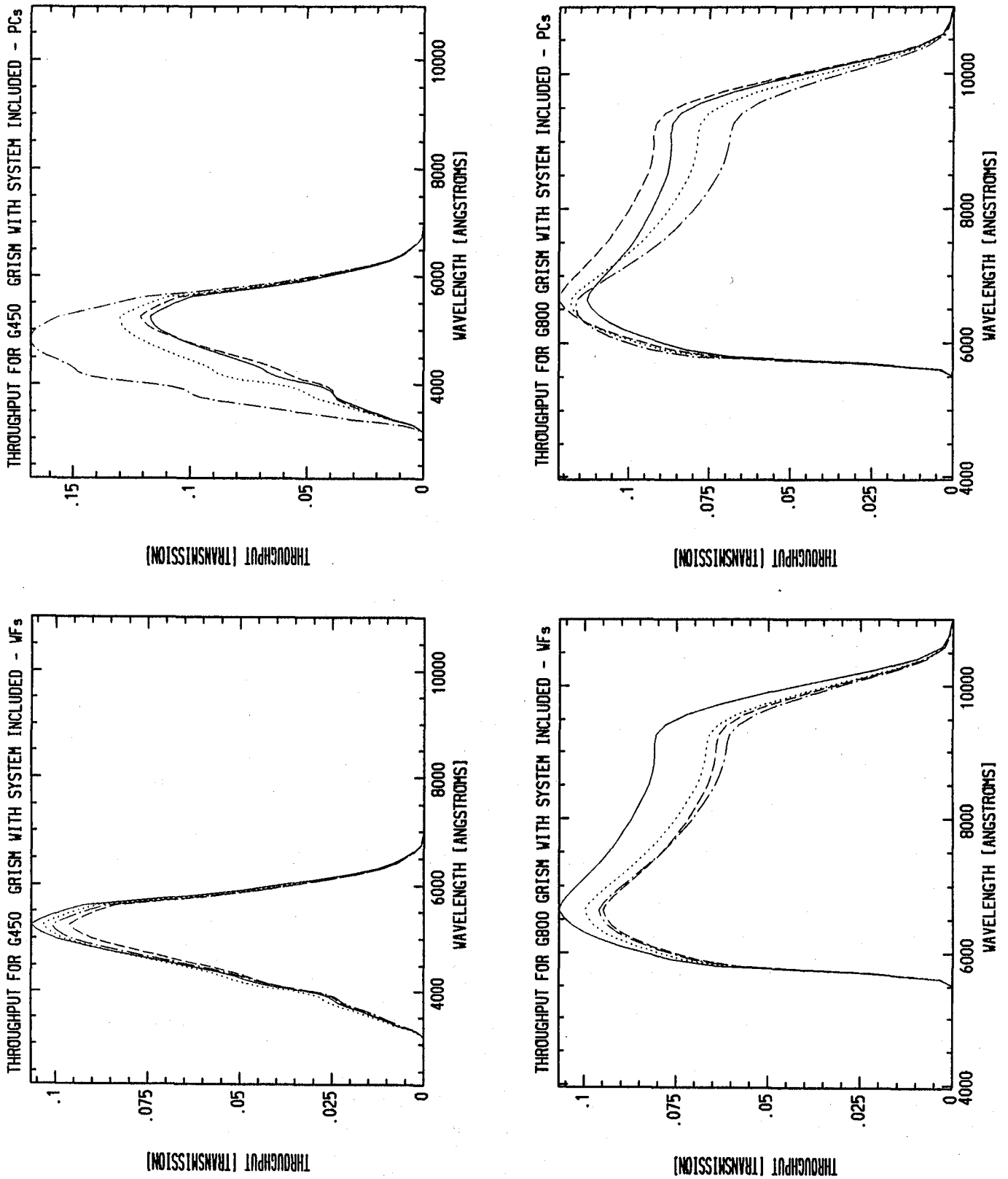

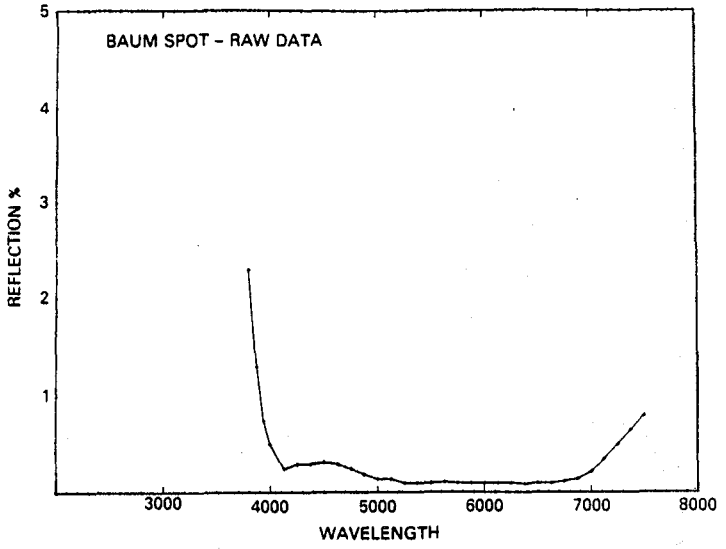

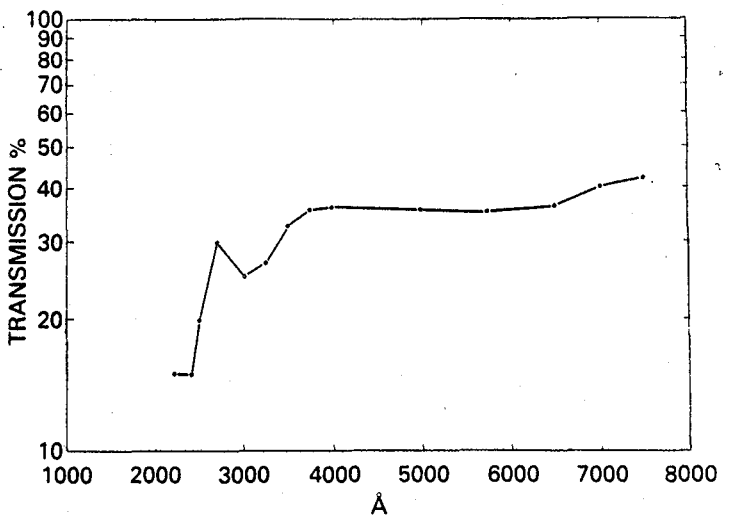

(left) Figure 3.3.1 Reflectance of Baum Spot
(right) Figure 3.2.4 Nominal transmission of WF/PC polarizers

3.5 CCD ORIENTATION AND READ-OUT

The relation between the pixels and lines for the four CCDs associated with each camera is shown in Figure 3.5.1. The 45° difference between the WFC and PC reflects the pyramid rotational difference for the two cameras. The counts for pixels and lines increase for the indicated CCDs in the manner described in Figure 3.5.1. Note that each CCD is similarly sequenced, so that their axes are defined by a 90° rotation from the adjacent CCD. If a given image were displayed from all the CCDs of a given camera (with pixels in the "X" direction and lines in the "Y" direction), each successive display would appear rotated by 90° from its predecessor. Any one, two, three of all four CCDs may be read out from either camera, in numerical order. The default operational mode will be to read out all four CCDs from the relevant camera.

The square area completely covered on the sky by the 4-part mosaic is thus 1543×1543 pixels in the WFC (154.5×154.5 arc sec) and 1531×1531 pixels in the PC (65.8×65.8 arcsec). Figure 3.5.1 illustrates the projected orientation of the WF/PC CCDs onto the sky . The diagram should be used in conjunction with the transparent overlay inserted at the back of the Call for Proposals (October 1985), The overlay does not show the relative enumeration of the CCDs in the cameras.

There is an optically inactive border of approximately 25 pixels along the two edges of each CCD which butt against the fields of view of neighboring CCDs (see Figure 3.5.1). The Kelsall spots are imaged at the boundaries of the optically active and inactive areas of each

TABLE 3.4.1

EXPOSURE TIMES

Exposure Time Sec.	Exposure Time Sec.	Exposure Time Sec.
0.11	140.	4.3E3
0.12	160.	4.4E3
0.14	180.	4.5E3
0.16	200.	4.6E3
0.18	230.	4.7E3
0.20	260.	4.8E3
0.23	300.	4.9E3
0.26	350.	5.0E3
0.30	400.	5.1E3
0.35	500.	5.2E3
0.40	600.	5.3E3
0.5	700.	5.4E3
0.6	800.	5.5E3
0.7	900.	5.6E3
0.8	1.0E3	5.8E3
1.0	1.1E3	6.0E3
1.2	1.2E3	6.2E3
1.4	1.3E3	6.4E3
1.6	1.4E3	6.6E3
1.8	1.5E3	6.8E3
2.0	1.6E3	7.0E3
2.3	1.7E3	7.5E3
2.6	1.8E3	8.0E3
3.0	1.9E3	8.5E3
3.5	2.0E3	9.0E3
4.0	2.1E3	1.0E4
5.0	2.2E3	1.5E4
6.0	2.3E3	2.0E4
7.0	2.4E3	2.5E4
8.0	2.5E3	3.0E4
10.	2.6E3	4.0E4
12.	2.7E3	5.0E4
14.	2.8E3	7.5E4
16.	2.9E3	1.0E5
18.	3.0E3	
20.	3.1E3	
23.	3.2E3	
26.	3.3E3	
30.	3.4E3	
35.	3.5E3	
40.	3.6E3	
50.	3.7E3	
60.	3.8E3	
70.	3.9E3	
80.	4.0E3	
100	4.1E3	
120	4.2E3	

CCD, where the optically active areas are defined by the following pixel dimensions:

	x	y		x	y
WF 1	783	767	PC 5	767	757
2	783	773	6	774	763
3	772	770	7	768	771
4	773	769	8	781	770

Registration of images from more than one CCD is aided by a series of 11 pinholes along each of the common pyramid edges ('Kelsall' spots), which may be illuminated in a special calibration exposure.

The WF/PC has two readout formats, namely full single-pixel resolution, and (2×2) pixel summation. Each line of science data is started with two words of engineering data, following which there are 799 (Single-pixel format) or 400 (2×2 format) 16-bit positive numbers as read from the CCDs for the line. For the single-pixel format, the CCD pixels are followed by 12 offset or 'bias' words, i.e., 'overclocked' pixels, making a total of 813 words per line for 800 lines. In the (2×2) format, there are 402 words per line for 400 lines. Either pixel format may be used to read out the WFC or PC.

The advantage of (2×2) 'on-chip' pixel summation is that readout noise is maintained at ~13 electrons rms for the summed (i.e., larger) pixels. This pixel summation is useful for some photometric observations of extended sources. Note, however, that cosmic ray removal is more difficult in (2×2) format when using the PSF method (see Section 4.6). The area of sky affected by cosmic rays is also increased, but deferred charge (q.v., Section 4.7.1) may be alleviated by summing pixels containing sky background. Note also that the electronic bias is not as well determined in the (2×2) mode, because there are no "over-clocked" or extended register pixels. For each line of data, the bias value for one pixel is contained in the engineering data, but without the least significant bit.

In a fundamental way, the WF/PC has a single science mode: it acts as a photometric, area imager. The Operating Mode in the Exposure Logsheet will, therefore, always read *IMAGE*. By choice of elements from the SOFA that are included in the light beam, however, three distinct photometric modes are permitted, viz., filter photometry (using wide, medium or narrow band filters), photopolarimetry (using a polarizer plus a filter in the 250–800 nm range), and slitless spectroscopy (using a transmission grating).

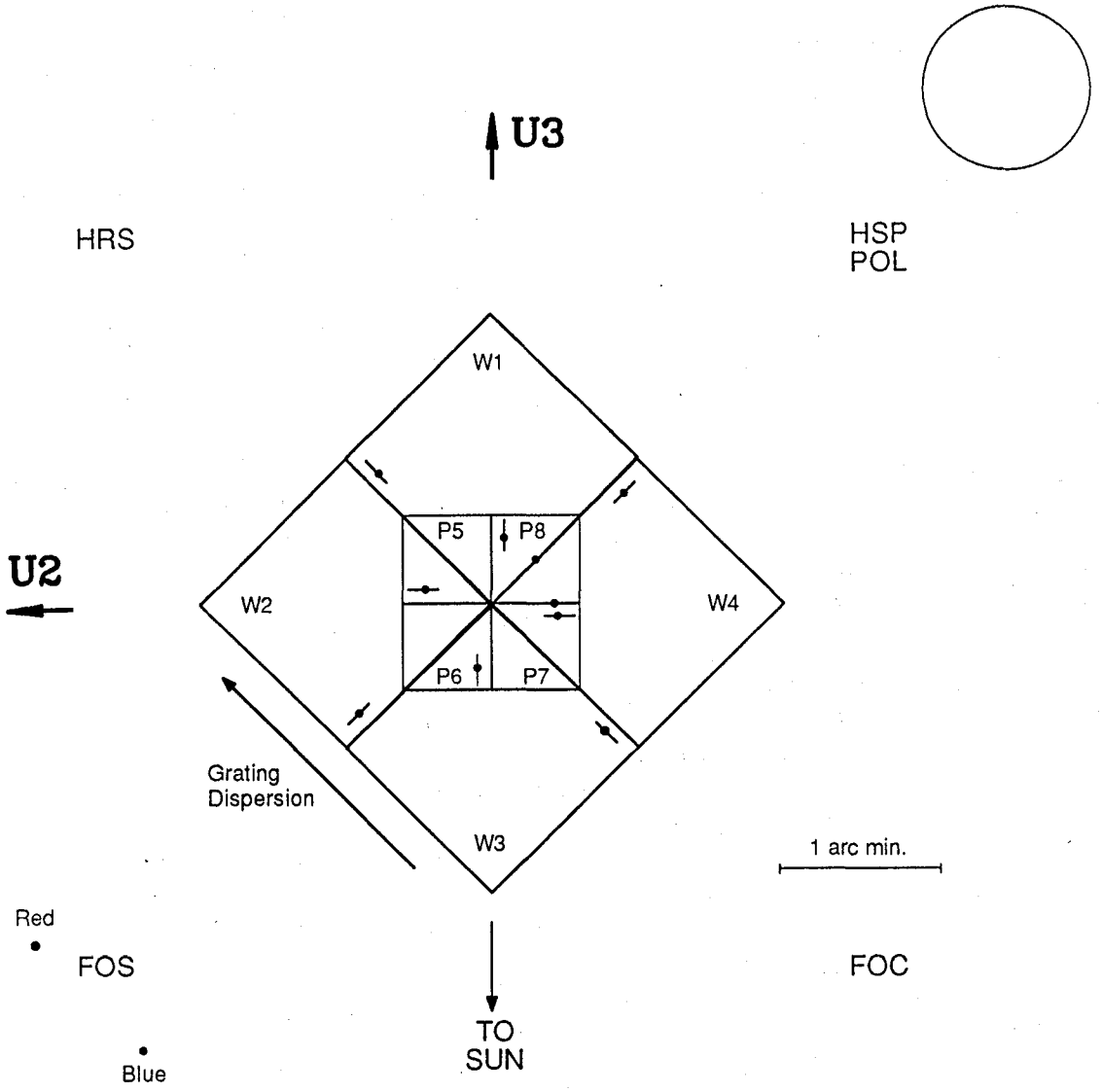

Figure 3.5.1 Overlay of the FOV of the WF/PC CCDs on the sky. The orientation of this overlay is the same as that published in the CP (insert, back cover). The direction of blooming along the columns of each CCD is indicated by the bars on either side of the (saturated) solid dot. Each CCD is read out from the corner nearest the centre of the diagram, with column (pixel) and row (line) numbers increasing from the diagram center. Columns and rows are parallel and orthogonal to the bar, respectively. The direction of wavelength dispersion is also indicated, when the gratings are used. Diffraction spikes caused by the Optical Telescope Assembly and by the internal Cassegrain optics of the WF/PC are parallel to the edges of the Planetary Camera CCDs. The neutral density or 'Baum' spot is at the center of P8 and one-quarter of the way along each axis from the origin of W4. The default pointing positions when all 4 CCDs of each camera are used are on P6 and W2, approximately 10 arc seconds along each axis from the origin.

4.0 INSTRUMENT PERFORMANCE

4.1 QUANTUM EFFICIENCY

The overall spectral response of the system is quantified in Table 4.1.1 and is shown in Figure 4.1.1. These do not include filter transmissions. The data presented here represent the UV-flooded response of the CCDs, with negative charge on the illuminated surfaces. The QE of the CCDs has generally been enhanced in the UV and blue, with respect to the baseline values contained in the October 1985 version of this Handbook, with smaller improvement for $\lambda > 7000$Å. In particular, the response trough which previously existed around 4000 Å is filled in for some CCDs so that the QE rises monotonically from the 2000–3000 Å region (where QE enhancement is relatively small following UV flood) to 6000 Å, where the enhancement is again relatively small.

The following table presents the QE of the WF/PC plus OTA for each camera head and CCD as a function of wavelength. The data are for the UV-flooded condition, after the equivalent of 4 orbits of UV flood for the WFC and 15 orbits for the PC. Data are smoothed interpolations through Thermal-Vac test points, and include everything except the filter transmissions (*q.v.*, section 3.2 and Table 5.1.1).

QE shortward of 2000 Angstroms

Absolute Q.E. of the camera, as measured at 1500 Angstroms, fell from 3% to 1% on the time scale of 2 to 3 days when the CCDs were cooled to their operating temperature near -80C during thermal-vacuum testing. At the same time, the Q.E at 2400 Angstroms fell from 6.4% to about 6.1%, while there was no significant change in the Q.E. at 4100 Angstroms or longer wavelengths over the same time periods. The cause of the Q.E fall shortward of 2000 Angstroms is believed to have been contamination by at least two undetermined molecules, but not H_2O, as determined using measurements made with a thermal quartz-crystal microbalance placed inside the camera housing. One contaminant had an accumulation temperature of 8 to 10C (i.e. the contaminant can be boiled off at temperatures above this) , and the second contaminant had an accumulation temperature of -40 to -50C. The high-temperature contaminant was associated with the camera housing, probably the electronics. Removal of this contaminant in orbit will be achieved using special procedures. The low temperature component was of undetermined origin, but can be boiled off relatively easily by warming the CCDs to about -30C for a time equal to one orbital period. The contaminants, when boiled off the CCD windows, tend to collect on the cold internal surface of the radiator or on the cold parts of the "heat pipes" which transfer heat from the thermo-electric coolers to the radiator.

An on-orbit decontamination plan for the camera has been developed for the OV/SV period. The plan entails a one-orbit warm-up before performing observations with the camera at wavelengths less than 2000 Angstroms. Calibration of absolute q.e. will be performed as close in time as possible to such a suite of observations.

Good flat fields at these wavelengths will, in any case, be difficult or impossible to obtain, so that photometric accuracy will not be better than about 10%.

Q.E at Lyman alpha was measured to be less than or equal to 0.3 %, several times less than the expected value. The Magnesium Fluoride entrance aperture has lower transmission than the design goal at Lyman α.

Table 4.1.1
Quantum Efficiency of WF/PC + OTA

λ (Å)	WF1	WF2	WF3	WF4	PC5	PC6	PC7	PC8
1100	0.0000	0.0000	0.0000	0.0000	0.0000	0.0000	0.0000	0.0000
1200	0.0008	0.0008	0.0008	0.0008	0.0007	0.0002	0.0008	0.0002
1300	0.0035	0.0037	0.0035	0.0036	0.0032	0.0011	0.0037	0.0012
1400	0.0071	0.0074	0.0071	0.0072	0.0069	0.0025	0.0080	0.0030
1500	0.0122	0.0126	0.0122	0.0122	0.0126	0.0051	0.0143	0.0063
1600	0.0140	0.0145	0.0141	0.0138	0.0153	0.0067	0.0172	0.0088
1700	0.0161	0.0166	0.0163	0.0157	0.0185	0.0088	0.0206	0.0121
1800	0.0184	0.0189	0.0189	0.0178	0.0223	0.0114	0.0246	0.0165
1900	0.0199	0.0204	0.0205	0.0189	0.0252	0.0139	0.0275	0.0208
2000	0.0243	0.0249	0.0252	0.0229	0.0322	0.0190	0.0348	0.0297
2100	0.0299	0.0305	0.0312	0.0278	0.0412	0.0260	0.0442	0.0422
2200	0.0356	0.0362	0.0374	0.0328	0.0511	0.0344	0.0544	0.0578
2300	0.0389	0.0396	0.0411	0.0356	0.0581	0.0415	0.0614	0.0723
2400	0.0408	0.0415	0.0434	0.0370	0.0632	0.0479	0.0664	0.0862
2500	0.0428	0.0434	0.0457	0.0384	0.0685	0.0549	0.0715	0.1019
2600	0.0438	0.0444	0.0471	0.0391	0.0726	0.0613	0.0753	0.1175
2700	0.0427	0.0431	0.0460	0.0377	0.0730	0.0649	0.0752	0.1280
2800	0.0397	0.0401	0.0430	0.0348	0.0701	0.0655	0.0718	0.1328
2900	0.0385	0.0386	0.0419	0.0337	0.0689	0.0671	0.0716	0.1416
3000	0.0374	0.0374	0.0409	0.0329	0.0676	0.0681	0.0714	0.1488
3100	0.0374	0.0372	0.0410	0.0330	0.0676	0.0700	0.0728	0.1579
3200	0.0381	0.0377	0.0419	0.0338	0.0688	0.0727	0.0754	0.1687
3300	0.0393	0.0387	0.0433	0.0350	0.0706	0.0759	0.0788	0.1803
3400	0.0414	0.0406	0.0456	0.0371	0.0737	0.0801	0.0837	0.1943
3500	0.0446	0.0437	0.0492	0.0403	0.0784	0.0856	0.0908	0.2118
3600	0.0487	0.0474	0.0537	0.0444	0.0836	0.0904	0.0993	0.2276
3700	0.0529	0.0513	0.0583	0.0489	0.0874	0.0918	0.1074	0.2346
3800	0.0560	0.0540	0.0615	0.0523	0.0887	0.0895	0.1128	0.2310
3900	0.0579	0.0558	0.0636	0.0547	0.0887	0.0859	0.1160	0.2230
4000	0.0661	0.0635	0.0724	0.0629	0.0981	0.0909	0.1314	0.2362
4100	0.0838	0.0804	0.0917	0.0801	0.1217	0.1086	0.1657	0.2817
4200	0.0951	0.0903	0.1024	0.0914	0.1322	0.1174	0.1778	0.2826
4300	0.1029	0.0967	0.1093	0.0992	0.1388	0.1257	0.1824	0.2799
4400	0.1133	0.1054	0.1185	0.1094	0.1480	0.1369	0.1899	0.2803
4500	0.1280	0.1180	0.1320	0.1238	0.1622	0.1531	0.2029	0.2870

Quantum Efficiency of WF/PC + OTA (Cont'd.)

λ (Å)	WF1	WF2	WF3	WF4	PC5	PC6	PC7	PC8
4600	0.1438	0.1316	0.1465	0.1392	0.1770	0.1704	0.2160	0.2920
4700	0.1598	0.1453	0.1608	0.1546	0.1914	0.1877	0.2281	0.2946
4800	0.1756	0.1589	0.1748	0.1695	0.2052	0.2045	0.2394	0.2964
4900	0.1905	0.1719	0.1881	0.1834	0.2183	0.2204	0.2503	0.2990
5000	0.2039	0.1838	0.1999	0.1954	0.2298	0.2344	0.2600	0.3022
5100	0.2148	0.1936	0.2096	0.2049	0.2392	0.2458	0.2679	0.3055
5200	0.2233	0.2015	0.2170	0.2120	0.2463	0.2546	0.2740	0.3089
5300	0.2297	0.2076	0.2225	0.2169	0.2515	0.2612	0.2786	0.3121
5400	0.2344	0.2121	0.2265	0.2202	0.2552	0.2659	0.2818	0.3150
5500	0.2377	0.2153	0.2292	0.2223	0.2576	0.2692	0.2838	0.3169
5600	0.2400	0.2176	0.2310	0.2236	0.2592	0.2715	0.2847	0.3175
5700	0.2417	0.2192	0.2322	0.2243	0.2601	0.2733	0.2849	0.3171
5800	0.2429	0.2203	0.2329	0.2247	0.2606	0.2746	0.2846	0.3158
5900	0.2440	0.2211	0.2334	0.2250	0.2610	0.2757	0.2839	0.3142
6000	0.2450	0.2217	0.2338	0.2252	0.2614	0.2770	0.2833	0.3123
6100	0.2461	0.2223	0.2342	0.2255	0.2620	0.2783	0.2826	0.3104
6200	0.2468	0.2225	0.2343	0.2255	0.2622	0.2793	0.2815	0.3078
6300	0.2466	0.2217	0.2334	0.2246	0.2615	0.2793	0.2792	0.3040
6400	0.2449	0.2195	0.2310	0.2222	0.2593	0.2777	0.2753	0.2983
6500	0.2413	0.2154	0.2267	0.2181	0.2551	0.2739	0.2691	0.2902
6600	0.2354	0.2093	0.2202	0.2118	0.2486	0.2675	0.2605	0.2796
6700	0.2278	0.2016	0.2122	0.2040	0.2404	0.2593	0.2501	0.2673
6800	0.2194	0.1932	0.2034	0.1954	0.2314	0.2500	0.2389	0.2543
6900	0.2108	0.1846	0.1943	0.1866	0.2222	0.2404	0.2276	0.2415
7000	0.2026	0.1764	0.1857	0.1781	0.2136	0.2313	0.2170	0.2296
7100	0.1953	0.1690	0.1779	0.1704	0.2058	0.2231	0.2074	0.2191
7200	0.1887	0.1623	0.1708	0.1634	0.1990	0.2157	0.1988	0.2099
7300	0.1827	0.1563	0.1644	0.1569	0.1928	0.2090	0.1911	0.2017
7400	0.1773	0.1508	0.1585	0.1510	0.1872	0.2029	0.1841	0.1945
7500	0.1724	0.1457	0.1532	0.1456	0.1822	0.1973	0.1778	0.1881
7600	0.1680	0.1412	0.1483	0.1407	0.1777	0.1923	0.1722	0.1825
7700	0.1640	0.1370	0.1439	0.1361	0.1736	0.1877	0.1671	0.1775
7800	0.1604	0.1333	0.1399	0.1320	0.1700	0.1835	0.1625	0.1731
7900	0.1571	0.1299	0.1362	0.1283	0.1667	0.1797	0.1584	0.1692

Quantum Efficiency of WF/PC + OTA (Cont'd.)

λ (Å)	WF1	WF2	WF3	WF4	PC5	PC6	PC7	PC8
8000	0.1541	0.1268	0.1329	0.1248	0.1637	0.1763	0.1546	0.1658
8100	0.1514	0.1240	0.1298	0.1217	0.1610	0.1731	0.1512	0.1627
8200	0.1489	0.1214	0.1271	0.1188	0.1585	0.1702	0.1482	0.1600
8300	0.1467	0.1192	0.1247	0.1163	0.1564	0.1677	0.1455	0.1577
8400	0.1451	0.1173	0.1226	0.1141	0.1548	0.1657	0.1433	0.1559
8500	0.1439	0.1160	0.1212	0.1125	0.1537	0.1643	0.1418	0.1548
8600	0.1434	0.1152	0.1203	0.1114	0.1534	0.1638	0.1409	0.1544
8700	0.1437	0.1150	0.1200	0.1109	0.1538	0.1639	0.1408	0.1548
8800	0.1445	0.1153	0.1203	0.1110	0.1549	0.1649	0.1413	0.1558
8900	0.1460	0.1161	0.1211	0.1115	0.1566	0.1665	0.1424	0.1575
9000	0.1480	0.1174	0.1223	0.1125	0.1588	0.1687	0.1440	0.1598
9100	0.1502	0.1189	0.1238	0.1136	0.1614	0.1712	0.1459	0.1624
9200	0.1521	0.1200	0.1250	0.1145	0.1635	0.1733	0.1474	0.1645
9300	0.1527	0.1202	0.1251	0.1145	0.1643	0.1739	0.1478	0.1653
9400	0.1512	0.1188	0.1236	0.1129	0.1628	0.1722	0.1461	0.1638
9500	0.1469	0.1152	0.1197	0.1092	0.1582	0.1672	0.1417	0.1592
9600	0.1392	0.1089	0.1132	0.1031	0.1501	0.1584	0.1341	0.1510
9700	0.1286	0.1004	0.1043	0.0949	0.1387	0.1463	0.1236	0.1395
9800	0.1155	0.0900	0.0935	0.0850	0.1246	0.1314	0.1109	0.1254
9900	0.1006	0.0783	0.0813	0.0738	0.1086	0.1144	0.0965	0.1093
10000	0.0844	0.0655	0.0680	0.0617	0.0912	0.0960	0.0808	0.0917
10100	0.0674	0.0522	0.0542	0.0491	0.0728	0.0766	0.0644	0.0733
10200	0.0504	0.0390	0.0405	0.0366	0.0545	0.0573	0.0482	0.0548
10300	0.0345	0.0267	0.0277	0.0250	0.0373	0.0392	0.0329	0.0376
10400	0.0209	0.0161	0.0167	0.0151	0.0226	0.0237	0.0199	0.0227
10500	0.0108	0.0083	0.0086	0.0078	0.0117	0.0122	0.0103	0.0117
10600	0.0051	0.0039	0.0040	0.0036	0.0055	0.0057	0.0048	0.0055
10700	0.0027	0.0021	0.0022	0.0019	0.0029	0.0031	0.0026	0.0030
10800	0.0021	0.0016	0.0016	0.0015	0.0022	0.0024	0.0020	0.0023
10900	0.0014	0.0011	0.0011	0.0010	0.0015	0.0016	0.0013	0.0016
11000	0.0004	0.0003	0.0003	0.0003	0.0005	0.0005	0.0004	0.0005

The sensitivity of PC8 is sufficiently greater than that of the other CCDs (particularly between 3000 and 5000 Å) that, for the same exposure time, use of PC8 will give similar S/N as that from any of the WF CCDs (if the observations are readout-noise limited).

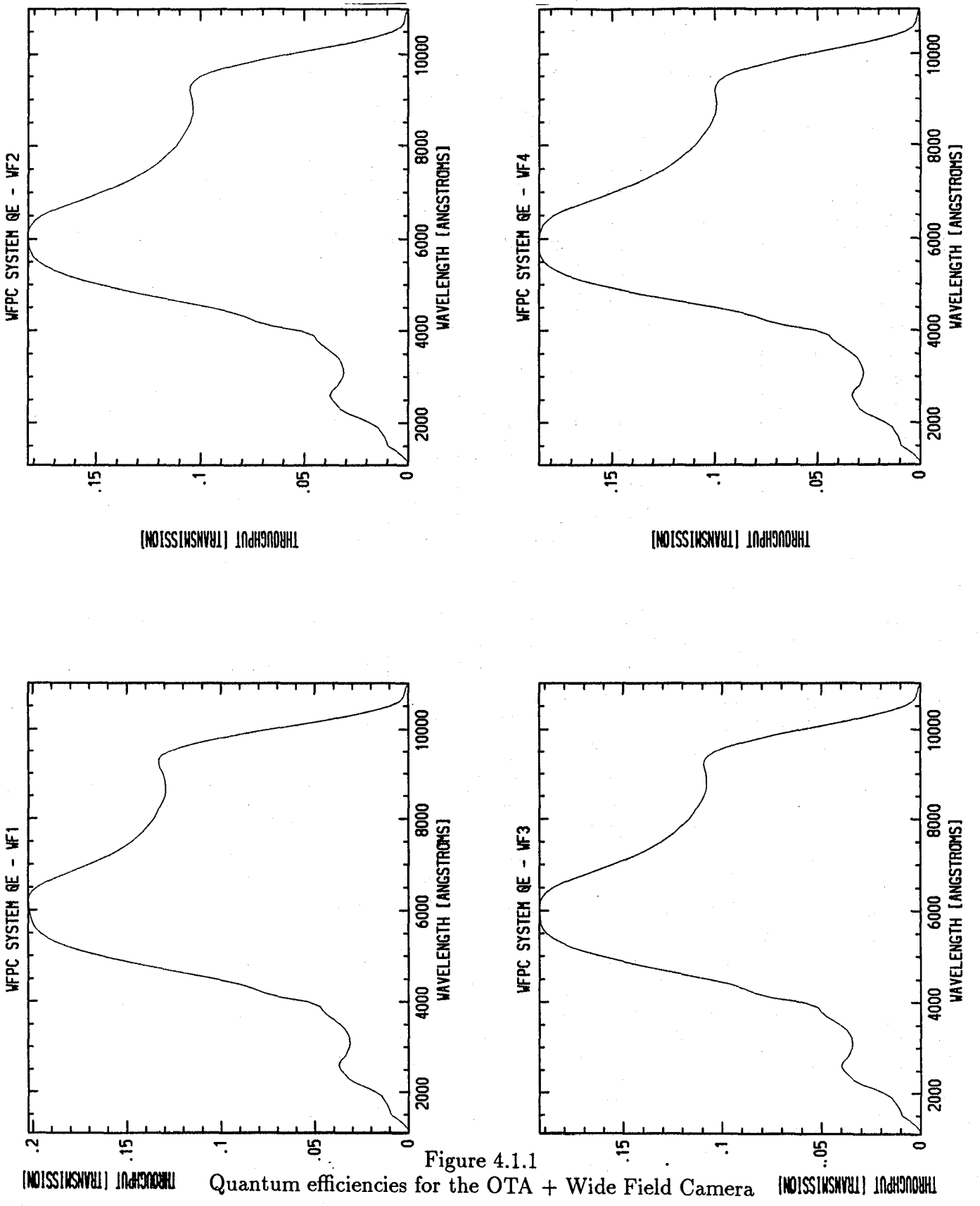

Figure 4.1.1
Quantum efficiencies for the OTA + Wide Field Camera

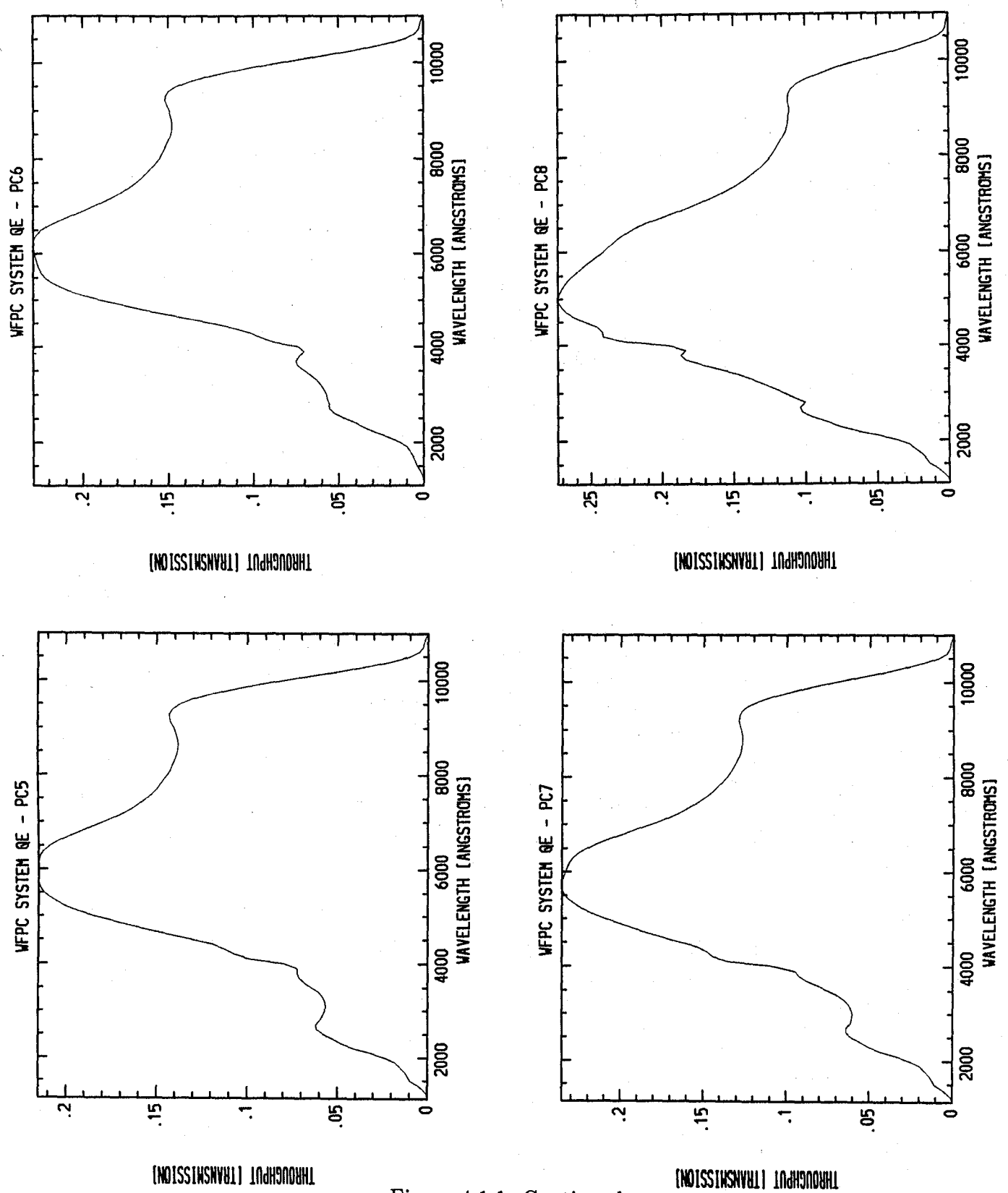

Figure 4.1.1 Continued
Quantum efficiencies for the OTA + Planetary Camera

4.2 QUANTUM EFFICIENCY STABILITY

The WF/PC CCDs, as fabricated, have a 'depletion layer' at the back surface and suffer the effect of 'quantum efficiency hysteresis' if they have not been exposed to light for a long period (months). The depletion layer (Figure 4.2.1) arises by virtue of 'holes' (i.e., electron vacancies), located within the native oxide on the silicon surface and, predominantly, at the interface between the oxide and the silicon. These holes cause the electron energy levels at the back of the CCD to bend downwards, i.e., a potential gradient exists which collects electrons in the interface and oxide traps. The resulting potential well extends about 0.6 μm into the CCD, and the problem is, therefore, especially severe for photons which are not converted by the coronene, i.e., photons with $\lambda \gtrsim 3700$Å, and which have an absorption length in silicon of less than 0.6 μm, i.e., photons with $\lambda \lesssim 5000$ Å. For a CCD with a depletion layer at the surface, incoming photons will produce photo-electrons which start to fill the traps. As the traps become full, further photo-electrons are collected in the buried channel at the front of the CCD, i.e., the CCD responds as it should. If the light source is now removed, the trapped electrons will be released on timescales dependent on the energy level of the trap, as well as temperature. The quantum efficiency of such a device thus varies depending on the history of previous exposure to light.

The solution to this problem for the WF/PC is 'UV flood.' Photons of $1800 < \lambda < 3000$Å generate photo-electrons in the silicon of sufficient energy to reach the conduction band in the oxide. At the back surface of the CCD, the electrons fill the traps and are attracted by oxygen atoms on the surface, thus charging the surface. A negative charge layer at the surface of the CCD produces an 'accumulation' layer in the silicon, i.e., a potential gradient which repels photo-electrons from the back surface so that they can be collected in the buried channel. The facility to UV flood the CCDs is provided within the WF/PC by a light channel from a mirror on the external radiator (Figure 2.2.1). The UV flood procedure involves pointing the $-V_1$ axis of the telescope at the sun and allowing UV photons to accumulate the CCD surfaces. The timescale for loss of the negative charge on the coronene is very long at the normal operating temperature of -95°C. Although the absolute quantum efficiency of the CCDs may fall until the next UV flood is performed, 'hysteresis' as such will be eliminated. UV flood will be performed as part of routine WF/PC operations, as necessary.

4.3 LINEARITY

The linearity of the WF/PC response is dependent on the absence of QE hysteresis and deferred charge. The camera system is required to follow the transfer function given below over the range from full scale of the ADC down to a S/N = 3.)

$\log_{10} \mathrm{DN_{out}} = \mathrm{A} \log_{10} \mathrm{P}_{in} \gamma$ where

$\mathrm{DN_{out}}$ = DN output

A = constant

P = photons in

$\gamma = 1.00 \pm 0.005$

S/N = signal/noise ratio

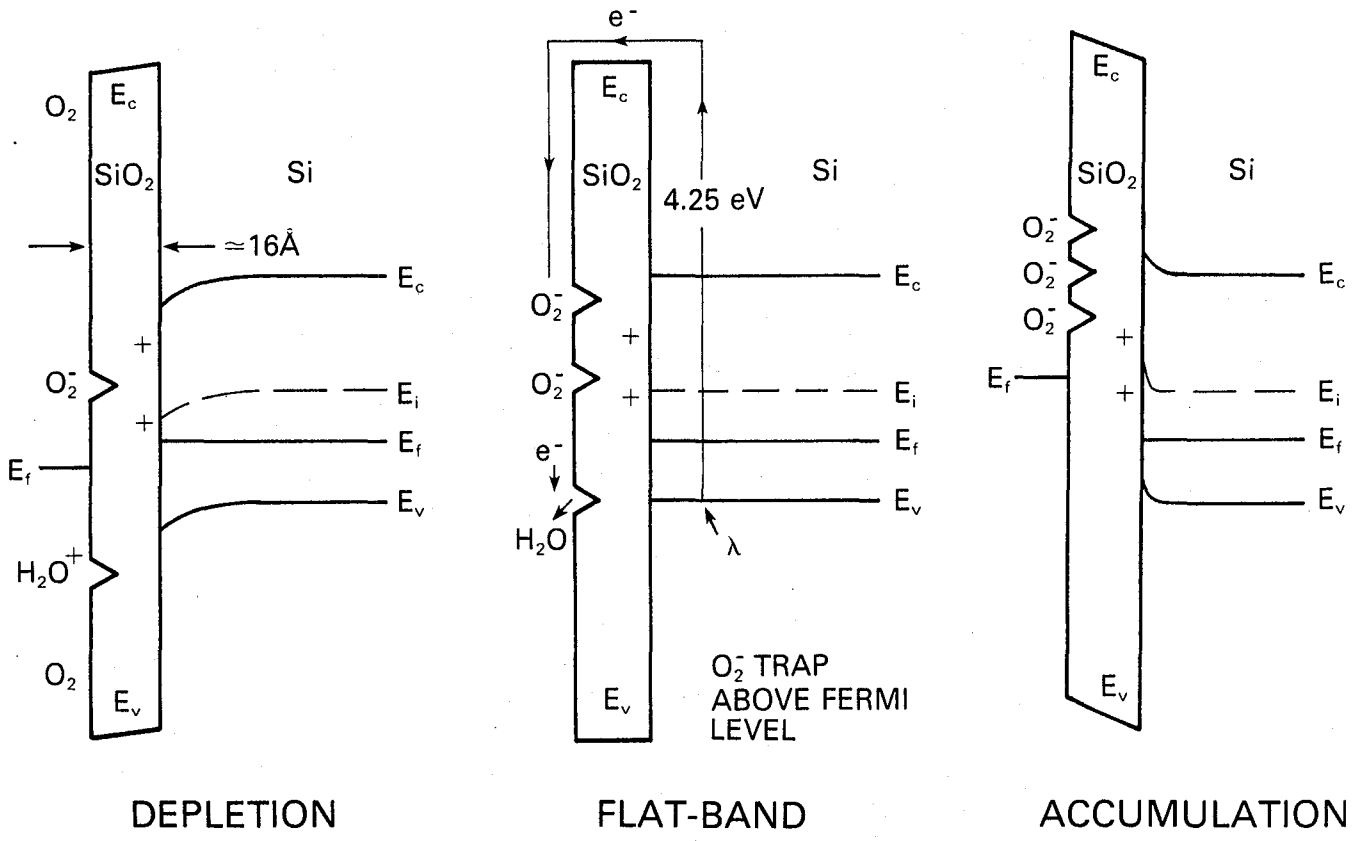

Figure 4.2.1Energy levels at the back (illuminated) CCD Surface (left) Interface states (holes) at the SiO_2/Si interface repel holes in the silicon and cause the energy levels to bend downwards near the oxide layer, producing "depletion," as shown here. (middle) The introduction of photo-electrons into the backside well, or the presence of some negative oxygen ions adsorbed onto the surface will produce a 'flat-band' condition. (right) If sufficient negative ions are adsorbed ($\sim 10^7$ per pixel), the interface becomes 'accumulated' with holes, and will tend to repel further photo-electrons into the buried channel of the CCD.

4.4 CCD READOUT NOISE, FULL WELL AND 'GAIN'

The average CCD readout noise, in the absence of signal shot noise or interference, is 13 electrons rms, with an average of 8 electrons per digital number (DN) count. The average signal-chain saturation level (4096 DN) is 33,000 electrons, with a minimum of 30,000 electrons.

4.5 POINT-SPREAD FUNCTION

The fraction of energy falling within a single pixel on the CCD is a function of wavelength, as shown in Figure 4.5.1. For the WFC, a point source centered on a pixel on-axis will collect about 60% of the incident energy, for a telescope pointing jitter of 7 milli arc sec, rms. For the PC, the corresponding fraction varies from a peak of 40% near 4000Å to 20% at 8000Å.

4.6 COSMIC-RAY BACKGROUND

For a faint-object observation, special efforts may have to be made to remove the time-integrated effects of charged particles (> 200 MeV protons, and secondary events.)

The primary cosmic-ray background outside the South Atlantic Anomaly (SAA) will be approximately 0.4 count cm^{-2} s^{-1}, caused by protons having energies $\gtrsim$ 200 MeV, i.e., 2 events s^{-1} per (1600 × 1600) frame. There will, in addition, be secondary events caused by interactions between the primaries and the material surrounding the CCDs, including the radiation shield, which will build up a certain amount of induced radio-activity by repeated SAA passage. These secondaries will contribute perhaps an additional $\sim$ 0.4 event cm^{-2} s^{-1}.

There are two methods which will be used to recognize cosmic ray events, viz., geometrical shape, and repeated observations. The geometrical shape discriminant may be used for some fraction of those cosmic-ray events which leave more than a few hundred electrons in the CCD. Such discrimination is more feasible for the PC in which the point spread function (PSF) of the telescope corresponds to 2 pixels FWHM. Cosmic ray events (muons) during thermal-vac testing were predominantly ($\sim$ 70%) confined to single pixels, in the absence of deferred charge (*q.v.*). Most of the muon-related events leave $\sim$ 300–800 electrons in the CCDs, and a similar amplitude range is expected for the minimum-ionizing protons in orbit. A low-amplitude tail to the distribution of event sizes, however, is more difficult to remove. Events which leave only $\sim$ 100 electrons in a total of one or more pixels are difficult or impossible to recognize using the PSF method. A second exposure is thus necessary to recognize such events. The post-observation data analysis will allow comparison of such sub-exposures for rejection of signal induced by cosmic ray secondaries.

Two rocket flights conducted by the x-ray astronomy group of Pennsylvania State University (led by Prof.G.Garmire, Principal Investigator, with John Nousek and Dave Burrows) carried a Texas Instruments 3-phase CCD to altitudes above 120 km for approximately 400 secs. on each flight. The measured cosmic ray event rate was approximately 0.33 cm^{-2} s^{-1}, or 0.5 events per $CCDs^{-1}$. WF/PC uses the same CCDs as the one flown, and although the amount of radiation shielding was less than that internal to the WF/PC, similar rates are expected from the WF/PC during operation. The events had amplitudes with a peak at around 300 electrons, with an amplitude distribution falling to half height at about 500 to

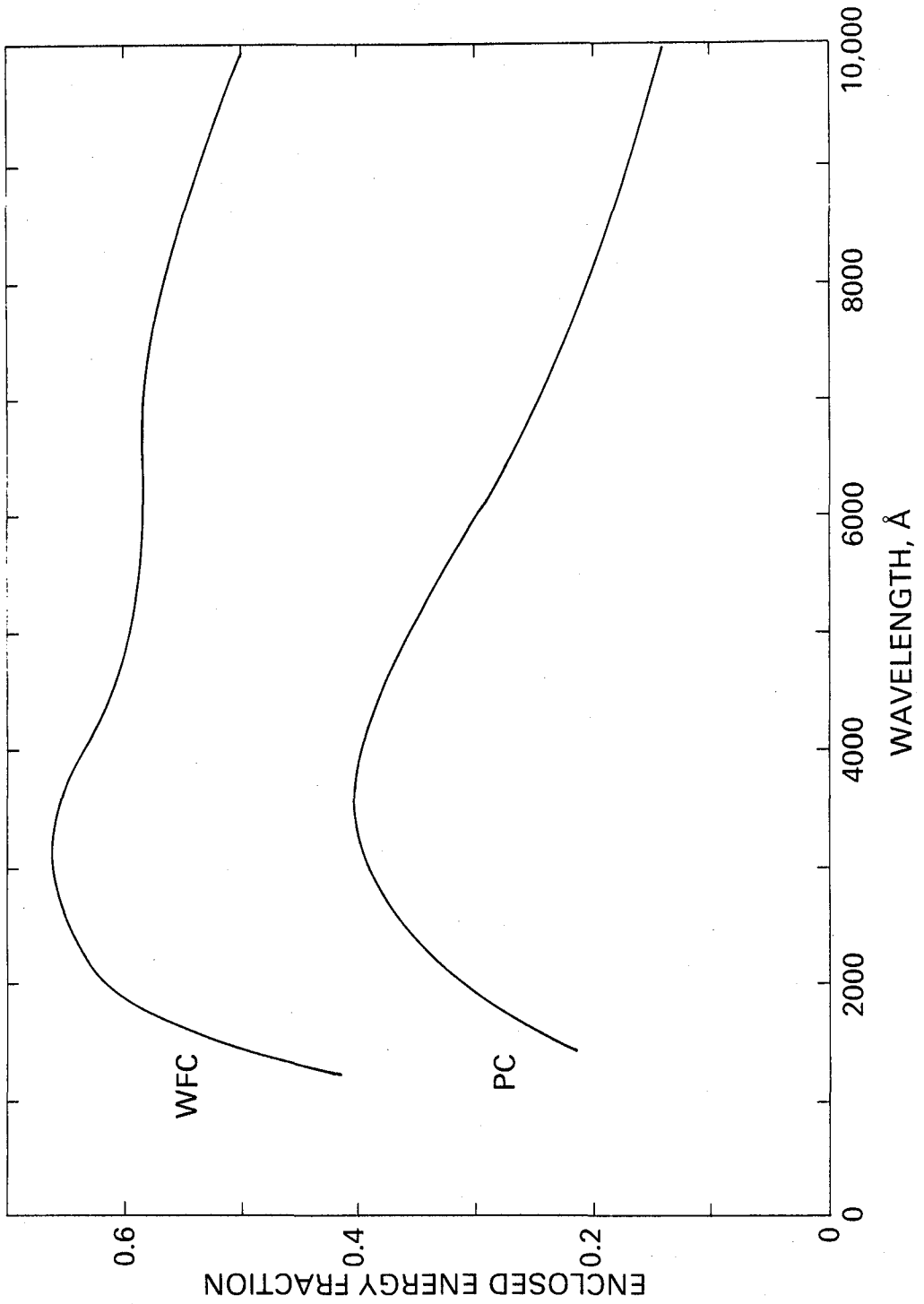

Figure 4.5.1 Enclosed energy fraction for an on-axis point source centered on a pixel of the WFC or PC, for a telescope pointing jitter of 7 milli arc secs. rms.

600 electrons, trailing off slowly to higher amplitudes. On the low energy side of the peak, a trough in the amplitude distribution was observed around 200 electrons, well above the read-out noise. These amplitude distributions were very similar to those generated by muons during WF/PC ground-based testing.

4.7 INSTRUMENT ANOMALIES

4.7.1 Deferred Charge

The TI CCDs in the WF/PC suffer from a low level non-linearity called "deferred charge," which results from a spurious potential pocket between the transfer gate and serial register. The effects are complex but basically very low level charge ($\leq 250e^-$/pixel) is transferred poorly and tends to cause tails behind faint images. Some charge ($\sim 50e^-$) is lost entirely so that it is not feasible to recover the photometry accurately even in uncrowded fields.

The only fix is to "preflash" much like a photographic plate with the internal lamps putting in $\sim$ 80 electrons/pixel either before or after the exposure. The cost is the photon noise in the preflash so that in this mode the effective readout noise will be $\sqrt{13^2 + 80}$ or about 15 electrons rms. This will need to be done for imaging work in the UV and when using narrow and medium-width filters with the WFC, since the sky will serve in the wide filters for sufficiently long exposures. A "preflash" is always advised for the PC.

A calibrated "preflash" image will be removed, if necessary, as part of the routine data reduction (see section 6.2).

4.7.2 Blooming and Residual Image

Blooming up and down the CCD column occurs when more than about 80,000 electrons ("full well capacity") are collected in any pixel. When the adjacent pixels up and down the column are full, the charge will flow into the next pixels along the column, and so on.

The orientation of the bloomed column(s) on the sky depends on the readout direction of the particular CCD (see Figure 3.5.1) and the roll angle of the spacecraft.

Residual images occur for pixels which collect more than about 200,000 electrons (this threshold varies by about a factor of 2 depending on location and CCD). Electrons are trapped at the interface between the buried channel and the insulating oxide beneath the electrodes, and are released later. The time constants for electron release are on the order of minutes to hours. The intensity of the residual image depends on the integration ("exposure") time and the length of time since the overexposure. Most of the CCDs have residuals which decay after about an hour, although some take several hours for the decay. There is some non-uniformity along the column in the level of residual image from bloomed images on some of the CCDs. On long ($\sim$ half-orbit) exposures through the wide V or wide I filters, stellar objects brighter than V $\sim$ 21 will leave residual images in the WFC.

In ground-based thermal-vacuum tests, the CCDs were over-exposed to a maximum of several thousand times the nominal pixel well capacity, and the decay of the resulting residual images was monitored, typically for several hours. In particular , it was found that, following an over-exposed image of point sources, a uniform residual level could be introduced by over-exposure to the internal flat-field lamps. The decay of this uniform residual level is such that, after an electronic "purging" and a wait of 20 to 60 minutes, the remaining residual is very uniform at the 1 to 2 DN level. It is therefore planned to carry out such a residual image purge following those observations expected to leave residual images which would compromise the subsequent images. Such residual purging will usually be performed on entry into earth occultation, and will be known as a "superpurge". Such a "super-purge"

leads to an enhanced "dark current", which will be subtracted from the image, as necessary, during the routine data reduction.

4.7.3 Red Leaks in UV Filters

The 'red leaks' in the UV filters are quantified in Figure 4.7.3.1 for F122M, F157W, F194W, F230W and F284W. Table 4.7.3.1 shows the red leak as a percentage of the total signal from the source. In the first column, the red leak is defined as flux longward of 3800Å; in the second column, the red leak is defined as flux longward of the wavelengths shown in the third column.

4.7.4 Overhead Time

Commands to the WF/PC are processed at spacecraft 'major frame' intervals of 1 minute. A filter may be returned 'home' and another filter selected in one major frame. An exposure takes a minimum of one minute, and a readout of less than 4 CCDs takes a further minute. A read-out of all 4 CCDs of the WFC or PC takes two minutes.

If a pre-flash is necessary to give enough signal to avoid deferred charge, then a minute needs to be allowed for filter change, a minute for the exposure on internal lamps, and a minute to return to the filter to be used for observation.

4.7.5 Missing Codes in the A/D Convertor

The A/D converters for both the WFC and PC produce 12-bit words, where words ending with binary bits 10 are re-assigned to other values i.e. the A/D convertors will never (or very rarely) produce output decimal words 2, 6, 10, 14.... 4094. Words ending with bit pattern 01, i.e. 1, 5, 9, 13.... 4093, are produced more often than they should be. True word values ending in 00 or 11 may also be re-assigned, but with less probability than true words ending in 10.

This problem is addressed in the first stage of the routine data reduction process. It is important to note, however, that no attempt is made to "correct" the digitisation process. Instead, an allowance for the missing code is made, such that a given pixel value may be assigned to a "bin" more than 1 DN in width, i.e. an allowance is made for ignorance in the "correct" DN value.

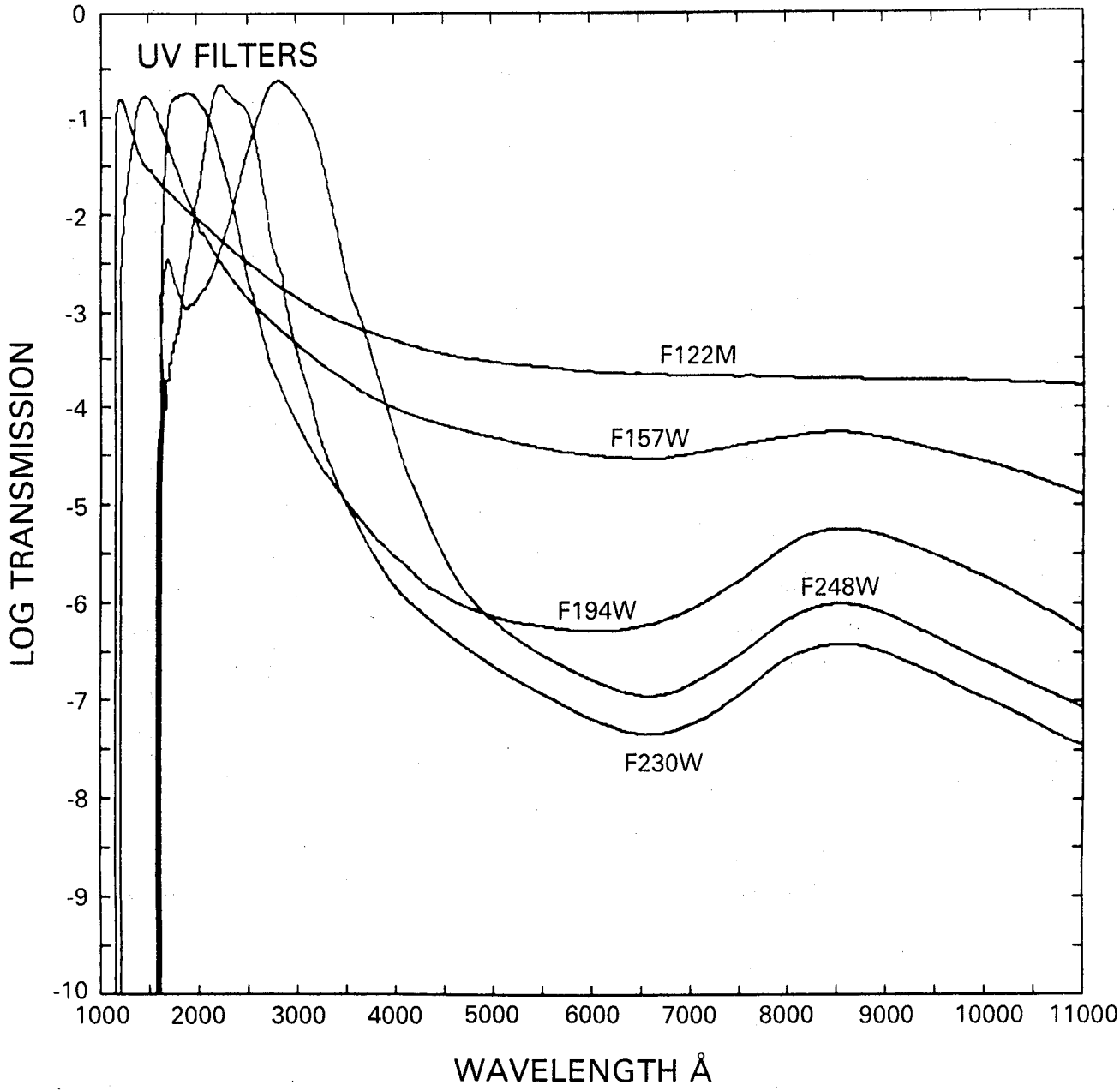

Figure 4.7.3.1
Transmission Curves for the UV Filters

Table 4.7.3.1 Red Leak in UV Filters

OBJECT	FILTER DESIGNATIONS	RED LEAK (%) ($\lambda > 3800$Å)	RED LEAK (%) $\lambda > \lambda_c$, Å	
BOV	F122M	5.3	76.2	1400
	F157W	0.4	6.1	2000
	F194W	0.0	0.2	2600
	F230W	0.0	0.0	2900
	F284W	0.0	0.0	3600
AOV	F122M	56.0	97.6	1400
	F157W	10.5	21.6	2000
	F194W	0.1	0.4	2600
	F230W	0.0	0.2	2900
	F284W	0.1	0.3	3600
GOV	F122M	94.5	100.0	1400
	F157W	90.3	99.8	2000
	F194W	18.2	23.2	2600
	F230W	0.4	1.9	2900
	F284W	0.3	0.8	3600
KOIII	F122M	98.6	100.0	1400
	F157W	96.3	98.6	2000
	F194W	34.0	35.5	2600
	F230W	1.2	2.0	2900
	F284W	1.0	2.0	3600
E gal.	F122M	98	100	1400
(z = 1)	F157W	95	98	2000
	F194W	55	58	2600
	F230W	3	2	2900
	F284W	0	1	3600
Sbc gal.	F122M	89	99	1400
(z = 1)	F157W	77	92	2000
	F194W	19	28	2600
	F230W	0	3	2900
	F284W	0	0	3600
Scd gal.	F122M	51	83	1400
(z = 1)	F157W	14	24	2000
	F194W	1	1	2600
	F230W	1	1	2900
	F284W	0	0	3600
QSO	F122M	60	98	1400
(z = 2)	F157W	29	63	2000
	F194W	1	2	2600
	F230W	0	1	2900
	F284W	0	1	3600

5.0 ESTIMATING EXPOSURE TIME AND SIGNAL TO NOISE RATIO

5.1 POINT SOURCES

Accurate predictions of exposure time will require knowledge of:

a. Overall spectral response of the system (Section 4.1)
b. Spectral transmission of 48 filters and grisms (Section 3.2)
c. Spectral energy distribution and spatial profile of the target
d. Criteria for specifying desirable charge levels

When the transmissions of filters are combined with the overall system response of Figure 4.1, we obtain a detective-quantum-efficiency plot (electrons-per-photon, Q_λ, as a function of λ) for each filter. This DQE plot links the output of the CCD to the photon flux at the input to the telescope.

The revised filter characteristics for the new QEs are listed in the following table. For each filter, five lines give the following information:

Line 1: filter name, filter-wheel position, and the following quantities (which are means over the eight CCDs): mean wavelength and width of the bandpass (as defined below) in Å; the dimensionless efficiency, $\int QT\, d\lambda/\lambda$; the equivalent Gaussian σ; the maximum value of QE × transmission over the bandpass of the filter; the derivative of the mean wavelength in Å with the spectral index α; and the effective number of pixels n_{eff} for both the WFC and the PC, respectively

Lines 2-5 (boxed): the values for $\int QT\, d\lambda/\lambda$, $\bar{\lambda}$, $\delta\bar{\lambda}$ and σ for each CCD. These parameters are defined as follows:

The efficiency is

$$\int Q(\lambda)T(\lambda)d\lambda/\lambda \ ,$$

where $Q(\lambda)$ is the QE of the camera + OTA and $T(\lambda)$ is the filter transmission, both as functions of the wavelength λ.

The mean wavelength is similar to that defined in Schneider, Gunn, and Hoessel (*Astrophys. J.*, **264**, 337, 1983):

$$\bar{\lambda} = \exp\left[\int Q(\lambda)T(\lambda)\ln(\lambda)d\lambda/\lambda \ \Big/ \int Q(\lambda)T(\lambda)d\lambda/\lambda\right] \ .$$

This rather unconventional definition has the property that the correspondingly defined mean frequency is just $c/\bar{\lambda}$; it is in some sense halfway between the conventional frequency mean and the wavelength mean.

The effective Gaussian σ is given by

$$\sigma^2 = \int Q(\lambda)T(\lambda)\left(\ln\frac{\lambda}{\bar{\lambda}}\right)^2\frac{d\lambda}{\lambda} \Big/ \int Q(\lambda)T(\lambda)\frac{d\lambda}{\lambda} \ .$$

The effective width of the bandpass is then

$$\delta\bar{\lambda} = 2[2\ln(2)]^{1/2}\sigma\bar{\lambda} \ ,$$

and it can be shown that

$$\frac{d\bar{\lambda}}{d\alpha} = \bar{\lambda}\sigma^2 \ .$$

Of rather more interest is the camera-to-camera variation of the mean wavelength, due to the variations in QE. One would expect this to be most serious in the long-wavelength bands, where the fall of the CCD QE is used to define the long-wavelength cutoff; the effect is not too bad, however. In the *I* (F785LP) band in the WFC, the range is only 23 Å, from 8907 Å (WF4) to 8930 Å (WF1). In *V* (F555W), the effect is predictably much smaller, 10 Å; in the PC, however, the effect of the much higher response of PC8 in the blue takes its toll, and there is a 55 Å spread. A 100 Å uncertainty in the 3500 Å lever arm is about a 3% color uncertainty in $V - I$ (which can, of course, be calibrated).

The WF/PC U, V and I system is fairly close as regards effective wavelengths to the Johnson UVI system, but cross-calibration will be necessary to convert to Johnson magnitudes.

Note that grating exposure times are not determined by the full passband; they are determined instead by the $\Delta\lambda$ falling within a single pixel in the vicinity of the blaze wavelength. Gratings can therefore be treated as narrowband filters with FWHM equal to the number of Ångstroms per pixel (Table 3.2.2), and grating images can then be treated as stellar images (except for a spread-function adjustment) when computing signal levels. Altogether, the three WF/PC gratings give rise to eight possible passband widths and therefore simulate eight different "filters" for which exposure times are to be calculated. Specifically, the $\Delta\lambda$ of each grating is different for f/12.9 than for f/30. Additionally, the ultraviolet grating has different $\Delta\lambda$s when used in the second-order spectrum than when used in the first order.

To estimate the number of electrons collected from a point source of apparent visual magnitude *V*, one can use the equation:

$$N_{el} = Ct\left[\int QTd\lambda/\lambda\right] \times 10^{-0.4(V+AB_\nu)} \ ,$$

where $C = 2.5 \times 10^{11}$, t is the exposure time in seconds, the QT integral is given in the following table, and AB_ν is given in Table 5.1.2 as a function of spectral type and wavelength. $V + AB_\nu$ is the monochromatic magnitude on the Oke system at the mean wavelength of the filter, *viz.*,

$$(V + AB_\nu) = -2.5 \log F_\nu - 48.60 \ ,$$

where F_ν is the flux in ergs cm^{-2} s^{-1} Hz^{-1} (Oke and Gunn, *Astrophys. J.*, **266**, 713, 1983).

In terms of F_ν,

$$N_{el} = Ct\left[\int QTd\lambda/\lambda\right] F_\nu \ ,$$

where $C = 6.9 \times 10^{30}$.

The last equation assumes a flat continuum. For a source of spectral index α, the shift in mean wavelength for each filter may be calculated from the tabulated $d\bar{\lambda}/d\alpha$. The value of F_ν should then be calculated at the appropriate wavelength for insertion into the above equation.

noise $\left\{N_{e\ell} + n_{eff}(t \times (sky + dark) + (RN)^2)\right\}^{\frac{1}{2}}$.

n_{eff} effective number of pixels, listed in Table 5.1.1 as n_{eff} (WF) or n_{eff} (PC).

sky $\simeq$ $28.0 + AB_\nu$ mag. per pixel (WFC)
$29.8 + AB_\nu$ mag. per pixel (PC)

and the corresponding electron count per pixel is found from the equation for $N_{e\ell}$ above and dark may be assumed negligible

RN = camera read noise = 13 electrons rms

The number of electrons collected, and corresponding signal-to-noise ratios, were given in Table 5.1.3 of the October 1985 version of the Instrument Handbook for spectral types B0, F0, and K0III and for several medium and wide filters as a function of stellar magnitude from $m_V = 21$ to $m_V = 29$. The magnitudes at which stars cause saturation of the signal-chain electronics ($\sim$ 30,000 electrons) were also noted. These Tables are not repeated here because of the differential response of each ccd, but the number of electrons collected simply scales as $\int QT\frac{d\lambda}{\lambda}$ for each ccd, so that Oct 85 Tables may be used as a check by simply comparing old and new values for $\int QT\frac{d\lambda}{\lambda}$ for a given filter / ccd combination.

Table 5.1.1 follows on the next 8 pages

WF/PC Filter Summary

	WF1	WF2	WF3	WF4	PC5	PC6	PC7	PC8

F122W 2a (1543/485) $\int QTd\lambda/\lambda$ = 0.00022 σ = 0.5149 QT_{max} = 0.0003 $d\bar{\lambda}/d\alpha$ = 619.1
n_{eff}(WF) = 2.1 n_{eff}(PC) = 3.0

$\int QTd\lambda/\lambda$	0.00019	0.00019	0.00019	0.00018	0.00023	0.00016	0.00026	0.00036
$\bar{\lambda}$	2256.	2187.	2236.	2195.	2330.	2802.	2304.	2319.
$\delta\bar{\lambda}$	2874.2	2670.5	2752.9	2733.0	2793.2	3522.9	2727.8	2521.0
σ	0.5411	0.5185	0.5229	0.5288	0.5092	0.5339	0.5029	0.4617

F157W 4a (1580/413) $\int QTd\lambda/\lambda$ = 0.00032 σ = 0.2563 QT_{max} = 0.0016 $d\bar{\lambda}/d\alpha$ = 113.1
n_{eff}(WF) = 2.1 n_{eff}(PC) = 3.2

$\int QTd\lambda/\lambda$	0.00030	0.00031	0.00031	0.00030	0.00033	0.00016	0.00037	0.00049
$\bar{\lambda}$	1648.	1640.	1650.	1636.	1685.	1823.	1677.	1699.
$\delta\bar{\lambda}$	957.8	903.0	937.7	906.7	1017.2	1444.2	988.7	999.4
σ	0.2468	0.2339	0.2414	0.2354	0.2563	0.3365	0.2503	0.2498

F194W 4b (1954/411) $\int QTd\lambda/\lambda$ = 0.00077 σ = 0.0943 QT_{max} = 0.0039 $d\bar{\lambda}/d\alpha$ = 17.5
n_{eff}(WF) = 2.1 n_{eff}(PC) = 3.7

$\int QTd\lambda/\lambda$	0.00065	0.00067	0.00067	0.00062	0.00084	0.00049	0.00092	0.00129
$\bar{\lambda}$	1951.	1951.	1953.	1948.	1965.	1989.	1963.	1970.
$\delta\bar{\lambda}$	431.2	427.7	429.9	426.8	437.2	461.6	434.3	435.9
σ	0.0938	0.0931	0.0935	0.0930	0.0945	0.0985	0.0940	0.0940

F230W 4c (2309/363) $\int QTd\lambda/\lambda$ = 0.00142 σ = 0.0673 QT_{max} = 0.0094 $d\bar{\lambda}/d\alpha$ = 10.5
n_{eff}(WF) = 2.2 n_{eff}(PC) = 4.3

$\int QTd\lambda/\lambda$	0.00108	0.00109	0.00114	0.00098	0.00161	0.00117	0.00170	0.00258
$\bar{\lambda}$	2307.	2307.	2308.	2305.	2316.	2330.	2314.	2319.
$\delta\bar{\lambda}$	364.3	364.0	364.6	363.5	366.9	372.1	366.6	368.6
σ	0.0671	0.0670	0.0671	0.0670	0.0673	0.0678	0.0673	0.0675

F284W 4d (2819/496) $\int QTd\lambda/\lambda$ = 0.00218 σ = 0.0791 QT_{max} = 0.0149 $d\bar{\lambda}/d\alpha$ = 17.6
n_{eff}(WF) = 2.2 n_{eff}(PC) = 5.3

$\int QTd\lambda/\lambda$	0.00142	0.00143	0.00154	0.00125	0.00246	0.00230	0.00257	0.00447
$\bar{\lambda}$	2804.	2802.	2806.	2802.	2813.	2832.	2816.	2835.
$\delta\bar{\lambda}$	530.8	530.1	528.7	536.0	514.8	501.8	522.2	525.8
σ	0.0804	0.0803	0.0800	0.0812	0.0777	0.0753	0.0788	0.0788

WF/PC Filter Summary (Cont'd.)

	WF1	WF2	WF3	WF4	PC5	PC6	PC7	PC8

F336W 2b (3361/410) $\int QTd\lambda/\lambda$ = 0.00537 σ = 0.0519 QT_{max} = 0.0376 $d\bar{\lambda}/d\alpha$ = 9.0
n_{eff}(WF) = 2.4 n_{eff}(PC) = 6.3

$\int QTd\lambda/\lambda$	0.00302	0.00297	0.00332	0.00271	0.00535	0.00573	0.00606	0.01377
$\bar{\lambda}$	3361.	3360.	3361.	3363.	3357.	3360.	3364.	3366.
$\delta\bar{\lambda}$	412.8	412.8	412.5	413.5	410.0	406.5	411.2	405.6
σ	0.0522	0.0522	0.0521	0.0522	0.0519	0.0514	0.0519	0.0512

F439W 2c (4352/465) $\int QTd\lambda/\lambda$ = 0.01349 σ = 0.0454 QT_{max} = 0.0997 $d\bar{\lambda}/d\alpha$ = 9.0
n_{eff}(WF) = 2.7 n_{eff}(PC) = 8.7

$\int QTd\lambda/\lambda$	0.00999	0.00933	0.01050	0.00962	0.01323	0.01223	0.01708	0.02590
$\bar{\lambda}$	4364.	4360.	4358.	4364.	4351.	4357.	4343.	4326.
$\delta\bar{\lambda}$	465.4	465.7	465.6	464.9	466.5	469.3	464.4	463.9
σ	0.0453	0.0454	0.0454	0.0452	0.0455	0.0457	0.0454	0.0455

F569W 5a (5598/967) $\int QTd\lambda/\lambda$ = 0.04632 σ = 0.0734 QT_{max} = 0.2253 $d\bar{\lambda}/d\alpha$ = 30.2
n_{eff}(WF) = 3.3 n_{eff}(PC) = 12.2

$\int QTd\lambda/\lambda$	0.04340	0.03922	0.04176	0.04049	0.04707	0.04926	0.05167	0.05768
$\bar{\lambda}$	5605.	5604.	5600.	5598.	5598.	5604.	5591.	5584.
$\delta\bar{\lambda}$	971.0	968.2	967.8	966.9	969.6	972.2	964.3	961.5
σ	0.0736	0.0734	0.0734	0.0733	0.0735	0.0737	0.0732	0.0731

F675W 5b (6684/910) $\int QTd\lambda/\lambda$ = 0.03890 σ = 0.0578 QT_{max} = 0.2238 $d\bar{\lambda}/d\alpha$ = 22.3
n_{eff}(WF) = 4.0 n_{eff}(PC) = 16.0

$\int QTd\lambda/\lambda$	0.03808	0.03361	0.03537	0.03397	0.04026	0.04332	0.04179	0.04483
$\bar{\lambda}$	6691.	6684.	6684.	6682.	6690.	6692.	6679.	6674.
$\delta\bar{\lambda}$	912.6	909.0	909.0	908.0	913.1	912.9	908.3	908.0
σ	0.0579	0.0577	0.0577	0.0577	0.0580	0.0579	0.0577	0.0578

F791W 5c (7906/1322) $\int QTd\lambda/\lambda$ = 0.03125 σ = 0.0710 QT_{max} = 0.1488 $d\bar{\lambda}/d\alpha$ = 39.9
n_{eff}(WF) = 5.0 n_{eff}(PC) = 20.8

$\int QTd\lambda/\lambda$	0.03197	0.02649	0.02777	0.02614	0.03395	0.03655	0.03238	0.03475
$\bar{\lambda}$	7916.	7900.	7899.	7892.	7919.	7915.	7900.	7909.
$\delta\bar{\lambda}$	1324.3	1320.7	1319.8	1317.0	1325.6	1323.6	1322.0	1327.3
σ	0.0710	0.0710	0.0710	0.0709	0.0711	0.0710	0.0711	0.0713

WF/PC Filter Summary (Cont'd.)

	WF1	WF2	WF3	WF4	PC5	PC6	PC7	PC8

F555W 9b (5416/1205) $\int QTd\lambda/\lambda = 0.06268$ $\sigma = 0.0945$ $QT_{max} = 0.2266$ $d\bar{\lambda}/d\alpha = 48.4$
n_{eff}(WF) = 3.2 n_{eff}(PC) = 11.8

$\int QTd\lambda/\lambda$	0.05766	0.05213	0.05590	0.05415	0.06360	0.06583	0.07085	0.08131
$\bar{\lambda}$	5434.	5433.	5425.	5424.	5416.	5429.	5400.	5374.
$\delta\bar{\lambda}$	1205.0	1203.4	1203.5	1200.0	1207.9	1207.9	1206.2	1211.9
σ	0.0942	0.0941	0.0942	0.0939	0.0947	0.0945	0.0949	0.0957

F622W 8c (6140/964) $\int QTd\lambda/\lambda = 0.04976$ $\sigma = 0.0667$ $QT_{max} = 0.2484$ $d\bar{\lambda}/d\alpha = 27.3$
n_{eff}(WF) = 3.6 n_{eff}(PC) = 13.9

$\int QTd\lambda/\lambda$	0.04766	0.04283	0.04520	0.04355	0.05079	0.05401	0.05445	0.05957
$\bar{\lambda}$	6146.	6143.	6141.	6140.	6143.	6147.	6134.	6128.
$\delta\bar{\lambda}$	966.9	963.7	964.4	964.6	967.5	967.9	963.5	961.3
σ	0.0668	0.0666	0.0667	0.0667	0.0669	0.0669	0.0667	0.0666

F702W 6d (6898/1493) $\int QTd\lambda/\lambda = 0.06164$ $\sigma = 0.0919$ $QT_{max} = 0.2386$ $d\bar{\lambda}/d\alpha = 58.3$
n_{eff}(WF) = 4.2 n_{eff}(PC) = 17.1

$\int QTd\lambda/\lambda$	0.06089	0.05303	0.05578	0.05334	0.06446	0.06934	0.06574	0.07058
$\bar{\lambda}$	6915.	6894.	6893.	6888.	6914.	6917.	6885.	6880.
$\delta\bar{\lambda}$	1502.8	1487.8	1486.7	1480.9	1505.6	1503.0	1486.7	1491.4
σ	0.0923	0.0916	0.0916	0.0913	0.0925	0.0923	0.0917	0.0921

F814W 10a (8137/1768) $\int QTd\lambda/\lambda = 0.04286$ $\sigma = 0.0923$ $QT_{max} = 0.1555$ $d\bar{\lambda}/d\alpha = 69.3$
n_{eff}(WF) = 5.2 n_{eff}(PC) = 21.6

$\int QTd\lambda/\lambda$	0.04404	0.03617	0.03787	0.03547	0.04688	0.05031	0.04425	0.04786
$\bar{\lambda}$	8152.	8128.	8125.	8113.	8157.	8151.	8129.	8145.
$\delta\bar{\lambda}$	1770.1	1765.2	1763.8	1759.1	1772.3	1768.8	1768.1	1777.3
σ	0.0922	0.0922	0.0922	0.0921	0.0923	0.0921	0.0924	0.0927

F785LP 10c (8922/1571) $\int QTd\lambda/\lambda = 0.03249$ $\sigma = 0.0748$ $QT_{max} = 0.1393$ $d\bar{\lambda}/d\alpha = 49.9$
n_{eff}(WF) = 6.0 n_{eff}(PC) = 25.3

$\int QTd\lambda/\lambda$	0.03391	0.02703	0.02819	0.02599	0.03635	0.03867	0.03315	0.03663
$\bar{\lambda}$	8930.	8917.	8915.	8907.	8934.	8929.	8920.	8932.
$\delta\bar{\lambda}$	1571.5	1570.7	1570.4	1569.3	1571.8	1571.3	1571.4	1573.0
σ	0.0747	0.0748	0.0748	0.0748	0.0747	0.0747	0.0748	0.0748

WF/PC Filter Summary (Cont'd.)

	WF1	WF2	WF3	WF4	PC5	PC6	PC7	PC8

F850LP 12a (9298/1153) $\int QTd\lambda/\lambda = 0.02157$ $\sigma = 0.0527$ $QT_{max} = 0.1375$ $d\bar{\lambda}/d\alpha = 25.8$
n_{eff}(WF) = 6.5 n_{eff}(PC) = 27.3

$\int QTd\lambda/\lambda$	0.02263	0.01784	0.01857	0.01700	0.02434	0.02578	0.02192	0.02449
$\bar{\lambda}$	9301.	9296.	9295.	9291.	9303.	9301.	9297.	9303.
$\delta\bar{\lambda}$	1153.6	1152.6	1152.3	1151.6	1153.9	1153.5	1152.8	1153.9
σ	0.0527	0.0526	0.0526	0.0526	0.0527	0.0527	0.0527	0.0527

F606W 12b (5844/1553) $\int QTd\lambda/\lambda = 0.08294$ $\sigma = 0.1129$ $QT_{max} = 0.2461$ $d\bar{\lambda}/d\alpha = 74.5$
n_{eff}(WF) = 3.4 n_{eff}(PC) = 13.1

$\int QTd\lambda/\lambda$	0.07825	0.07030	0.07474	0.07223	0.08463	0.08904	0.09192	0.10245
$\bar{\lambda}$	5865.	5859.	5851.	5848.	5847.	5862.	5824.	5798.
$\delta\bar{\lambda}$	1550.9	1544.8	1549.0	1548.0	1559.2	1556.3	1556.4	1563.3
σ	0.1123	0.1120	0.1124	0.1124	0.1132	0.1127	0.1135	0.1145

F725LP 12c (8496/1987) $\int QTd\lambda/\lambda = 0.04338$ $\sigma = 0.0993$ $QT_{max} = 0.1443$ $d\bar{\lambda}/d\alpha = 83.8$
n_{eff}(WF) = 5.6 n_{eff}(PC) = 23.4

$\int QTd\lambda/\lambda$	0.04490	0.03638	0.03802	0.03537	0.04795	0.05126	0.04455	0.04863
$\bar{\lambda}$	8512.	8486.	8482.	8468.	8518.	8510.	8489.	8510.
$\delta\bar{\lambda}$	1989.4	1984.7	1983.3	1978.7	1991.2	1988.4	1987.1	1995.0
σ	0.0992	0.0993	0.0993	0.0992	0.0993	0.0992	0.0994	0.0995

F368M 8a (3687/230) $\int QTd\lambda/\lambda = 0.00264$ $\sigma = 0.0266$ $QT_{max} = 0.0355$ $d\bar{\lambda}/d\alpha = 2.6$
n_{eff}(WF) = 2.4 n_{eff}(PC) = 7.0

$\int QTd\lambda/\lambda$	0.00153	0.00148	0.00168	0.00141	0.00253	0.00266	0.00310	0.00676
$\bar{\lambda}$	3689.	3689.	3689.	3690.	3686.	3683.	3689.	3684.
$\delta\bar{\lambda}$	231.6	231.5	231.5	231.8	230.4	228.7	231.3	228.8
σ	0.0267	0.0267	0.0266	0.0267	0.0265	0.0264	0.0266	0.0264

F413M 8b (4125/248) $\int QTd\lambda/\lambda = 0.00540$ $\sigma = 0.0256$ $QT_{max} = 0.0743$ $d\bar{\lambda}/d\alpha = 2.7$
n_{eff}(WF) = 2.6 n_{eff}(PC) = 8.0

$\int QTd\lambda/\lambda$	0.00365	0.00348	0.00396	0.00349	0.00521	0.00470	0.00700	0.01172
$\bar{\lambda}$	4129.	4128.	4128.	4129.	4125.	4124.	4125.	4119.
$\delta\bar{\lambda}$	248.6	248.3	248.1	248.5	248.3	250.5	246.7	247.2
σ	0.0256	0.0255	0.0255	0.0256	0.0256	0.0258	0.0254	0.0255

WF/PC Filter Summary (Cont'd.)

	WF1	WF2	WF3	WF4	PC5	PC6	PC7	PC8

F492M 8d (4906/364) $\int QTd\lambda/\lambda$ = 0.01252 σ = 0.0315 QT_{max} = 0.1282 $d\bar{\lambda}/d\alpha$ = 4.9
n_{eff}(WF) = 2.9 n_{eff}(PC) = 10.2

$\int QTd\lambda/\lambda$	0.01104	0.00998	0.01091	0.01061	0.01268	0.01277	0.01459	0.01759
$\bar{\lambda}$	4911.	4910.	4909.	4910.	4906.	4909.	4903.	4895.
$\delta\bar{\lambda}$	363.8	364.1	364.0	363.5	364.1	363.9	364.4	364.7
σ	0.0315	0.0315	0.0315	0.0314	0.0315	0.0315	0.0316	0.0316

F547M 9a (5454/438) $\int QTd\lambda/\lambda$ = 0.01757 σ = 0.0341 QT_{max} = 0.1637 $d\bar{\lambda}/d\alpha$ = 6.3
n_{eff}(WF) = 3.2 n_{eff}(PC) = 11.8

$\int QTd\lambda/\lambda$	0.01640	0.01484	0.01584	0.01538	0.01784	0.01860	0.01968	0.02201
$\bar{\lambda}$	5455.	5456.	5455.	5454.	5454.	5455.	5453.	5452.
$\delta\bar{\lambda}$	438.1	438.0	438.1	438.0	438.2	438.2	438.2	438.4
σ	0.0341	0.0341	0.0341	0.0341	0.0341	0.0341	0.0341	0.0341

F648M 9c (6469/371) $\int QTd\lambda/\lambda$ = 0.00976 σ = 0.0244 QT_{max} = 0.1344 $d\bar{\lambda}/d\alpha$ = 3.8
n_{eff}(WF) = 3.8 n_{eff}(PC) = 15.1

$\int QTd\lambda/\lambda$	0.00946	0.00845	0.00889	0.00855	0.01000	0.01073	0.01057	0.01141
$\bar{\lambda}$	6470.	6469.	6469.	6469.	6470.	6471.	6468.	6467.
$\delta\bar{\lambda}$	371.5	371.1	371.1	371.1	371.5	371.6	370.9	370.6
σ	0.0244	0.0244	0.0244	0.0244	0.0244	0.0244	0.0243	0.0243

F718M 9d (7160/595) $\int QTd\lambda/\lambda$ = 0.01038 σ = 0.0353 QT_{max} = 0.1187 $d\bar{\lambda}/d\alpha$ = 8.9
n_{eff}(WF) = 4.3 n_{eff}(PC) = 17.8

$\int QTd\lambda/\lambda$	0.01036	0.00893	0.00940	0.00899	0.01093	0.01184	0.01096	0.01160
$\bar{\lambda}$	7164.	7160.	7160.	7159.	7164.	7164.	7159.	7158.
$\delta\bar{\lambda}$	596.3	595.6	595.4	595.0	596.5	596.2	595.7	596.5
σ	0.0353	0.0353	0.0353	0.0353	0.0354	0.0353	0.0353	0.0354

F875M 10b (8762/556) $\int QTd\lambda/\lambda$ = 0.00955 σ = 0.0270 QT_{max} = 0.1223 $d\bar{\lambda}/d\alpha$ = 6.4
n_{eff}(WF) = 5.8 n_{eff}(PC) = 24.3

$\int QTd\lambda/\lambda$	0.00996	0.00796	0.00830	0.00767	0.01066	0.01136	0.00975	0.01073
$\bar{\lambda}$	8763.	8762.	8761.	8760.	8764.	8763.	8762.	8764.
$\delta\bar{\lambda}$	556.6	556.5	556.4	556.3	556.6	556.6	556.5	556.7
σ	0.0270	0.0270	0.0270	0.0270	0.0270	0.0270	0.0270	0.0270

WF/PC Filter Summary (Cont'd.)

	WF1	WF2	WF3	WF4	PC5	PC6	PC7	PC8

F1042M 10d (10167/481) $\int QTd\lambda/\lambda$ = 0.00149 σ = 0.0201 QT_{max} = 0.0436 $d\bar{\lambda}/d\alpha$ = 4.1
n_{eff}(WF) = 2.6 n_{eff}(PC) = 32.1

$\int QTd\lambda/\lambda$	0.00157	0.00122	0.00126	0.00114	0.00170	0.00179	0.00150	0.00171
$\bar{\lambda}$	10168.	10168.	10168.	10167.	10169.	10168.	10168.	10168.
$\delta\bar{\lambda}$	482.1	481.5	481.4	481.0	482.3	482.1	481.7	482.3
σ	0.0201	0.0201	0.0201	0.0201	0.0201	0.0201	0.0201	0.0201

F375N 7a (3755/82) $\int QTd\lambda/\lambda$ = 0.00093 σ = 0.0094 QT_{max} = 0.0344 $d\bar{\lambda}/d\alpha$ = 0.3
n_{eff}(WF) = 2.5 n_{eff}(PC) = 7.2

$\int QTd\lambda/\lambda$	0.00055	0.00053	0.00060	0.00051	0.00089	0.00091	0.00111	0.00234
$\bar{\lambda}$	3756.	3756.	3756.	3756.	3755.	3755.	3756.	3755.
$\delta\bar{\lambda}$	83.0	83.0	83.0	83.0	82.9	82.8	83.0	82.8
σ	0.0094	0.0094	0.0094	0.0094	0.0094	0.0094	0.0094	0.0094

F437N 7c (4366/22) $\int QTd\lambda/\lambda$ = 0.00034 σ = 0.0021 QT_{max} = 0.0679 $d\bar{\lambda}/d\alpha$ = 0.0
n_{eff}(WF) = 2.7 n_{eff}(PC) = 8.7

$\int QTd\lambda/\lambda$	0.00025	0.00024	0.00027	0.00025	0.00034	0.00031	0.00043	0.00065
$\bar{\lambda}$	4366.	4366.	4366.	4366.	4366.	4366.	4366.	4366.
$\delta\bar{\lambda}$	22.1	22.1	22.1	22.1	22.1	22.1	22.1	22.1
σ	0.0021	0.0021	0.0021	0.0021	0.0021	0.0021	0.0021	0.0021

F469N 11b (4687/27) $\int QTd\lambda/\lambda$ = 0.00062 σ = 0.0025 QT_{max} = 0.1073 $d\bar{\lambda}/d\alpha$ = 0.0
n_{eff}(WF) = 2.8 n_{eff}(PC) = 9.6

$\int QTd\lambda/\lambda$	0.00052	0.00047	0.00052	0.00050	0.00062	0.00061	0.00074	0.00096
$\bar{\lambda}$	4688.	4688.	4688.	4688.	4688.	4688.	4688.	4688.
$\delta\bar{\lambda}$	27.9	27.9	27.9	27.9	27.9	27.9	27.9	27.9
σ	0.0025	0.0025	0.0025	0.0025	0.0025	0.0025	0.0025	0.0025

F487N 11c (4869/31) $\int QTd\lambda/\lambda$ = 0.00079 σ = 0.0027 QT_{max} = 0.1176 $d\bar{\lambda}/d\alpha$ = 0.0
n_{eff}(WF) = 2.9 n_{eff}(PC) = 10.1

$\int QTd\lambda/\lambda$	0.00069	0.00062	0.00068	0.00067	0.00080	0.00080	0.00092	0.00111
$\bar{\lambda}$	4869.	4869.	4869.	4869.	4869.	4869.	4869.	4869.
$\delta\bar{\lambda}$	31.3	31.3	31.3	31.3	31.3	31.3	31.3	31.3
σ	0.0027	0.0027	0.0027	0.0027	0.0027	0.0027	0.0027	0.0027

WF/PC Filter Summary (Cont'd.)

	WF1	WF2	WF3	WF4	PC5	PC6	PC7	PC8

F502N 7b (5018/29) $\int QTd\lambda/\lambda$ = 0.00079 σ = 0.0025 QT_{max} = 0.1372 $d\bar{\lambda}/d\alpha$ = 0.0
n_{eff}(WF) = 2.9 n_{eff}(PC) = 10.5

$\int QTd\lambda/\lambda$	0.00072	0.00065	0.00070	0.00069	0.00081	0.00083	0.00091	0.00106
$\bar{\lambda}$	5019.	5019.	5019.	5019.	5019.	5019.	5019.	5019.
$\delta\bar{\lambda}$	29.9	29.9	29.9	29.9	29.9	29.9	29.9	29.9
σ	0.0025	0.0025	0.0025	0.0025	0.0025	0.0025	0.0025	0.0025

F517N 11d (5170/87) $\int QTd\lambda/\lambda$ = 0.00316 σ = 0.0072 QT_{max} = 0.1485 $d\bar{\lambda}/d\alpha$ = 0.3
n_{eff}(WF) = 3.0 n_{eff}(PC) = 10.9

$\int QTd\lambda/\lambda$	0.00290	0.00262	0.00282	0.00276	0.00321	0.00331	0.00358	0.00405
$\bar{\lambda}$	5170.	5170.	5170.	5170.	5170.	5170.	5170.	5170.
$\delta\bar{\lambda}$	87.7	87.7	87.7	87.7	87.7	87.7	87.7	87.7
σ	0.0072	0.0072	0.0072	0.0072	0.0072	0.0072	0.0072	0.0072

F588N 7d (5880/43) $\int QTd\lambda/\lambda$ = 0.00104 σ = 0.0031 QT_{max} = 0.1410 $d\bar{\lambda}/d\alpha$ = 0.1
n_{eff}(WF) = 3.4 n_{eff}(PC) = 13.1

$\int QTd\lambda/\lambda$	0.00099	0.00089	0.00094	0.00091	0.00106	0.00112	0.00115	0.00127
$\bar{\lambda}$	5880.	5880.	5880.	5880.	5880.	5880.	5880.	5880.
$\delta\bar{\lambda}$	43.6	43.6	43.6	43.6	43.6	43.6	43.6	43.6
σ	0.0031	0.0031	0.0031	0.0031	0.0031	0.0031	0.0031	0.0031

F631N 6a (6306/29) $\int QTd\lambda/\lambda$ = 0.00053 σ = 0.0020 QT_{max} = 0.1144 $d\bar{\lambda}/d\alpha$ = 0.0
n_{eff}(WF) = 3.7 n_{eff}(PC) = 14.5

$\int QTd\lambda/\lambda$	0.00051	0.00046	0.00048	0.00047	0.00054	0.00058	0.00058	0.00063
$\bar{\lambda}$	6307.	6307.	6307.	6307.	6307.	6307.	6307.	6307.
$\delta\bar{\lambda}$	29.8	29.8	29.8	29.8	29.8	29.8	29.8	29.8
σ	0.0020	0.0020	0.0020	0.0020	0.0020	0.0020	0.0020	0.0020

F656N 6b (6559/19) $\int QTd\lambda/\lambda$ = 0.00030 σ = 0.0013 QT_{max} = 0.1003 $d\bar{\lambda}/d\alpha$ = 0.0
n_{eff}(WF) = 3.9 n_{eff}(PC) = 15.4

$\int QTd\lambda/\lambda$	0.00029	0.00026	0.00027	0.00026	0.00030	0.00033	0.00032	0.00034
$\bar{\lambda}$	6559.	6559.	6559.	6559.	6559.	6559.	6559.	6559.
$\delta\bar{\lambda}$	19.8	19.8	19.8	19.8	19.8	19.8	19.8	19.8
σ	0.0013	0.0013	0.0013	0.0013	0.0013	0.0013	0.0013	0.0013

WF/PC Filter Summary (Cont'd.)

	WF1	WF2	WF3	WF4	PC5	PC6	PC7	PC8

F664N 6c (6637/131) $\int QTd\lambda/\lambda$ = 0.00328 σ = 0.0084 QT_{max} = 0.1289 $d\bar{\lambda}/d\alpha$ = 0.5
n_{eff}(WF) = 3.9 n_{eff}(PC) = 15.7

$\int QTd\lambda/\lambda$	0.00321	0.00284	0.00299	0.00288	0.00338	0.00364	0.00354	0.00379
$\bar{\lambda}$	6637.	6637.	6637.	6637.	6637.	6637.	6637.	6637.
$\delta\bar{\lambda}$	131.3	131.3	131.3	131.3	131.3	131.3	131.3	131.3
σ	0.0084	0.0084	0.0084	0.0084	0.0084	0.0084	0.0084	0.0084

F658N 5d (6576/20) $\int QTd\lambda/\lambda$ = 0.00029 σ = 0.0013 QT_{max} = 0.1004 $d\bar{\lambda}/d\alpha$ = 0.0
n_{eff}(WF) = 3.9 n_{eff}(PC) = 15.5

$\int QTd\lambda/\lambda$	0.00028	0.00025	0.00026	0.00025	0.00030	0.00032	0.00031	0.00033
$\bar{\lambda}$	6577.	6577.	6577.	6577.	6577.	6577.	6577.	6577.
$\delta\bar{\lambda}$	20.1	20.1	20.1	20.1	20.1	20.1	20.1	20.1
σ	0.0013	0.0013	0.0013	0.0013	0.0013	0.0013	0.0013	0.0013

F672N 1b (6723/50) $\int QTd\lambda/\lambda$ = 0.00136 σ = 0.0032 QT_{max} = 0.1927 $d\bar{\lambda}/d\alpha$ = 0.1
n_{eff}(WF) = 3.9 n_{eff}(PC) = 16.0

$\int QTd\lambda/\lambda$	0.00133	0.00117	0.00124	0.00119	0.00140	0.00151	0.00145	0.00155
$\bar{\lambda}$	6723.	6723.	6723.	6723.	6723.	6723.	6723.	6723.
$\delta\bar{\lambda}$	50.4	50.4	50.4	50.4	50.4	50.4	50.4	50.4
σ	0.0032	0.0032	0.0032	0.0032	0.0032	0.0032	0.0032	0.0032

F889N 12d (8888/51) $\int QTd\lambda/\lambda$ = 0.00065 σ = 0.0025 QT_{max} = 0.1165 $d\bar{\lambda}/d\alpha$ = 0.1
n_{eff}(WF) = 5.9 n_{eff}(PC) = 25.0

$\int QTd\lambda/\lambda$	0.00067	0.00054	0.00056	0.00052	0.00072	0.00077	0.00066	0.00073
$\bar{\lambda}$	8889.	8889.	8889.	8889.	8889.	8889.	8889.	8889.
$\delta\bar{\lambda}$	51.5	51.5	51.5	51.5	51.5	51.5	51.5	51.5
σ	0.0025	0.0025	0.0025	0.0025	0.0025	0.0025	0.0025	0.0025

F1083N 3d (10831/80) $\int QTd\lambda/\lambda$ = 0.00001 σ = 0.0032 QT_{max} = 0.0011 $d\bar{\lambda}/d\alpha$ = 0.1
n_{eff}(WF) = 8.3 n_{eff}(PC) = 34.8

$\int QTd\lambda/\lambda$	0.00001	0.00001	0.00001	0.00001	0.00001	0.00001	0.00001	0.00001
$\bar{\lambda}$	10831.	10831.	10831.	10831.	10831.	10831.	10831.	10831.
$\delta\bar{\lambda}$	80.8	80.8	80.8	80.8	80.8	80.8	80.8	80.8
σ	0.0032	0.0032	0.0032	0.0032	0.0032	0.0032	0.0032	0.0032

Note: Gratings, polarizers, F128LP and F8ND are omitted.

Table 5.1.2
AB_ν As a Function of Spectral Type and Wavelength

Index	0	1	2	3	4	5	6	7	8	9	10	11
λ, Å	sky	B0	A0	F0	G0	K0III	M0III	gE	Sa	Sbc	Scd	IrI
1500	2.45	-1.60	2.22	7.22	8.90	13.00	15.00	6.82	5.40	4.03	2.67	1.77
2000	5.46	-1.50	1.35	4.10	6.35	10.30	12.30	6.41	4.80	3.18	2.29	1.40
2500	5.46	-1.20	1.11	3.11	4.61	8.11	9.36	5.43	4.10	2.86	2.15	1.36
3000	3.12	-0.78	1.21	1.99	2.46	5.46	6.21	3.63	3.00	2.46	1.76	1.24
3500	2.00	-0.62	1.00	1.38	1.63	2.13	4.63	2.49	2.01	1.54	1.35	0.94
4000	1.03	-0.46	-0.23	0.29	0.67	1.16	2.26	1.40	1.12	0.84	0.65	0.43
4500	0.55	-0.36	-0.16	0.06	0.26	0.46	0.96	0.55	0.44	0.34	0.28	0.34
5000	0.18	-0.22	-0.09	0.03	0.08	0.20	0.51	0.21	0.19	0.17	0.13	0.17
6000	-0.11	0.16	0.11	0.03	-0.04	-0.24	-0.46	-0.19	-0.17	-0.14	-0.11	0.13
7000	-0.33	0.46	0.22	0.05	-0.12	-0.42	-0.76	-0.52	-0.44	-0.37	-0.26	-0.04
8000	-0.55	0.76	0.33	0.08	-0.21	-0.61	-1.06	-0.81	-0.70	-0.60	-0.39	-0.21
9000	-0.65	0.96	0.36	0.09	-0.23	-0.66	-1.12	-1.07	- .95	-0.84	-0.47	-0.33
10000	-0.75	1.17	0.40	0.10	-0.25	-0.72	-1.19	-1.29	-1.16	-1.04	-0.58	-0.45
11000	-1.01	1.37	0.43	0.11	-0.27	-0.75	-1.25	-1.51	-1.36	-1.21	-0.66	-0.51
12000	-1.11	1.57	0.45	0.12	-0.29	-0.78	-1.31	-1.69	-1.52	-1.35	-0.70	-0.54
B-V	1.10	-0.31	0.00	0.27	0.58	1.07	1.60	1.00	0.80	0.60	0.45	0.30

In the calculation of sky background on p.68, the surface brightness of the sky has been taken as $m_v = 23$ (arcsec)$^{-2}$. The actual sky brightness depends on the heliocentric ecliptic latitude and longitude (λ - $\lambda\odot$), in a manner summarized in Table 5.1.4, taken from the F.O.S. Instrument Handbook by H. Ford.

Table 5.1.4

	Ecliptic Latitude			
λ - $\lambda\odot$	0	30	60	90
180	22.1	22.7	23.2	23.3
145	22.4	22.9	23.3	23.3
110	22.3	22.9	23.3	23.3

5.2 EXTENDED SOURCES

For high-z galaxies, a much smaller fraction of light falls in the central pixel than for a stellar source; it is plotted against redshift in Figure 5.2.1, for giant elliptical galaxies, expressed as the magnitude difference between the central pixel and the total galaxy. For other types of galaxies, a morphological term can be added to the values in Figure 5.2.1; for example, 0.6 mag for lenticulars, 0.7 for S, 0.8 for Sab, 0.9 for Sbc, 1.2 for Scd, and 1.8 for Im. A further premium of 1.2 mag must be added if the f/30 camera is used instead of f/12.9.

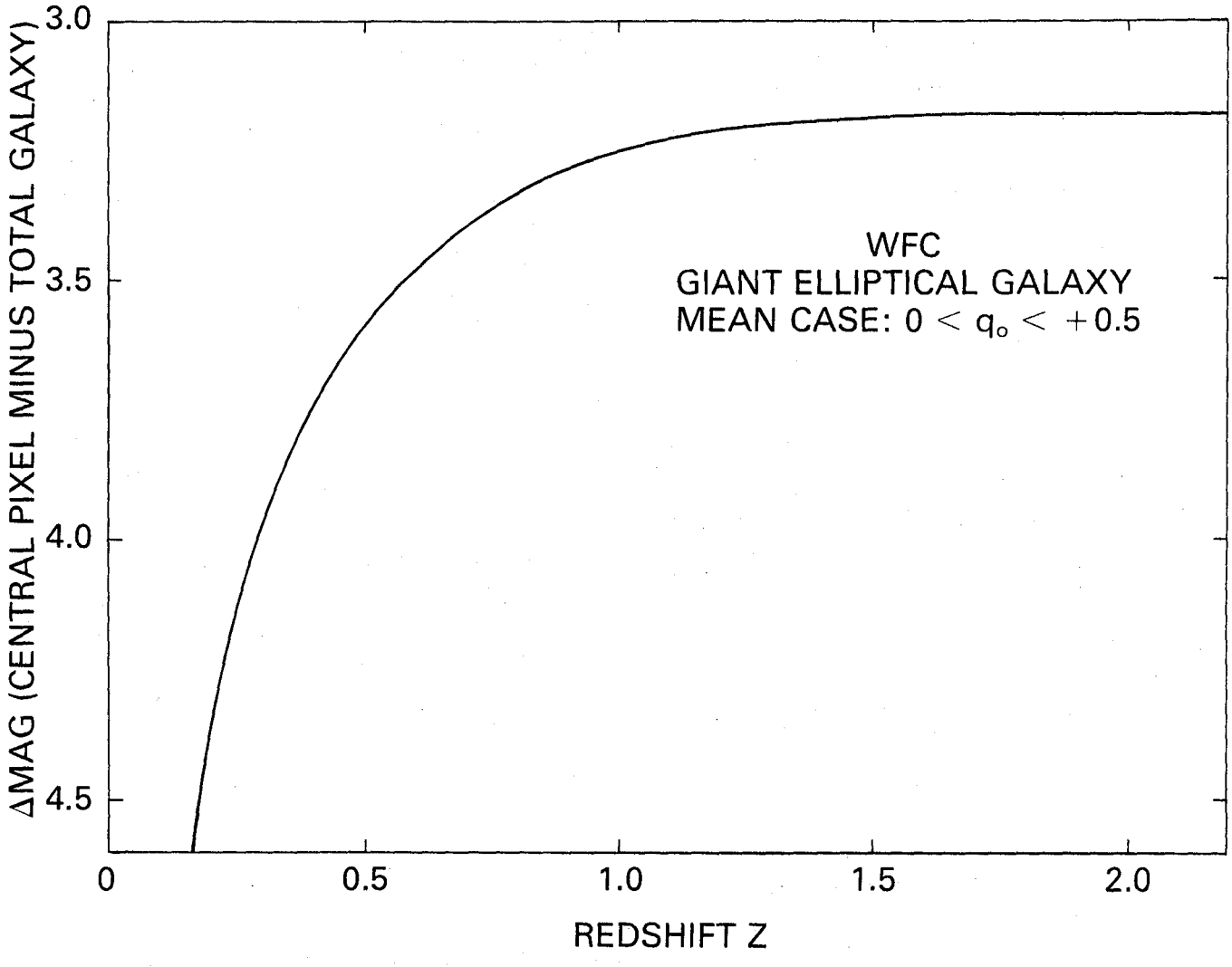

Figure 5.2.1 Giant Elliptical Galaxy

6.0 CALIBRATION AND DATA REDUCTION

6.1 CALIBRATION FRAMES

Standard calibration frames will be obtained and maintained in the calibration data base at the ST ScI. This includes the maintenance of flat-field calibration files, dark current images, pre-flash images, as well as standard star calibration frames for absolute sensitivity, plate scale distortion, grating dispersion, polarization properties, etc. These reference files will be provided to the STScI by the WF/PC IDT during the Science Verification period, and will be updated on a time-available basis after the end of that period. These reference data will be maintained to a precision which is routinely attainable. For especially precise measurements, special calibration reference data may need to be obtained by means of calibration observations which may constitute part of the observing proposal.

An imagescan will require the OTA to step and stop or to scan continuously. This may be used to observe bright standards and as an aid for detecting short-period variables. One application would be to observe a "standard" star with the star in different areas of the FOV. Only one readout of the CCDs would be taken. This procedure can be used to achieve higher statistical accuracy and to reduce the volume of data on the downlink.

6.1.1 Flat Fields

The removal of the pixel-by-pixel variation in the optical/electrical sensitivity of the WF/PC is usually known as flat-fielding or flattening. To obtain data for this, a "flat field" (an exposure of a spatially uniform source) needs to be observed through the telescope and desired filter. Real flat fields are always external; however, the WF/PC internal light sources that illuminate the CCDs can be used to monitor the stability of the flat fields (less the telescope), using exposures called INTFLATs. This internal capability uses a light source that cannot be guaranteed to be stable and therefore does not provide absolute data on the sensitivity of the CCDs and the performance of the WF/PC internal optics; furthermore, the internal flat fields may include 'ghost' images of the WF/PC Cassegrain optics, which do not appear in external images. Flat fields will be obtained using the sunlit earth, as part of routine calibration.

6.1.2 Dark Frames

Dark frames are long exposures that are taken with no light incident on the CCDs. They are used to detect CCD counts (the dark current) caused by thermal generation (at the interfaces between the silicon and oxide layers) as well as the rate of charged particle and secondary radiation events. At the normal CCD operating temperature, the "dark current" is $\lesssim$ 0.003 electrons/pixel/second, except for several hours after a "super-purge" used to ameliorate the residual image problem (*q.v.*)

6.1.3 Bias Frames

Bias frames are readouts of the CCDs without an exposure (so the dark current is negligible). They are used to measure the bias built into the system to ensure that the ADC input is above zero and, hence, to determine the pedestal for a zero signal (these frames, of course, are not automatically bias-subtracted in the data reduction process). The bias level

for frames of single-pixel data (813×800) will be determined in the routine data processing pipeline from the 'overclocked' pixels at the end of each line, where there is no signal.

6.1.4 Kelsall Spots (K-spots)

Kelsall spots can be imposed on any type of frame to find focus shifts or relative motions between CCDs. They also aid in registration of four frames (one per CCD) as a celestial scene. Normally, however, a separate frame for them will be taken because of the effect of the ND spot (with the K-spot lamp energized, CCD saturation is caused).

6.2 DATA PRODUCTION AND DATA PRODUCTS

The routine science data processing of WF/PC data consists of allowing for missing code in the analog-to digital conversion process, followed by bias subtraction and normalization for relative sensitivity variations over the image (i.e., flat-fielding). Various pixel conditions are flagged as bad or potentially bad. The resulting images will be available on magnetic tape in FITS format, and as photographic prints. The reformatted raw data will also be available, along with the relevant calibration data.

6.2.1 RSDP Pipeline

Currently implemented capabilities include the following :
Allowance for missing code in analog-to-digital conversion
Bias level removal (800 x 800 mode only)
Bias image subtraction
Preflash image scaling and subtraction
Dark image scaling and subtraction
Flat field image correction

The following conditions are flagged in the Data Quality File (DQF):
Transmission failures and possible failures
Known bad pixels (e.g. blocked columns)
Pixels at the maximum digital level
Bad pixels in reference images (e.g. flat)

The following histograms are generated :

Input image
After A to D fixup
Output image

Serial Register charge transfer fix-up (for images without preflash)
Additional keywords (e.g. object identifier)
Additional keywords (e.g. photometric parameters)

6.2.2 Data Formats

FITS tape output:

option will be provided to export WF/PC images as four (4) images on FITS tape (i.e. one FITS image for each chip read out). These FITS files will have simple headers with all SDAS "group" parameters presented as simple FITS keywords.

Output products:

The following are generally considered part of a data set :
Edited Image and DQF
(not processed in pipeline)
Standard Header Packet
Extracted Engineering Data
Trailer File

Header Contents:

Image and Reference File Headers
Standard Header Packet
Further data reduction and analysis may be performed under the ST ScI's science data analysis software system (SDAS). Standard routines will be available, operating under IRAF, for the analysis of data for image photometry, spectral analysis, polarimetry and astrometry. Details of the routines and their output are contained in the SDAS user's manual.